Ana Isabel Batista Rita

Mestre em Engenharia Química

Study, development and implementations of methodologies that allow optimizing refinery wastewater treatment processes and minimize impact risks on the surrounding

Dissertação para obtenção do Grau de Doutor

em Engenharia da Refinação, Petroquímica e Química

Orientador: Doutora Sandra Marisa Lourenço Sanches, Investigador Doutorado, Hovione FarmaCiência S.A.

Co-orientadores: Professor Luís Miguel Palma Madeira, Professor Associado com Agregação, FEUP

Professor João Paulo Serejo Goulão Crespo, Professor Catedrático, FCT/UNL

Coordenador Empresarial: Maria António de Oliveira Varandas Gonçalves Colaço Rodrigues dos Santos, Responsável de Ambiente da Refinaria de Sines, Galp

Júri:

Presidente: Professor José Paulo Barbosa Mota, Professor Catedrático, FCT/UNL

Arguente(s): Professora Rosa Maria de Oliveira Quinta-Ferreira, Professor Catedrático, UC

Doutora Maria João Filipe Rosa, Investigador Doutorado, LNEC

Vogal(ais): Professor Luís Miguel Palma Madeira, Professor Associado com Agregação, FEUP

Professora Isabel Maria Rôla Coelhoso, Professor Associado com Agregação, FCT/UNL

Maria António de Oliveira Varandas Gonçalves Colaço Rodrigues dos Santos, Responsável da Área de Ambiente da Refinaria de Sines, Galp

FACULDADE DE CIÊNCIAS E TECNOLOGIA
UNIVERSIDADE NOVA DE LISBOA

Dezembro 2020

Study, development and implementations of methodologies that allow optimizing refinery wastewater treatment processes and minimize impact risks on the surrounding

À minha querida família.

Ao meu pai, em particular.

Ao Tiago.

Acknowledgments

O presente trabalho foi co-financiado pela Fundação para a Ciência e Tecnologia (FCT) através do programa OPCH – Programa Operacional Capital Humano (co-financiado pelo PT2020 e Fundos Sociais Europeus) e fundos nacionais do MCTES e grupo Galp, através da bolsa PD/BDE/114356/2016. Agradece-se todo o apoio prestado pelo programa iNOVA4Health - UID/Multi/04462/2013, financiado pela FCT e Ministério da Educação e Ciência (MEC), através de fundos nacionais e co-financiado pelo Fundo Europeu de Desenvolvimento Regional (FEDER), sob o acordo de colaboração do PT2020 bem como o financiamento do Programa INTERFACE, através do Fundo de Inovação, Tecnologia e Economia Circular (FITEC). De igual forma, agradece-se todo o apoio prestado pelo Laboratório Associado para a Química Verde (LAQV) – Requi*m*te, o qual é financiado por fundos nacionais provenciados pela FCT e MEC (UID/QUI/50006/2013) e co-financiado pelo FEDER sob o acordo de colaboração do PT2020 (POCI-01-0145-FEDER - 007265). O presente trabalho foi igualmente financiado pelo Fundo Base UIDB/00511/2020 do Laboratório de Engenharia de Processo, Ambiente, Biotecnologia e Energia (LEPABE) – financiado por fundos nacionais através da FCT/MCTES (PIDDAC).

Agradece-se também ao Programa Doutoral de Engenharia da Refinação, Petroquímica e Química (EngIQ) e às instituições de ensino Faculdade de Ciências e Tecnologia da Universidade Nova de Lisboa (UNL-FCT) e Faculdade de Engenharia da Universidade do Porto (FEUP).

À minha equipa de orientação, os meus mais sinceros agradecimentos pela vossa genuína dedicação ao longo dos últimos 5 anos – à Doutora Sandra Sanches, a minha orientadora principal, ao Professor Luís Miguel Madeira, o meu co-orientador e à Engenheira Maria Santos, a minha coordenadora empresarial. Também um agradecimento especial ao Doutor Jorge Ribeiro, que muito ajudou na conceção do 1º capítulo da presente tese bem como no arranque e planeamento dos trabalhos durante os primeiros 2 anos.

Pretendo deixar um profundo agradecimento ao apoio imperscindível do Professor Fernando Martins, coordenador do Programa Doutoral EngIQ, e do Professor João Crespo,

coordenador do Programa Doutoral EngIQ na UNL-FCT. Sempre mostraram prontidão e disponibilidade para me auxiliar sobre prazos, questões mais burocráticas e em particular o Professor João Crespo que muito auxiliou na definição do plano de tarefas sobre os estudos de separação por membranas, em conjunto com a Doutora Sandra Sanches.

Agradeço a todas as pessoas da UNL-FCT, Instituto de Biologia Experimental e Tecnológica (IBET), FEUP e Refinaria de Matosinhos que de bom agrado desenvolveram análises extremamente essenciais para a conceção dos vários capítulos aqui apresentados e sem qualquer entrave me esclareceram sempre que necessário: Doutora Carmen Rodrigues, Doutora Luísa Neves e aluna Ana Rita Nabais, Doutora Rosa Huertas e Engenheiros Ana Luísa Monteiro e Ricardo Albuquerque.

À equipa da Refinaria de Sines eu podia ficar aqui a agradecer individualmente porque a amizade e disponibilidade que me foi prestada por todos assim o exige, mas não tenho espaço para tantas pessoas. Por isso, quero deixar desde já um pedido de desculpas a quem não incluí aqui, mas que toda a equipa da Refinaria de Sines saiba que levo comigo excelentes ensinamentos e que deixam uma enorme boa recordação dos anos em que aí estive. No entanto não posso deixar de agradecer em particular a um determinado conjunto de pessoas que realmente se destacaram nesta incrível amizade e disponibilidade: Maria Santos e Sandra Dias, a equipa do Ambiente da Refinaria de Sines, onde me senti verdadeiramente em casa e todos os dias foram um gosto! Da equipa do Laboratório, tenho de agradecer em particular à Isabel Grilo, por sempre autorizar com um sorriso e compreensão todas as horas extraordinárias e o uso disto e daquilo e ainda mais de qualquer coisa. Um obrigada è equipa dos chefes de turno do Laboratório, todos excecionais, e em particular às analistas Carla Costa e Ana Cavaco, lições sábias que me deram, meninas! Da equipa da Movimentação de Produtos, à Susete Valente um super obrigada por tudo, uma bela amizade que levo comigo, aliada ao belo cheiro de alguns efluentes aqui e ali. Quero agradecer de igual forma à equipa de chefes de turno, sempre impecáveis e com um sorriso a receberem-me sempre que lá aparecia para ir ver isto ou aquilo, ou pedir também alguma coisa. Aos operadores desta área, bem que merecem que eu agradeça, que tantas amostras e tantas boleias me deram e me ajudaram. De igual forma quero deixar um agradecimento especial aos chefes de turno da Fábrica I e operadores da área I, por tantas amostras de soda exausta tão mal cheirosa tirarem para mim, por vezes milhares de litros! Como por vezes os últimos são os primeiros, não posso passar sem deixar aqui uma verdadeira palavra de agradecimento por tanta ajuda que a equipa do PRS me deu, ao ajudar com transportes para

todo o lado da refinaria, de coisas demasiado grandes e pesadas para um carro. E também pela amizade genuína que criei com a Raquel Chainho e com a Joana Brito, que levo comigo para além das portas da refinaria, também como tantas outras aqui mencionadas.

Às restantes pessoas que passaram comigo tempo na área do Ambiente e ao grupo dos almoços que me acolheu assim que cheguei, um muito muito obrigada! Belos tempos.

Aos meus amigos, em particular à Andreia, obrigada pelo vosso tempo e amizade, e sem dúvida, paciência!

À minha querida família, que sempre esteve comigo e sempre me apoiou, mesmo nos momentos mais sombrios, adoro-vos. Em particular, ao meu pai que partiu pouco antes da conclusão desta tese, mas que foi o primeiro a insistir para eu iniciar o doutoramento e sempre insistiu fervorosamente que eu a terminasse, aqui está o fim, pai. Aos meus futuros sogros, obrigada por me terem sempre tratado como filha! Finalmente, ao meu companheiro de tantas lutas e vitórias, Tiago, agradeço-te em particular por tudo, e continuemos para o que há-de vir.

Abstract

The main objective of the work developed in this thesis was to address spent caustic treatment as a way to decrease the high organic load of this effluent and reduce its great impact on the quality of the wastewater sent to wastewater treatment plants, particularly in terms of oil and grease (O&G) contamination. The naphthenic spent caustic generated by *Galp* refinery in Sines was used as case study.

Spent caustic effluents are very challenging due to their very hazardous nature in terms of toxicity as well as their extreme pH (approximately 12-13). Spent caustic treatment is presently a challenge for refineries, due to its composition rich in mercaptans, sulphides and other aromatic compounds. In general, proton nuclear magnetic ressonance (NMR), Fourier transform infrared spectroscopy (FT-IR) and gas chromatography – mass spectromery (GC-MS) analyses suggested that aromatic structures account for a significant part of the organic structures that constitute naphthenic spent caustic, which are also present in the final wastewater. It was found that acid crudes processing with lower molecular-weight acid components seem to have a great impact on polar O&G concentration increase in spent caustic and therefore in the final wastewater.

Nanofiltration (NF) is a very effective technology when treatment and separation/recovery of specific components is required since it is able to remove low molecular weight organic molecules like hydrocarbons and phenolic compounds. The potential application of polymeric and ceramic membranes was addressed by conducting ageing studies (only in the case of polymeric membranes) and NF experiments to assess their retention properties and lifespan. Contrarily to expectations, neither of the tested types of membranes presented attractive results for spent caustic treatment, due to very quick losses of their retention properties; analysis by FT-IR and Inductively coupled plasma atomic emission spectroscopy (ICP-AES) corroborated the ocurrence of desintegration mechanisms in the structure of the tested membranes.

A different strategy based on chemical treatments was followed to treat spent caustic: (i) neutralization, followed by Fenton oxidation post-treatment (approach 1) and (ii) neutralization, followed by liquid-liquid extraction (approach 2). Approach 1 (lab scale tests) allowed to remove 95 % of polar O&G, with a 70% decrease in the acute toxicity after treatment. Approach 2 (pilot scale tests) allowed to remove 99 % of polar O&G. Both technologies allowed direct discharge of treated spent caustic into the Sines refinery wastewater circuit, with approach 2 being the best option since it presented the highest annual savings (1.58 M€) in the yearly effluent management cost.

The results obtained in the present thesis may be useful for the development/optimization of industrial-scale plants in petroleum refineries for the treatment of naphthenic spent caustic effluents, providing an effective treatment technology proposal, with interesting effluent management cost reduction.

Keywords: Oil refinery, Naphthenic spent caustic effluents, Oil and grease, Nanofiltration, Neutralization, Fenton oxidation.

Resumo

O presente trabalho teve como principal objetivo o tratamento da soda exausta como forma de diminuir a elevada carga orgânica deste efluente e assim reduzir o seu impacto no efluente final descarregado para a estação de tratamento, particularmente em termos da contaminação por óleos e gorduras (O&G). Para tal, a soda exausta nafténica produzida na refineria de Sines (*Galp*) foi utilizada como caso de estudo.

A soda exausta constitui um verdadeiro desafio devido à sua natureza tóxica e ao seu pH extremo (aproximadamente 12-13). Este efluente tem-se apresentado como um enigma para as refinarias no que concerne ao tratamento de efluentes, tendo em conta a sua composição rica em mercaptanos, sulfuretos e outros compostos aromáticos. No geral, as análises de ressonância magnética nuclear de protão (NMR), espectroscopia de infravermelho com transformada de Fourier (FT-IR) e cromatografia gasosa com espectroscopia de massa (GC-MS) sugerem que as estruturas aromáticas representam uma parte significativa das estruturas orgânicas que constituem a soda exausta nafténica, as quais também estão presentes no efluente final. Verificou-se que o processamento de crudes ácidos com compostos ácidos de baixo peso molecular apresentam maior impacto no aumento da concentração de O&G de natureza polar na soda exausta e por consequência no efluente final.

A nanofiltração (NF) caracteriza-se por ser uma tecnologia eficiente quando o tratamento e separação/recuperação de compostos específicos é necessário, uma vez que consegue remover moléculas orgânicas de baixo peso molecular como hidrocarbonetos e compostos fenólicos. O potencial de tratamento da soda exausta foi estudado com membranas polimérica e cerâmica, avaliando-se para tal o tempo de vida útil das membranas (apenas no caso da membrana polimérica). Contrariamente às expectativas, nenhum dos tipos de membranas testados apresentou resultados interessantes para o tratamento da soda exausta, devido a perdas muito rápidas de propriedades retentivas; efetivamente, análises por FT-IR e espectroscopia de emissão atómica de indução por plasma e espectroscopia de absorção

atómica com câmara de grafite (ICP-AES) corroboraram a ocorrência de mecanismos de desintegração na estrutura das membranas testadas.

Foi testada uma estratégia diferente para tratar a soda exausta, baseada em tratamentos químicos: (i) neutralização, seguida de oxidação Fenton como pós-tratamento (1ª abordagem) e (ii) neutralização, seguida de extração líquido-líquido (2ª abordagem). A 1ª abordagem (realizada à escala laboratorial) permitiu remover 95 % de O&G de natureza polar, com uma redução de 70 % da toxicidade aguda após tratamento. A 2ª abordagem (realizada à escala piloto) permitiu remover 99 % de O&G de natureza polar. Ambas as tecnologias produziram um efluente tratado com características aceitáveis para descarga no circuito de tratamento de efluentes da refinaria de Sines. A 2ª abordagem foi considerada a melhor opção, uma vez que apresentou a maior poupança no custo anual com a gestão de efluentes (1.58 M€).

Os resultados obtidos na presente tese poderão ser úteis no desenvolvimento/otimização de unidades à escala industrial em refinarias de petróleo para o tratamento de sodas exaustas nafténicas, providenciando para tal uma proposta de tecnologia de tratamento eficiente, com uma redução interessante no custo anual com a gestão de efluentes.

Palavras-chave: Refinaria de petróleo, Soda exausta nafténica, Óleos e gorduras, Nanofiltração, Neutralização, Oxidação Fenton.

List of Abbreviations

A - Effective filtration area (m^2)

AOPs - Advanced oxidation processes

ATR - Attenuated total reflectance

CAPEX - Capital expenditure

$CDCl_3$ - Deuterochloroform

COD - Chemical oxygen demand (mg O_2/L)

CP/MAS - Cross polarization-magic angle spinning

DBE - Double bond equivalents

DI - Distilled

EA - Ethyl acetate

ESI FT-ICR MS - Negative-ion electrospray ionization Fourier transform ion cyclotron mass spectrometry

FD - Fractional distillation

FT-IR - Fourier transform infrared spectroscopy

GC-MS - Gas chromatography-mass spectrometry

^{1}H NMR - Proton nuclear magnetic ressonance

HC - Hydrodynamic cavitation

HPSEC - High-pressure size exclusion chromatography

ICP-AES - Inductively coupled plasma atomic emission spectroscopy

k' - Specific uptake rate of dissolved oxygen (mg O_2.mg^{-1}.h^{-1})

LLE - Liquid-liquid extraction

LOD - Limit of detection

L_P - Hydraulic permeability ($Lh^{-1}bar^{-1}m^{-2}$)

LPG - Liquid petroleum gas

MBR - Membrane bioreactor

MEK - Methyl ethyl ketone

MW - Molecular weight

MWCO - Molecular weight cut-off

NF - Nanofiltration

O&G - Oil and grease

OPEX - Operational expenditure

PAHs - Polycyclic aromatic hydrocarbons

PD - Penalizing discharge

PES - Polyethersulphone

PLS - Project to latent structures

PMS - Peroxymonosulphates

PS - Persulphates

PS - Polysulphone

PWP - Pure water permeability

R - Ratio between spent caustic and fresh kerosene flow rates

Re – Reynolds number

RM - Ribeira de Moinhos

RO – Reverse Osmosis

RT - Retention time (min)

SEC - Size exclusion chromatography

SEM - EDS - Scanning electron microscopy - Energy dispersive X-ray spectroscopy

SDD - Silicon drift detector

SMEWW - Standard method for examination of water and wastewater

TAN - Total acid number

TCE - Tetrachloroethylene

TMP - Transmembrane pressure (bar)

TMS - Tetramethylsilane

t - Time of nanofiltration test (h)

TOC - Total organic carbon (mg C/L)

TSS - Total suspended solids (mg/L)

UV - Ultraviolet light

UV-Vis - Ultraviolet-visible

V_P - Permeate volume (L)

VOCs - Volatile organic compounds

WWTP - Wastewater treatment plant

Contents

List of Figures

List of Tables

1 Introduction

1.1 Contextualization

Processing of crude oil and the generation of petroleum refinery effluents has been a global issue in the last years due to ever growing energy demand. Increasingly stringent regulations are now worldwide imposed to encourage industries to treat and reuse wastewater since availability of quality water is decreasing. Conventional processes often employed to treat refinery effluents cannot remove several hazardous pollutants. From the economic and environmental perspectives, the development of sustainable and effective technologies to treat refinery effluents and provide reuse of resources is crucial.

Galp is a portuguese enterprise that operates in the energetic sector, already with more than 30 years of presence in the national and international market. *Galp* has two refineries, one in Matosinhos and another in Sines. The development of this work focused on the latter – Sines refinery, the biggest and most complex portuguese refinery, with about 12.5 million ton of processed crude oil per year [1], and a variety of final products (gases, petrol, jet/kerosene, diesel fuels and other fuels). Sines refinery produces in average 3 Mm^3 per year of wastewater, which is discharged into Ribeira dos Moinhos wastewater treatment plant (RM WWTP). This WWTP is located near the refinery and accumulates the wastewaters of the adjacent industries and the domestic wastewaters from the nearby populations. Despite this diversity of sources, the Sines refinery wastewater still represents about 90% of the total income for the RM WWTP [2,3]. Figure 1.1 presents annual effluent management costs taxed to Sines refinery since 2014.

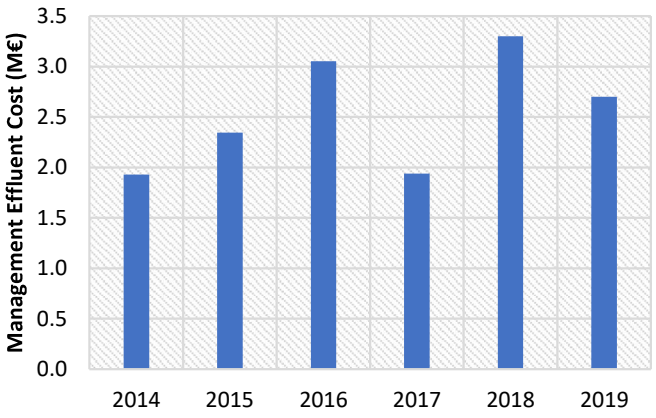

Figure 1.1 - Effluent management cost annually taxed to Sines refinery by RM WWTP.

Sines refinery is divided in three plants and the present work is dedicated to Plant I, regarding the kerosene Merox unit, as explained in more detail below.

At Sines refinery, effluents generated in the different processes of crude oil refining are collected in a retention basin, homogenized, pre-treated by dissolved air flotation and oxidized in an aerated basin, and sent to RM WWTP, which performs the remaining treatment, ensuring the legal discharge specifications (Figure 1.2).

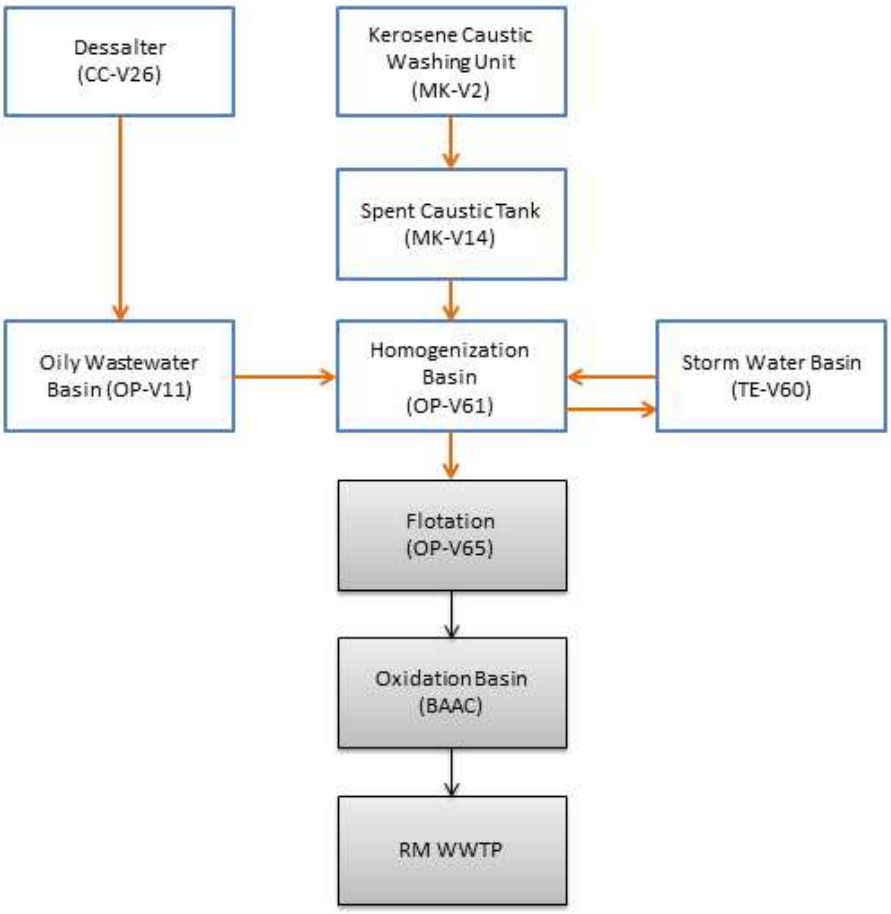

Figure 1.2 - Sines refinery wastewater circuit, with emphasis on the kerosene caustic washing unit.

After primary treatment, wastewater is discharged to RM WWTP, for final treatments before discharge into a water body. The discharge of the refinery wastewater to this external WWTP is subjected to rules defined in Águas de Santo André (2007) [4], which, among different considerations, establishes the charges to be applied based on the discharged wastewater volume and quality. The wastewater analytical composition is determined twice per week with composed samples collected with an automatic sampler located between the refinery and the treatment plant. The parameters analyzed are sulphides, phenolic compounds, chemical oxygen demand (COD), oil and grease (O&G), ammonia, total suspended solids (TSS) and pH. Based on the results of these parameters and the total volume discharged, the taxation is classified according to the matrix presented in Table 1.1.

Table 1.1 - Effluent classification according to quality [4].

Parameter	Unit	Class 1	Class 2	Class 3	Class 4	Class 5
Sulphides	**mg/L**	]l.q.;2]	]2;4]	]4;7]	]7;10]	]10;20]
Phenolic compounds	**mg/L**	]l.q.;5]	]5;10]	]10;15]	]15;20]	]20;40]
COD	**mgO_2/L**	]l.q.;150]	]150;300]	]300;600]	]600;1000]	]1000;2000]
O&G	**mg/L**	]l.q.;5]	]5;20]	]20;35]	]35;50]	]50;100]
Ammonia	**mg/L**	]l.q.;125]	n.a.	n.a.	n.a.	n.a.
pH	**Sorensen scale**	[6;9]	n.a.	n.a.	n.a.	[4.5;10]
TSS	**mg/L**	]l.q.;100]	]100;200]	]200;300]	]300;500]	]500;1000]

l.q. – quantification limit; n.a. – non-applicable

The wastewater classification is defined by the parameter that presents the highest class in the analyses of the composed sample, e.g. if all parameters have analytical values that define them as class 1, but phenolic compounds indicate a class 3, the effluent is defined as class 3 for charging.

If class 5 or class 1 (in case of ammonia) limits are exceeded, the discharge of the wastewater will be penalized and an extra factor of 15 % will be applied to the charges in the following 45 days. The extra factor is cumulative up to a maximum of 5 events, i.e. 75 % of extra charge. The charge of the effluent is proportional to the volume sent to RM WWTP.

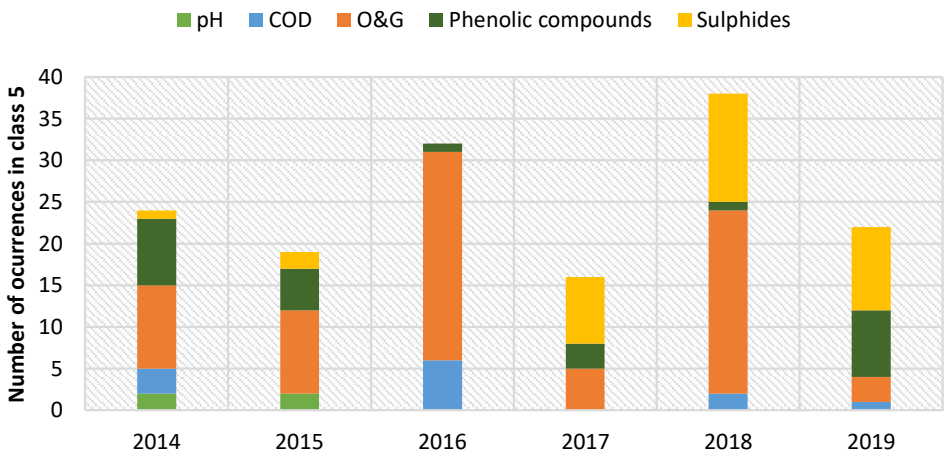

Figure 1.3 - Distribution of occurrences by contaminant in class 5.

Figure 1.3 shows that O&G is in general the main responsible parameter for class 5 taxations over the past 6 years at Sines refinery. The year of 2017 was an abnormal year in terms of precipitation, therefore the accumulation in Sines refinery basins was high, increasing the contamination levels for the following year discharges. Also, a shutdown for maintenance and cleaning occurred by the end of 2018 in Plant II (mainly responsible for sulphides and phenolic compounds' occurrences) that was noticeable in 2019 discharges. Another shutdown happened in the summer of 2019 in Plant I (mainly responsible for O&G occurrences), which major impact was noticed by the end of 2019 and the first half of 2020 (data not shown).

It is, however, considered that it is still possible to further upgrade the quality of the final wastewater. Since the most problematic contaminant in this effluent is O&G, emphasis will be, therefore, given to the minimization of this contaminant class.

1.2 Oil and Grease

O&G can be divided into two types: non-polar and polar. The first type comprises hydrocarbon compounds that are insoluble in water (linear and ramified chain hydrocarbons). The second type includes the dissolved organic compounds in wastewater (heterocyclic, aromatic and phenolic compounds as well as unsaturated substances and elements that have polar arrangements like naphthenic acids, which are important polar substances) [2,5].

The technologies used to treat O&G are selected based on the type of O&G (non-polar or polar). Non-polar O&G is usually treated with gravity separators: the oil ascends to the surface of the contaminated water and is then removed. Such gravity separators will not separate oil droplets smaller than the size of free oil nor will break down emulsions. Another alternative tecnhnology is the aerated lagoon: air is provided through the contaminated water and the oil emerges to the surface, where it is removed [6]. When a free oil water mixture is brought to a relatively quiescent state and given sufficient time, the oil droplets will coalesce and eventually separate from wastewater, forming a continuous floating oil layer which may be skimmed off; however, in most industries, there is not enough time to wait for coalescence. In some units, an electric field is applied in order to accelerate the coalescence. Other alternative is the addition of coagulants, for example, aluminium derivatives. Polar O&G removal is usually addressed with biological oxidation technologies such as aerated lagoons, trickeling filters, activated sludge treatments and eventually advanced oxidation treatments, where the main objective is to

biologically degrade the organic compounds or chemically convert them into non-toxic elements such as minerals and carbon dioxide (CO_2) [6].

Table 1.2 shows the contribution of the different refinery process streams for the O&G concentration in the global wastewater. This analysis is also extended to pH, given that this is one of the limiting factors for the proper functioning of the wastewater treatment technologies proposed in this work.

Table 1.2 - Qualitative characteristics of the effluents by fundamental refining processes. Adapted from [2].

Fundamental Process	Free Oil	Emulsified Oil	pH
Fuel-oil and products storage	XXX	XX	0
Fuel-oil desalination	X	XXX	X
Fuel-oil distillation	XX	XXX	X
Thermal cracking	X	- -	XX
Catalytic cracking	X	X	XXX
Catalytic hydrogenation	- -	- -	- -
Reforming	X	0	0
Polimerization	X	0	X
Alquilation	X	0	XX
Isomerization	- -	- -	- -
Solvent refining	- -	X	X
Extraction and fractionation	X	0	- -
Thermal hydrogenation	- -	0	XX

XXX – main contribution; XX – moderate contribution; X – small contribution; 0 – no problems; - - – no data

The research strategy followed in a previous work [7] consisted in identifying the sources of water contamination for O&G and ammonia (and developing possible source reduction and/or wastewater treatment solutions in order to mitigate or eliminate their impact). This was accomplished by developing a mass balance to the refinery wastewater circuit for prediction and identification of contamination sources of O&G, through a predictive model based on a Project to Latent Structures (PLS) approach. The PLS model identified spent caustic discharge as the main O&G contamination source in the kerosene caustic washing unit [7].

Santos *et al.* (2013) [7] went through an extensive experimental work that consisted in the collection of samples in several points for 24 months (Figure 1.4). The records before that period were also used for framing and contamination evolution comparison.

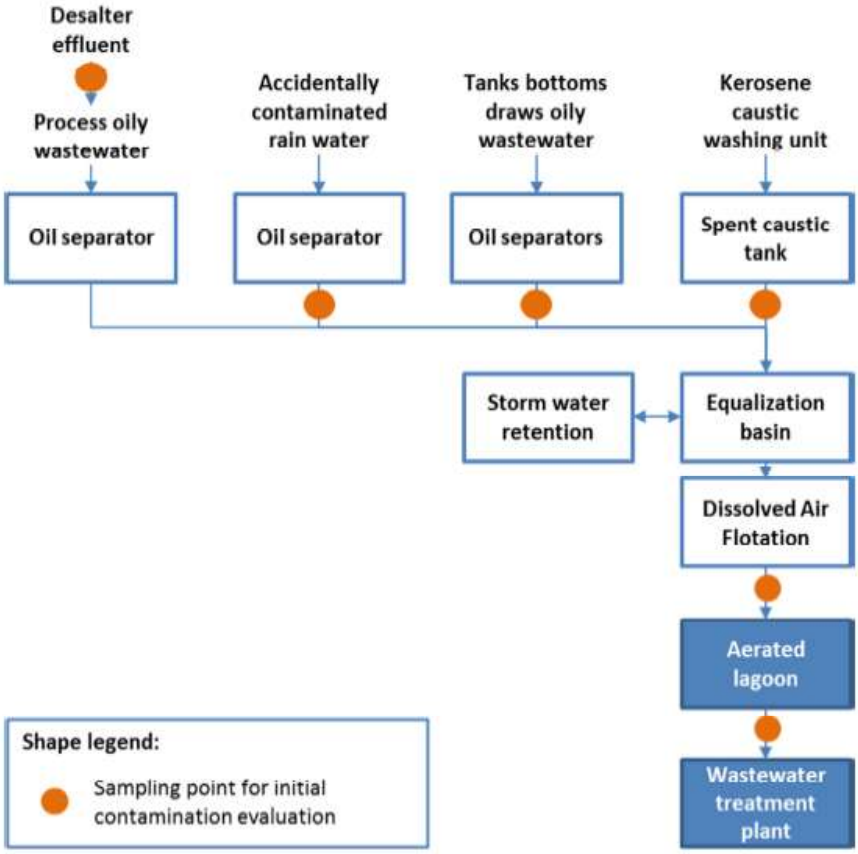

Figure 1.4 - Schematic representation of Sines refinery wastewater circuit and identification of sample collection points for O&G analysis.

To identify the emission source, the mass balance became necessary. The main results obtained by Santos *et al.* (2013) [7] are summarized in Figure 1.5, where the major contribution of spent caustic for the polar O&G contamination levels of the final effluent are shown.

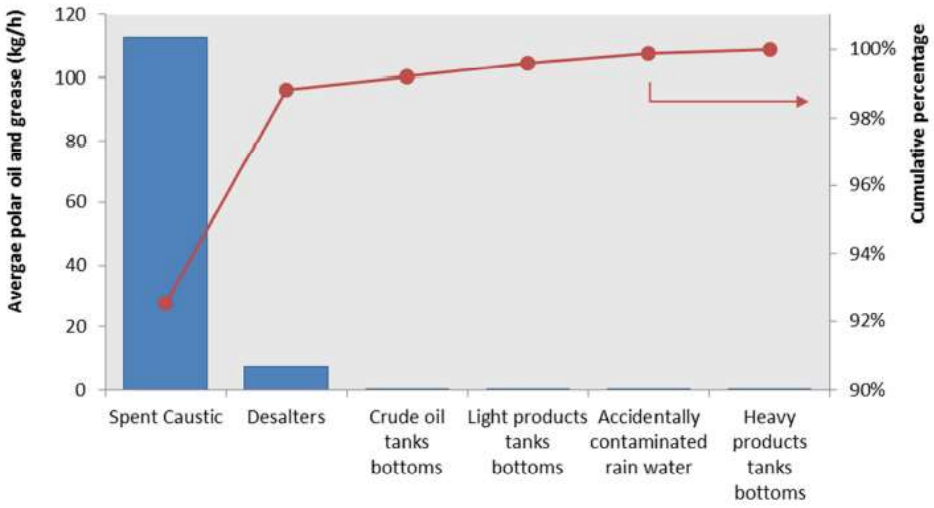

Figure 1.5 - Average polar O&G mass flow rate contribution of different emission points for O&G wastewater contamination at the discharge point for RM WWTP [6].

The high concentrations of O&G are mainly related to processing crude oils with higher concentrations of sulphur and acidic compounds, which are responsible for strong unpleasant odors, corrosion and effluent quality decrease. Sines refinery uses a process based on extraction and oxidation for the removal of these compounds, which is licensed by UOP, known as Merox unit. This process is used worldwide in refineries for mercaptan and acidic compounds removal from liquid petroleum gas (LPG), naphtha, gasoline or kerosene [8]. In the particular case of this work [7], the identified emission source of O&G contamination was the kerosene cut in the Merox unit (located in Plant I, the effluent is collected in tank MK-V2). The MK-V2 effluent consists of a spent caustic soda solution, and throughout this work, will be referred to as spent caustic.

Spent caustic is a challenging effluent in refineries worldwide due to its hazardous nature, especially the kerosene Merox spent caustic, which may account for more than 90% of the total contamination generated by refineries in terms of O&G [7]. Among refineries, the characteristics of spent caustics may vary greatly. Naphthenic spent caustic, in particular, forms during the kerosene Merox pre-washing step, being essentially a caustic solution rich in mercaptans, sulphides and other aromatic compounds with a natural pH between 12 and 14 [8].

Spent caustic may have different compositions according to the production process. It can be sulphidic (in ethylene plants or refining cracking units – lighter cuts), naphthenic (refining jet/kerosene units) – like the one used in Sines refinery – or cresylic (refining gasoline units). In general, sulphidic spent caustics present much lower COD than naphthenic/cresylic spent

caustics but contain much higher concentrations of sulphides [9]. Most literature on spent caustic remediation describes experimental works developed with sulphidic spent caustic, not addressing other types of spent caustic. The source of the crude oil, the refining processes employed and the emission regulations all influence the quality and quantity of spent caustic [10].

The UOP Merox process attempts to treat kerosene by a sweetening process. Before the reaction, there is a pre-washing step, where kerosene is submitted to a liquid-liquid extraction process with a fresh caustic soda solution, with an electric field application to help differentiate the two formed phases. The resulting aqueous solution is the so-called naphthenic spent caustic. This type of spent caustic cannot be recycled, contrary to the other types, which therefore makes such a wastewater with relevant impact in the refinery context [8].

Phenolic derivatives, monoaromatic and polycyclic aromatic compounds, cycloalkanes, ethers, ketones and some esters are often found in caustic refinery effluents. Several authors have proposed different characterization methods based on liquid-liquid microextraction to study such complex aqueous matrices and extract information that helps describing and identifying families of compounds [11–17]. Naphthenic spent caustic may contain as much as 30,000 ppm of polar O&G and presents very high COD (as much as 140,000 ppm) [18]. Moreover, it usually presents a very high concentration of naphthenic acids (2 – 15 wt. %) that promote foam formation, sulphides (< 0.1 wt. %) and NaOH (1 – 4 wt. %) [19]. Spent caustic has an average pH around 13 and is a highly odorous waste due to its composition, rich in mercaptans, sulphides and some volatile organics, which inhibit biological treatment [19,20].

Wastewater treatment has been attempted with various technologies and much different variations in each technology. The selection of one or other technology in a certain situation depends on the quality standards to be met and the most effective treatment with the lowest reasonable cost [21]. The treatment of an effluent with such a difficult pH range might be potentially problematic, in terms of safety and equipment corrosion. On the other hand, effluent treatment directly at the source enables valorisation within the process and might be considerably cheaper due to the reduction in volume. Due to these very harsh conditions of naphthenic spent caustic, the treatment of this effluent will be evaluated in this thesis using different technologies to eliminate/remove specific contaminants and avoid their discharge into Sines refinery wastewater basin. The technologies addressed in these thesis will be described in the following sections.

1.3 Pressure-driven Membrane Separation Processes

Membrane filtration has become an important technology to address water and wastewater treatment. As technology develops and more stringent regulations are to be met, membrane filtration started to demonstrate its potential to treat toxic and contaminated effluents. Membranes are now able to treat a variety of effluents (petroleum refinery effluents, dairy industry effluents, textile dye effluents, etc), since they have been gaining chemical stability and physical resistance for industrial applications [22].

The chemical nature of the membrane, the pore size and other characteristics determine its efficiency to retain certain solutes over others. Membrane separation processes can be classified according to the pore size (Figure 1.6).

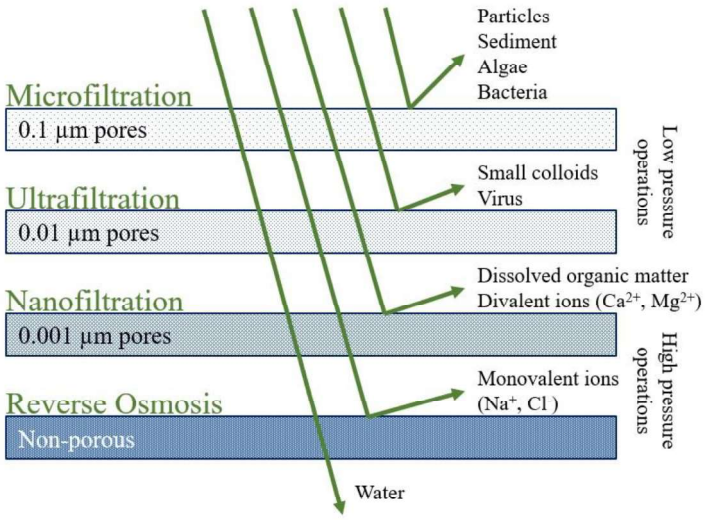

Figure 1.6 - Membrane separation process classification (adapted from [23]).

This classification can be made according to the membrane pore size (normally in nm or µm) or molecular weight cut-off (MWCO), which refers to the lowest molecular weight solute (in daltons) in which 90% of the solute is retained by the membrane, or the molecular weight of the molecule (e.g. globular protein) that is 90% retained by the membrane. Pressure is applied to increase the mass transfer of the selected components through the membrane.

1.3.1 Nanofiltration

Nanofiltration (NF, one of the membrane technologies shown in Figure 1.6) is very effective when treatment and separation/recovery of specific components is required since it is able to remove bacteria, low molecular weight organic molecules like hydrocarbons and phenolic compounds, and a certain level of divalent ions [24]. Since this thesis is focused on the treatment of effluents containing dissolved oils, NF may have the potential to deal with such effluents. However, wider acceptance of this process to treat oily wastewaters by industries is limited by membrane fouling [25], a critical factor in the treatment of this type of effluent. Fouling is caused by adsorption/deposition of components on membrane surface and intrapore structure, and results in flux decline, leading to frequent cleanings, membrane replacement and, ultimately, increased operating costs.

Cleaning processes for membranes can be either physical or chemical. Usually physical cleaning comprises backflushing, which is the mechanism of reversing the flow and mechanically remove foulants from the surface of the membrane (e.g. by crossflow). Chemical cleaning implies an interruption for scouring the membrane with mineral or organic acids, caustic soda or sodium hypochlorite (more usually in membrane bioreactors – MBRs) [26]. Ageing studies are a common way to test the lifespan and chemical resistance of membranes to certain conditions (oxidant agents, pH of the medium, salt concentration, etc). The potential for NF treatment with new membranes is constantly being tested with model wastewaters and cleaning solutions; these studies are a very important step before advancing to pilot testing to assess NF treatment performance [27–35]. It seems that NF treatment studies with real naphthenic spent caustic were only tested in [25], from where one might conclude that very few information is available concerning NF treatment of naphthenic spent caustic.

There are several properties that must be assessed before choosing a membrane, as they determine the retentive capacity of the solute, given the interactions between the solute and the membrane. These properties consist of the molecular weight cut-off (MWCO), porosity, hydrophobicity, pure water permeability (PWP), surface/pore charge and roughness [36].

Polymeric membranes are the most commonly used for NF treatment, however ceramic membranes have also started to be considered as their MWCO has been decreasing and these membrane are more resistant to high temperatures and chemicals. Not many studies exist for low MWCO ceramic membranes addressing membrane performance during ageing studies [37]

and/or membrane separation processes such as NF, specially for extreme pH effluents, like spent caustic.

As mentioned above, organic fouling seems to be a challenge for NF membranes, nevertheless studies [37] have found that ceramic membranes appear to be more resistant to fouling and possess high chemical resistance to cleaning, contrarily to polymeric membranes, therefore leading one to assume that maybe ceramic membranes could be more suitable to treat spent caustic rather than polymeric membranes. Studies with other matrices also show that, for example in the removal of polycyclic aromatic hydrocarbons (PAHs) from wastewaters, size exclusion may be the primary removal mechanism for ceramic membranes while, for example, hydrophobic interactions played a minor role [37], compared to polymeric membranes.

A Koch MPF-34 polymeric membrane and a TiO_2 ceramic membrane supported on Al_2O_3 were used to treat acid-mine waters (pH 1.0) with positive results (maximum concentration factor of 4.19 for the polymeric membrane and 3.29 for the ceramic membrane to achieve 80 % of permeate recovery, which was the maximum recovery tested), however the authors refer a need for lower MWCO ceramic membrane [38]. It seems that both ceramic and polymeric membranes may be chemically resistant to very low pH values, but no conclusion was made regarding very high pH values. Santos *et al.* (2016) [25] attempted to treat refinery spent caustic with a NF Koch MPF-34 spiral wound configuration polymeric membrane. In such study, very high rejections were obtained for key components of spent caustic effluents (99.9 % for O&G and 97.7 % for COD) at the optimal concentration factor of 3. On the other hand, this study did not include testing the membrane on the long term nor assess the main membrane structure changes with high pH exposure time, turning the reported results only valid for first time application (fresh membrane). Therefore, more studies are necessary to determine the membrane lifespan in order to evaluate its potential for industrial treatment.

1.4 Chemical Treatments

Advanced oxidation processes (AOPs) posess very high efficiency in removing recalcitrant organic compounds through chemical oxidation with a very strong oxidant agent, the hydroxyl radical ($HO^{\bullet}$) [39]. Neutralization is commonly applied before Fenton oxidation to control initial pH, as the later operates at very narrow pH ranges, typically from 2.5-4. Neutralization as a single

treatment is not usually interesting, as the resulting effluent might retain most of its compounds [9]. Apart from Fenton oxidation, an alternative would be liquid-liquid extraction since the addition of acid during neutralization leads to the formation of two phases. Again, liquid-liquid extraction as a single treatment does not attract much attention given that it produces another effluent [6]; however, because this second effluent can be reintroduced into the process, the interest of this combined process alternative greatly increases. These technologies will be briefly addressed in the following sections.

1.4.1 Neutralization

Neutralization is a common practice in wastewater treatment and waste stabilization. When dealing with an aggressive stream that causes, for example, corrosivity, neutralization is the primary treatment used. Other common use is to apply neutralization as a pre-treatment before a variety of biological, chemical, and physical treatment processes.

In chemical industrial wastewater treatment, neutralization of excess alkalinity or acidity is often required. One of the critical items in neutralizing the water is to determine the nature of the substances that cause acidity or alkalinity. Some processes like biological treatment require pH of the wastewater to be near neutral, while other processes like metal precipitation require pH to be alkaline [20]. Several chemical processes, where pH plays a significant role through neutralization, may be metal adsorption and biosorption, chemical precipitation, water softening, coagulation, water fluoridation, and water oxidation [40–43].

Neutralization can be carried out in either batch or continuous mode. In batch mode, the effluent is retained until its quality meets specifications before release. Several processes can be simultaneously carried out when the process is performed batchwise. Batch processes are good for small scale treatment plants or small waste volume. For large volumes, a continuous neutralization process is typically used. Neutralization tanks should be constructed with a corrosion-resistant material or should be lined to prevent corrosion [20]. Addition of an acid or an alkali should be controlled by continuous pH measurement, either by withdrawing samples periodically and measuring the pH or by installing an online pH meter that gives continuous pH readings. The commonly used acids for pH adjustment of alkaline wastewaters are sulfuric acid (H_2SO_4), hydrochloric acid (HCl), and nitric acid (HNO_3). Among them, sulfuric acid is the most widely used neutralizing agent [44].

Acid neutralization consists on a reconversion of the acid components, separating them into an oily phase, instead of degrading them [9,20]. Seyedin and Hassanzadeganroudsari [9] reported an efficient removal of COD (70%) by neutralization, depending on the operating conditions, and diminishing the concentration of organic contaminants in the aqueous phase [45]. Eq (1.1) to (1.5) describe the main steps involved in the neutralization of typical salts and/or other organic compounds (thus the R for a generic group) that are usually present in spent caustic effluents [20].

$$2NaOH + H_2SO_4 \rightarrow Na_2SO_4 + 2H_2O \quad (1.1)$$

$$2Na_2S + H_2SO_4 \rightarrow Na_2SO_4 + 2NaHS \quad (1.2)$$

$$2Na_2CO_3 + H_2SO_4 \rightarrow Na_2SO_4 + 2NaHCO_3 \quad (1.3)$$

$$2NaSR + H_2SO_4 \rightarrow Na_2SO_4 + 2RSH \quad (1.4)$$

$$2NaOR + H_2SO_4 \rightarrow Na_2SO_4 + 2ROH \quad (1.5)$$

However, because of volatile organic compounds (VOCs) and hydrogen sulfide (H_2S) release, neutralization cannot be considered as a single treatment [46,47], thus, its combination with other processes is required.

1.4.2 Advanced oxidation processes: Fenton oxidation

AOPs refer to several chemical oxidation methods whose common characteristics are the production of hydroxyl radicals, $HO^{\bullet}$, which $HO^{\bullet}$ is a highly reactive and non-selective species able to attack and degrade many persistent organic molecules. Usually, for petroleum refinery wastewater tratment, flotation/coagulation/filtration (primary treatment) are followed by the removal of dissolved components like polycyclic aromatic hydrocarbons (PAHs) and other hydrocarbons, heavy metals, etc. (secondary treatment), which may be accomplished by AOPs [20]. The successful implementation of AOPs depends on the pre-treatment, which should remove suspended solids, colloids, grease and other components that may interfere with the process [48].

Among numerous AOPs, the Fenton process is widely known for its use in the degradation of several organic pollutants (pharmaceuticals, pesticides, polyaromatics, phenols, etc.) [49]. Transition metal salts (iron salts, for example), ozone and UV-light can activate H_2O_2 to form hydroxyl radicals, which are strong oxidants [39]. The chemistry of the Fenton's reagent, which comprises a mixture of ferrous iron salt (catalyst) and H_2O_2 (oxidant) [39], involves in short the

following main reactions, where Eq (1.6) represents the hydroxyl radicals generation and Eq (1.7) the ferrous iron (catalyst) regeneration:

$$Fe^{2+} + H_2O_2 \rightarrow Fe^{3+} + OH^- + HO^\bullet \quad (1.6)$$

$$Fe^{3+} + H_2O_2 \rightarrow Fe^{2+} + H^+ + HO^\bullet{}_2 \quad (1.7)$$

In the Fenton process, equation Eq (1.7) is the limiting step given that its associated rate constant is very low, around 0.02-0.01 $M^{-1}s^{-1}$ [50]. With this, it becomes essential to increase the efficiency of the process through the increase of H_2O_2 and Fe^{2+} concentrations. However, such high concentrations may lead to the inhibition of the reaction due to the radical scavenging effects:

$$H_2O_2 + HO^\bullet \rightarrow HO^\bullet{}_2 + H_2 \quad (1.8)$$

$$Fe^{2+} + HO^\bullet \rightarrow Fe^{3+} + OH^- \quad (1.9)$$

Other important factor that affects Fenton's process efficiency is the pH. The optimal pH values range from 2.5 to 4 [51]. For higher pH values, Fe^{3+} form complexes with OH^-, leading to a precipitate, and inhibiting Fe^{2+} regeneration and the production of additional $HO^\bullet$ [39]. On the other hand, at very acidic conditions reaction between ferrous ion and hydrogen peroxide becomes too slow.

Temperature may have a positive effect on these processes since it increases the rate of radicals generation and organics degradation [49]. But, on the other hand, special attention must be paid to the H_2O_2 decomposition with an increase in temperature [49], leading to a common volcano-type plot when process efficiency is represented versus operating temperature. So, optimal temperatures have to be determined with care.

Alnaizy [19] reported high COD removal from refinery spent caustic effluent using the Fenton processes (approximately 95%) and reported that the treatment is less expensive than other classic treatments. A new study topic for Fenton processes are alkaline Fenton oxidation, in order to avoid the need for neutralization. However, low efficiency in COD removal (43%) and dissolved organic matter removal (86%) are reported compared to neutral and acid pH conditions [46,52]. Other types of AOPs, less investigated for refinery effluents [53–56], may demonstrate positive results, but their application is always limited or presents a drawback that favours Fenton oxidation; another possibility is to combine different treatment technologies. For example, the combination of hydrodynamic cavitation (HC) and Fenton process has

demonstrated high efficiency in the oxidation of hardly degradable organic contaminants, but phenol oxidation performance is still low compared with other higher molecular weight contaminants, denoting a bottleneck of this approach concerning smaller organic molecules [53,57]. AOPs based on persulphates have also demonstrated potential to oxidize several organic pollutants, both in terms of technology and investment. Persulphates (PS)- and peroxymonosulphates (PMS)-based AOPs are in science very similar to Fenton, but here the oxidation species is the sulphate radical, which exhibits also a high oxidation potential and extended lifetime. Authors argument [e.g. [39]] that the oxidation potential of hydroxyl radicals is higher than sulphate radicals, which could mean that although hydroxyl radicals need a lower pH medium to enhance activity, the expected degradation of COD and other organic contaminants would be higher. Other technologies such as photocatalytic AOPs have demonstrated to be successful in organic contaminants oxidation at basic pH conditions, however their application is more complex and implies additional separation steps to remove/recover the catalyst [54,55]. Another promising trend in research to oxidize organic contaminants of industrial effluents at basic pH conditions is hydrodynamic and acoustic cavitation processes coupled with AOPs (ozonation, H_2O_2 oxidation, peroxone, UV-C, and others). Studies demonstrate that COD removal is still low/moderate (in the range of 40-50 %) but the potential is high, due to smaller process costs and avoidance of dangerous reactions (for example neutralization); however, by-products formation is still a matter to be addressed for all AOPs [56,58].

1.4.3 Liquid-liquid Extraction

Solvent extraction (or liquid extraction) as a unit operation is widely practiced in the chemical and petrochemical industries for the separation of aromatics, manufacturing of lubricating oil, etc. Liquid-liquid extraction (LLE) is primarily used in wastewater treatment for the removal of phenols, cresols and other phenolic compounds. These wastewater streams arise principally in petroleum industries, coke-oven plants in the steel industry and in the plastics industry [6].

The oil industry uses fractional distillation (FD) or LLE, and the emphasis of the technique is on obtaining the optimal benefit for the crude oil in refining or recovery operations. However, the use of distillation or extraction as a decontamination treatment of wastewater still requires further research and data. In this respect, catalytic vacuum distillation has been shown to reduce

COD by 99% [59], in particular with the use of NaOH as a promoter. On the other hand, an extraction technique used to treat pond sludge removed 67.5% [60] and 40%–60% of COD using the solvents methyl ethyl ketone (MEK) and ethyl acetate (EA) [61]. Only more recently has the systematic use of liquid–liquid extraction as preliminary treatment for the decontamination of wastewater been studied. A study that assesses refinery wastewater treatment with dicholoromethane presented quite positive results such as 90.5 % COD decrease [62], with very appealing results concerning process time and energy consumptions.

Although LLE may lead to the generation of more effluent, its combination with oxidation technologies such as AOPs has previously shown to enable very high removals of organics such as aromatic compounds (around 99%) [63]. Sabri *et al.* [64] assessed the treatment of spent caustic combining LLE with ionic liquids and obtained an extremely high removal of COD (99.8%). LLE has also been considered an efficient extraction process for the removal of other organic contaminants such as phenols from spent caustic [65].

1.5 Objectives

In this PhD project, the objective is to address spent caustic treatment as a way to decrease the high organic load of spent caustic effluent and reduce its impact in the global effluent in terms of O&G contamination. The naphthenic spent caustic generated by *Galp* refinery in Sines will be used as case study. To reach this goal, spent caustic will be first characterized by different techniques (NMR, FT-IR and GC-MS) in order to identify the organic contaminants responsible for such high COD and O&G concentrations, as well as high pH. The economic impact of treating this effluent will be assessed, in Sines refinery context. The conclusions to be drawn are useful to define treatment strategies at the source, where the effluent is more concentrated but the flow is minimal, of 2 m^3/h. NF potential will be studied with a polymeric and a ceramic membrane, given their well known efectivensess to treat wastewaters with high organic load in an environmentally-friendly way. After membrane processes, chemical treatments will be applied in combined processes: neutralization prior to Fenton oxidation or prior to LLE, as such technologies are consistent and well kown in refinery processes (neutralization and LLE) and Fenton oxidation is a promising wastewater treatment technology focused on converting organic group structures into minerals and CO_2. The technologies discriminated above will be economically evaluated, and compared to the existing wastewater treatment, at Sines refinery.

1.6 Thesis Outline

Chapter 1 presents a brief state of the art on the thematics and technologies addressed in the thesis, as well as its scope, objectives, motivation and strategy followed throughout this PhD project.

Chapter 2 presents an overview of naphthenic spent caustic, why it causes contamination of the final wastewater in Sines refinery and what types of contaminants are responsible for it, through the application of NMR, FT-IR and GC-MS techniques to spent caustic and final wastewater. The conclusions draw from this chapter allowed to define treatment technologies, studied in the next chapters.

Chapter 3 assesses the potential for treatment of naphthenic spent caustic by nanofiltration using polymeric (Koch SelRO MPF-34 flatsheet 200 Da) and ceramic (Inopor TiO_2 tubular 200 Da) membranes. An ageing study is also presented for the polymeric membrane to evaluate its lifespan. Several characterization techniques were employed to address modifications in the membranes' structure and composition that could explain the differences in their permeability and retentive properties over time.

Chapter 4 describes all the testing performed to treat naphthenic spent caustic with chemical treatments, particularly the two approaches followed: i) neutralization followed by Fenton oxidation (tested at lab scale) and ii) neutralization followed by liquid-liquid extraction (tested at pilot scale). This section ends with a simple economic analysis for such approaches, comparing the expected annual savings with current Sines refinery situation.

Each chapter (2-4) includes a summary of the work developed, a short introduction, a description of the materials and methods used, a discussion of the results and the respective conclusions.

Chapter 5 summarizes the conclusions of each chapter and provides suggestions for future work.

2 Unraveling the relation between processed crude oils and the composition of spent caustic effluents as well as the respective economic impact*

* Submitted as: **Rita, A. I.**, Monteiro, A. L., Albuquerque, R. M., Santos, M., Ribeiro, J. C., Madeira, L. M., Sanches, S, *Unraveling the relation between processed crude oils and the composition of spent caustic effluents as well as the respective economic impact*

2.1 Abstract

Spent caustic discharges are responsible for increasing oil and grease (O&G) matter in refineries wastewater, leading to increasing treatment costs due to low water quality and environmental constraints associated with high O&G concentration discharges. As a way to settle and optimize treatment technologies for such complex effluents, more insight regarding the effluents impact and deeper characterization is necessary. The present study intends to assess the possibility of existing a relationship between the processed crude oils with the polar O&G concentration in naphthenic spent caustic as well as in the final wastewater; Sines refinery was considered as case-study. Also, in order to get insights about the nature of the polar O&G compounds, their structures and their prevalence in the effluent treatment system was carried out through detailed analytical characterization studies. Proton nuclear magnetic resonance (1H NMR), Fourier transform infrared spectroscopy (FT-IR) and gas chromatography-mass spectrometry (GC-MS) were chosen. It was found out that, for Sines refinery, spent caustic discharges may increase the refinery effluent management cost up to 3 €/ton of processed crude oil, everytime a high kerosene cut acid crude oil is processed. It was also found that the typical spent caustic O&G effluents are composed by organic contaminants with very low molecular weight (MW), with aromatic and polar arragements, like phenolic groups and naphthenic acids. This outcome is crucial for subsquently establishing the best technologies able to deal with such complex effluents.

Keywords

Refinery, Merox, Naphthenic spent caustic effluent, oil and grease, GC-MS, FT-IR, ^{1}H NMR

2.2 Introduction

Crude oil is a highly complex mixture that typically contains thousands of components. Within the large number of constituents of crude oil, there is an oxygen-containing species known as naphthenic acids. These species are in general responsible for corrosion processes in piping and the creation of emulsions difficult to treat [66]. Naphthenic acids are defined as carboxylic acids that include one or more saturated ring structures, with five- and six- membered rings being the most common. In addition to ring-containing acids, linear carboxylic acids are often included in the naphthenic acid class [67]. Depending on their structure and boiling point, these acid compounds may leave atmospheric distillation in a lower cut [20,66,68]. Alkaline liquid-liquid extraction seems to work very well in extracting these compounds from crude oil and respective distilled cuts leading to well established technologies such as the Desalting and the Merox process [69]. In the particular case of kerosene, the resulting aqueous phase is called naphthenic spent caustic, an aqueous solution rich in organic oxygenated compounds (derived from naphthenic acids) that may have sulphur and nitrogen in their structures and phenolic compounds [8]. Oily matter in naphthenic spent caustic is composed essentially by polar compounds. Spent caustic cannot be recirculated. Instead, it is mixed with other spent caustic solutions and finally discharged into the effluent treatment system, which causes environmental distress.

A property of crude oil that may help predict naphthenic acids presence is TAN. TAN is measured as the amount of potassium hydroxide, in milligrams, required to neutralize one gram of oil, indicating the total concentration of acid species present in crude oil. It is not specific to a particular acid but refers to all possible acidic components in the crude. A TAN > 0.5 mg KOH/g is conventionally considered to be high [66]. This property can also be applied to mid-distilled cuts, in a way to estimate acidic components present in kerosene, gasolines, etc.

Many studies have already attempted to characterize waters (from natural sources), effluents (from Wastewater Treatment Plants (WWTP) and industrial sources) and other products, such as crude oils [69,70,79,80,71–78]. In the particular case of refinery effluents, it is a complex challenge to determine the exact concentrations and classes of the different organic compounds with varying

structures and properties. Given this, various analytical techniques are used individually or in combination to provide adequate information on these substances or classes [81].

Sines Refinery wastewater tariffs are calculated by Ribeira dos Moinhos wastewater treatment plant (RM WWTP), based on two factors: flow rate and quality. Flow rate usually varies between 250 and 450 m^3/h. Quality depends on contaminants concentrations [4], in particular organic contaminants, chemical oxygen demand (COD) and pH. These parameters define wastewater class tariffs on a daily basis, which have different costs – the higher the class, the higher the cost that Sines refinery has to pay to RM WWTP for the treatment of the effluents. Sines refinery objective is to obtain a classification for the wastewaters that corresponds to class 3 (total O&G between 20 and 35 mg/L), but across the years the most predominant class seems to be class 5 (total O&G between 50 and 100 mg/L), with a particular impact due to polar O&G occurrences. The prevalence of higher concentrations of polar O&G in the final wastewater became more common around 2008, with the beginning of acid crudes processing, in a turnaround of crude oil market shares in which Sines refinery had to adapt.

The kerosene that is produced in the atmospheric distillation is pre-washed with fresh caustic soda (3º Bé) in a mixing valve to eliminate acid compounds and other derivatives. The mixture then flows to a sweetening process, where the mercaptans are converted to disulphides, and after this the treated petroleum is stored. The effluent that results from the pre-treatment step (before sweetening) is the naphthenic spent caustic soda solution that causes the polar O&G contamination in the effluent. The contaminants concentrations in this effluent greatly depend on the characteristics of the kerosene to be treated, which depends on the properties of the crudes that are being processed.

There are some differences to be observed between older characterization methods and more recent ones. Older methods are based on fractionation of organic matter through resin adsorption columns (as a physical process) and afterwards the different fractions were analysed with high-pressure size exclusion chromatography (HPSEC) [80], elemental analyses [77], liquid and gas chromatography coupled to mass spectrometry [70,74,76], UV absorbance, nuclear magnetic resonance (NMR), size exclusion chromatography (SEC), Fourier transform infrared spectroscopy (FT-IR) [72], among others. Recent characterization studies are based on more advanced techniques such as negative-ion electrospray ionization Fourier transform ion cyclotron mass spectrometry (ESI

FT-ICR MS), and simpler versions such as FT-IR and ESI [75,78,79]. The objective of the present study was to give an insight of the main organic group contributors to polar O&G and to estimate the average molecular weight (MW), as well as functional organic groups structures and arrangements, and their relative prevalence in the wastewater. Three classical quantitative methods were used in a complementing sequence: proton nuclear magnetic resonance (^{1}H NMR), FT-IR and gas chromatography – mass spectrometry (GC-MS).

High acid crudes have been acquired by Sines refinery. Processing acid crudes presents a challenge for refineries, given the numerous problems that come with it. A previous work [7] concluded that approximately 90% of polar oily matter in the final wastewater is due to naphthenic spent caustic discharges. It was found that the kerosene sweetening process is the main origin. It becomes necessary to understand the source of these polar compounds, how they affect naphthenic spent caustic and contaminate the final wastewater as well as the type of structures they have in order to develop adequate treatment processes that could avoid the environmental distress of direct discharge into the wastewater circuit. The scope of this work is to study the relation between the characteristics of the crudes that enter the process with the polar O&G content in the Merox pre-treatment effluent and in the final wastewater. Also in this study, experimental results of GC-MS, ^{1}H NMR, and FT-IR were used to determine the typical organic functional groups and other common structures of three naphthenic spent caustic samples of different crude-mix compositions. Also, two final wastewater samples were analysed by GC-MS so that conclusions can be taken about O&G contamination in the final wastewater and the main source of O&G contamination.

2.3 Experimental

2.3.1 Materials

2.3.1.1 Reagents

Hydrochoric acid (HCl, 37 %), was provided by Fluka, Honeywell (USA). Silica gel (grade 923) was provided by Grace Davidson (USA). Tetrachloroethylene was provided by PanReac AppliChem (USA).

Cotton filter papers, grade 40, with a diameter of 150 mm and a pore size 8 µm were provided by Whatman, GE (USA). This material was used as part of Standard Methods for the Examination of Water and Wastewater (SMEWW) 5520 C/F – analysis of oil and grease in wastewater.

2.3.2 Characterization procedures

2.3.2.1 Oil and Grease

The standard method followed to determine O&G contents on final wastewater and spent caustic samples was the SMEWW 5520 C/F [82].

2.3.2.2 Extraction Method

The analytical method (adapted from SMEWW5520 C/F) used to quantify oily matter is based on an acid extraction of the organic compounds, therefore major chemical transformations may occur in the original compounds of spent caustic. In order to overcome possible chemical transformations and study all existing compounds, characterization procedures were performed on original spent caustic samples (natural pH) and spent caustic with pH adjusted to 3.0 with HCl.

The extraction method was developed at Galp as a mean to quantify polar O&G specifically for the present work. It was adapted from SMEWW 5520 C/F [82]. This method has two variants: one applied to spent caustic and the other applied to the final wastewater. The main difference relies in the acidification step, where the acid concentration is much higher for spent caustics compared to the final wastewater.

The procedure starts by collecting 50 mL of spent caustic and lowering the pH to 2 or less with concentrated HCl. When the characterization was to be performed on an acidified (modified – pH) spent caustic, a 50 mL sample of the previously acidified solution was mixed with 50 mL of tetrachoroethylene (TCE) in a separating funnel. When the characterization was on an original (natural – pH) spent caustic, then a 50 mL sample of spent caustic was directly mixed with TCE in a separating funnel. Two phases were formed, from where the organic phase was extracted and then decanted into a flask with a funnel and filter paper with ~10 g of Na_2SO_4 to absorb any traces of water that could still be present in the extract. Finally, 15 mL of treated extract were kept in a glass vial to be later analysed. When preparing wastewater sample, the procedure was similar but instead of acidifying with concentrated HCl to pH equal or lower than 2, the acidification was executed with diluted HCl 1 N.

2.3.3 GC-MS

GC-MS analyses were performed on both acidified and natural – pH spent caustic samples, as well as to acidified and natural – pH final wastewater samples.

GC-MS was carried out using a HP 5975B quadropole mass selective detector (Agilent Technologies, USA). The mass spectral ionization temperature was set at 230 ^{o}C. The mass spectrometer was operated in the electron impact ionization mode at a voltage of 70 eV. It was turned on between 0 and 5.50 min, turned off between 5.50 and 7.00 min and turned on between 7.70 min until the rest of the analysis. Turning on and off the detector proved to be a necessary step due to the solvent used, to avoid the saturation of the detector, which may diminish the sensibility of the test. The solvent used in this analysis was the same as in the Extraction Method (section 2.2.1), TCE. Mass spectra were taken over the m/z range of 40-450. The flow rate of the helium carrier gas on the TG-5MS column (30 m x 0.5 mm I.D., 0.25 µm thickness, Thermo Scientific, USA) was 1 mL/min. The injection was performed in splitless mode with the injector temperature at 250 ºC. The column was held at 40 ^{o}C for 5 min, increased to 300 ^{o}C with a temperature rate of 10 ^{o}C/min, then held for 10 min at this level.

2.3.4 FT-IR

FT-IR analyses were performed on both acidified and natural – pH spent caustic samples.

The FT-IR analysis of spent caustic samples was performed using a PerkinElmer Spectrum Two portable infrared spectrometer. The spectral measurement range was 4000 - 450 cm^{-1}, with the resolution and scanning times of 4 cm^{-1} and 4, respectively. The acidified samples were not dried, they stayed in the form of an oil, so a drop of sample was placed between the round KBr cell windows, spreading the sample and making sure that no air bubbles were formed. On the contrary, the non-acidified samples were dried and then dissolved in TCE. A few drops of this solution were placed and spread on the cell. Then, the tablets were sent to the oven. Afterwards, the cell was closed, and the spectra was collected. FT-IR spectra were studied using the curve-fitting analysis in OMNIC Quantpad 8.2 software.

2.3.5 ^{1}H NMR

NMR analyses were performed on both acidified and natural – pH spent caustic samples.

NMR analysis for spent caustic samples were carried out in a Thermo picoSpin 80 spectrometer with cross polarization-magic angle spinning (CP/MAS). Both acidified and non-acidified spent caustic samples were concentrated by solvent evaporation, in a water bath under a N_2 stream. For non-acidified samples, it was necessary to perform several concentration stages to obtain a spectra with identifiable peaks and the obtained "concentrated" was sprinkled with deuterochloroform ($CDCl_3$) with 1 % of tetramethylsilane (TMS), to allow reference of each peak of the spectra. In the case of acidified samples, the evaporation is more difficult and the obtained product is viscous, requiring the dilution of the "concentrated" solutions with 30 % $CDCl_3$ with 1 % TMS, as a way to reference the obtained peaks and a to obtain a good baseline. Obtained spectra was the result of 128 scans, that were subsequently analysed using miniNova software (smoothing, chemical shift adjustment, baseline adjustment and phase correction). The resonance frequency of ^{1}H NMR was 80 MHz and the spectral width was 10 Hz; the delay time was 5 sec.

2.4 Results

2.4.1 Characterization of the effluents

Three naphthenic spent caustic samples were collected in March 2018 at Sines Refinery. These three spent caustic samples derive from the crude-mix present in Table 2.1, which also contains the respective kerosene cut TAN values and total O&G, as well as the characteristics of two final wastewater samples that were also collected in March 2018.

Table 2.1 - Compositions of three crude-mix processed at Sines Refinery in March 2018, their respective kerosene cuts content in oil and grease, their TAN and two samples of final wastewater.

Crude-mix					
Crude Oil	**Content (%)**	**Crude Oil**	**Content (%)**	**Crude Oil**	**Content (%)**
Ural	74	Azeri Light	64	Zafiro Blend	59
W.T.I.	11	Zafiro Blend	24	Ural	11
RAT	11	Saharan Blend	6	W.T.I.	15
Others	4	Others	6	RAT	10
				Others	5
Collected on 9th March 2018		**Collected on 17th March 2018**		**Collected on 22th March 2018**	
Spent Caustic					
Kerosene cut TAN (mgKOH/g)	0.09	**Kerosene cut TAN (mgKOH/g)**	0.27	**Kerosene cut TAN (mgKOH/g)**	0.16
Total O&G (mg/L)	5989	**Total O&G (mg/L)**	46118	**Total O&G (mg/L)**	40755
Polar O&G (mg/L)	5505	**Polar O&G (mg/L)**	33155	**Polar O&G (mg/L)**	30974
Final Wastewater					
		Collected on 14th March 2018		**Collected on 19th March 2018**	
Total O&G (mg/L)		55		81	
Polar O&G (mg/L)		12		37	

2.4.2 Acid Crudes, TAN and polar O&G

Naphthenic acids are a naturally occurring, complex mixture of cycloaliphatic carboxylic acids existing in petroleum. It derives from petroleum distillates, where the term *naphthenic acid* – as used in the petroleum industry – refers collectively to all of the carboxylic acids present in crude oil [66]. Acid crude oils are grades of crude oil that contain substantial amounts of naphthenic acids and other acids. They are also called high acid crudes after the most common measure of acidity: the *TAN*. Crude oils are distilled into several cuts, where the kerosene cut is composed essentially by 170 - 230 ºC boiling point compounds (variant range according to each refining process), being each cut extensively analysed in order to characterize the crude oil. In the present work, acid crudes are named after a TAN higher than 0.10 mgKOH/g in the kerosene cut.

Speight [66] and Dalmaschio et al. [81] refer to TAN analysis as a consistent naphthenic acid measurement, and both authors describe the TAN values obtained for the different cuts in a distillation column with a direct relation with the increasing boiling point. The naphthenic acid family has different compounds, with necessarily different boiling points. Usually, compounds with high molecular weight (MW) have higher boiling point. Table 2.2 enumerates all crudes processed in Sines refinery in 2016 with a TAN in the kerosene cut higher than 0.10 mg KOH/g. Following this, Figure 2.1 exhibits the TAN profile for each crude present on Table 2.1 after atmospheric distillation, in the respective heavier cuts.

Table 2.2 - Original crude TAN values for all acid crudes processed in 2016 in Sines Refinery.

Acid Crude Name (kerosene TAN > 0.10 mg KOH/g)	TAN value in original crude (mg KOH/g)
Azeri Light	0.39
CLOV	0.68
Marlim	1.40
Mondo	0.58
Pazflor	1.51
Roncador	0.17
Forties	0.09

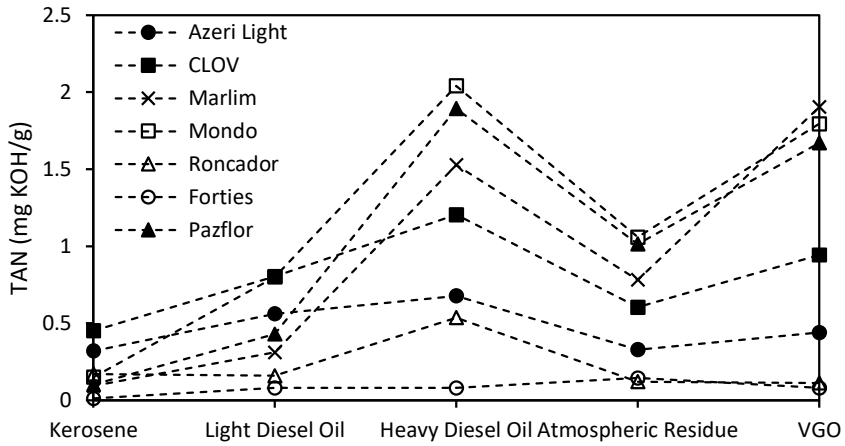

Figure 2.1 - TAN distribution for distillation heavier cuts of seven high crudes processed in Sines Refinery in 2016.

According to the distillation results for each crude enumerated in Table 2.2, the two higher kerosene cut TAN values correspond to crude oils Azeri Light and CLOV. However, on Table 2.2, they are not the more acidic crudes, which could mean that from all the seven crudes listed, these two crude oils acid compounds possibly present lower MW compounds with extremely thermal and chemical resistance, to endure desalting operation and thermal degradation [20,66,81,83]. Or, on the contrary, the acid compounds naturally present in these crude oils are very susceptible to thermal cracking, therefore originating heavier fractions of low MW acid compounds [66]. From these seven crudes, it has been known in Sines refinery that in 2016, only Azeri Light and CLOV presented such impact on polar O&G contamination of the final wastewater. Figure 2.2 illustrates this observation by showing the example of March 2016, where all effluent discharge tariffs are due to O&G concentrations above class 3. However, to better analyse Figure 2.2, it should be known that a delay of at least 48 h occurs between crude oil processing and effluent discharge; therefore, a tariff that occurred for example on the 7th day in the final wastewater will correspond to a crude-mix processed on the 5th day with a strong accumulation effect from the crude-mix processed in the 4th day.

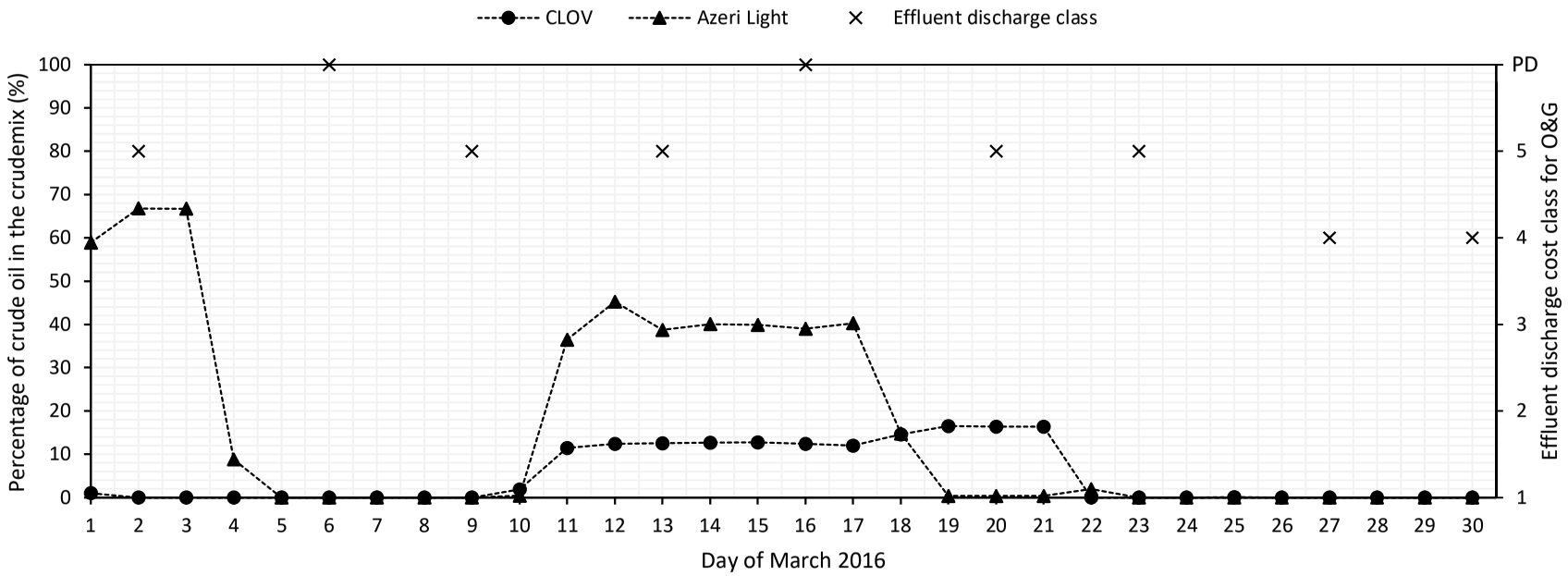

Figure 2.2 - Effluent discharge taxations in March 2016 versus crude oils CLOV and Azeri Light percentages in daily crude-mixes. PD – penalizing discharge.

Several samples of naphthenic spent caustic were analysed in 2016, together with the respective final wastewater produced in Sines refinery, for O&G contamination, and related with respective TAN values in the kerosene cuts, as illustrated in Figure 2.3.

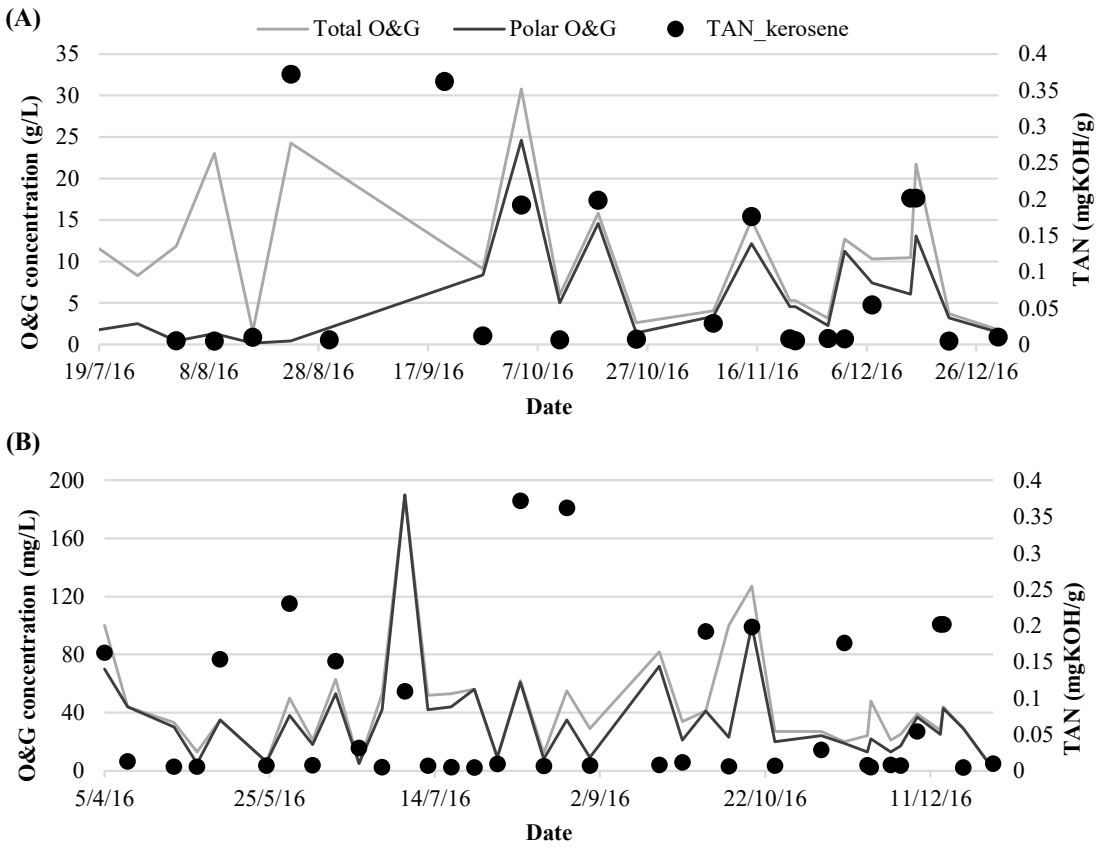

Figure 2.3 - O&G contamination in naphthenic spent caustic (A) and respective final wastewater (B) samples versus TAN value in respective kerosene cut.

From Figure 2.3, a relation between TAN in the kerosene cut and O&G contamination is observed, in accordance with previous studies [7]. Actually, it may be noticed that the higher the TAN in the kerosene cut, the higher is the O&G concentration in both the naphthenic spent caustic (Figure 2.3 A) and the refinery final wastewater (Figure 2.3 B). This observation led to modelling attempts of the entire wastewater circuits in order to estimate the class of the final wastewater before the refinery discharge. However, models may need update as soon as any variable changes. Nevertheless, due to the observation made previously, it would be interesting to characterize final wastewater and spent caustic samples to address the nature of the O&G compounds, to conclude

about their prevalence in the system and if they suffer any structural change. The Sines refinery wastewater circuit is extensive, but previous studies [7] concluded that naphthenic spent caustic is responsible for 90 % of polar O&G contamination in the final wastewater, although the naphthenic spent caustic flow consists only of 0.57 % of the final wastewater flow rate. Conclusions from characterization studies may help defining treatment strategies and provide more knowledge on refinery naphthenic acid compounds (that constitute part of polar O&G). This will be dealt with in section 2.4.4.

2.4.3 Economic impact per ton of acid crude oil

An attempt was made to calculate the real impact of acid crudes processing (Table 2.1) in the total effluent cost for the year of 2016. This study was very helpful in the crudes plan management, in a way to help choosing the optimal crude-mix considering minimum global costs. Access was granted to the daily production balance for all the crudes processed in the refinery in 2016 (in ton), and the chemicals used in the effluent treatment system for the year of 2016.

Assuming that the desired class for the effluent discharge would be according to Sines refinery annual objective (class 3), all the days with effluent discharge cost above class 3 and acid crudes processing (Azeri Light and/or CLOV), the difference in cost was calculated as described in Eq (2.1).

$$\Delta Effluent(€) = Real\ CostEffluent(€) - \text{Goal}\ CostEffluent(€) \quad (2.1)$$

The *Real Cost* parameter represents the sum of daily effluent costs for all the days with class above 3 (4, 5 and PD), when acid crudes Azeri Light and/or CLOV were processed. The *Goal Cost* parameter represents the sum of daily effluent costs for all the days that were considered in the first parameter but recalculated for class 3 (the objective class) and without any penalty. This means that the objective of the refinery would be processing acid crudes without impacting the effluent costs. The consumption of chemicals (H_2O_2, flocculant and coagulant) that are used in the effluent treatment system also varies, therefore alterations must be included, as described in Eq (2.2).

$$\Delta Chemicals(€) = Real\ CostChemicals(€) - \text{Goal}\ CostChemicals(€) \quad (2.2)$$

The *Real Cost* parameter reports the cost of chemicals for the days that had class above 3 and acid crudes processing, just like in Eq (2.1). The *Goal Cost* corresponds to the normal consumption of chemicals in the refinery (the average of all days without acid crudes, so it can also include punctual analyses with high classes but not derived from acid crudes). Both equations (Eq (2.1) and Eq (2.2)) present daily values (where class is above 3 and acid crudes are processed), and for these days the volume of Azeri Light and/or CLOV crude(s) were considered. In the days when both these acid crudes were processed, a weighted fraction of each was considered.

$$f_i = ton_i\ (ton/day)/ton\ acid\ crudes\ (ton/day) \quad (2.3)$$

$$Total\ Impact\ (€/day) = \Delta Effluent(€/day) + \Delta Chemicals(€/day) \quad (2.4)$$

$$Impact_i(€/day.ton) = Total\ Impact(€/day)/(\ f_i \times ton\ acid\ crudes(ton)) \quad (2.5)$$

In Eq (2.3), i = Azeri Light or CLOV, when only one of them is processed, f_i = 1. The *Impact* parameter is, evidently, a daily result. After that, the sum of all values is considered. With this, it is possible to obtain the economic impact of acid crudes processing per ton of Azeri Light or CLOV: $Impact_{Azeri\ Light}$ (€/ton$_{\text{Azeri Light}}$) and $Impact_{CLOV}$ (€/ton$_{\text{CLOV}}$).

However, it was very difficult to obtain accurate costs for the chemicals used in the effluent treatment system. The obtained costs may correspond to slightly higher values than the real costs. To compensate for this, the considered costs were estimated in 70% of the obtained costs, as presented in Figure 2.4.

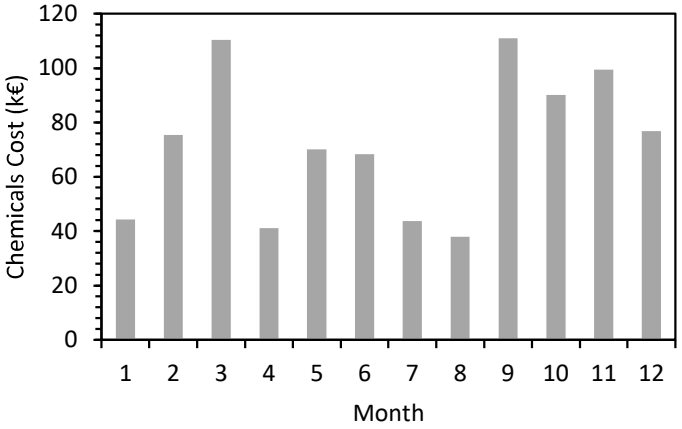

Figure 2.4 - Monthly costs that were considered for chemicals necessary to the effluent management cost in 2016.

Considering all the above, the impact of the acid crude oils Azeri Light and CLOV in the effluent treatment costs for the year of 2016 was estimated as an increase of 0.957 €/ton$_{\text{Azeri Light}}$ and 3.065 €/ton$_{\text{CLOV}}$, respectively. Considering that approximately 1478.5 kton of Azeri Light and 543.1 kton of CLOV were processed in 2016 by Sines refinery, the impact on the effluent management cost was extensive. Therefore, a more detailed attention must be paid to the increase on effluent management costs when acid crudes with a particularly high kerosene cut TAN are to be processed. In order to study the organic compounds that derive from this type of crude oil processing and that responsible for contaminating the wastewater circuit in Sines refinery, characterization studies will be performed in the next chapter to provide more knowledge on refinery naphthenic acid compounds (that constitute part of polar O&G).

2.4.4 Characterization of kerosene Merox spent caustic and final wastewater

2.4.4.1 ^{1}H NMR analysis

^{1}H NMR analyses were only applicable to spent caustic samples collected in 17th March and 22nd March 2018 (Table 2.1). Both original (natural pH) and acidified forms were analysed in order to understand the impact of acid addition to spent caustic, as explained previously. Results obtained are shown in Figure 2.5.

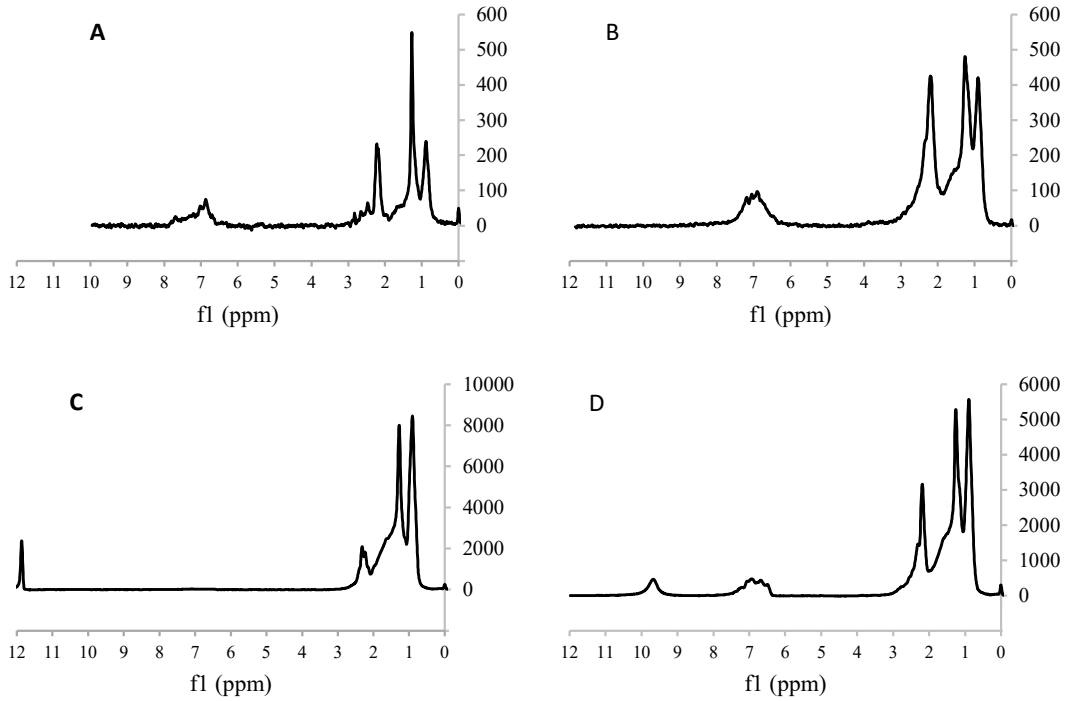

Figure 2.5 - ^{1}H NMR of spent caustic samples in original and acidified forms for 17th March (A; C) and 22nd March (B; D).

The first observation is the higher intensity of the peaks in the acidified forms in all spectra, in particular, for aliphatic hydrogens (-CH_2 and -CH_3) with a chemical shift between 0.8 and 1.2 ppm and H_α (from a methyl group attached to an aromatic ring) with a chemical shift between 2.0 and 2.5 ppm. It could mean that acidifying spent caustics may lead to an increase on CH_2 and CH_3 protons number, possibly related to the great pH variation of acidification of spent caustics. It may indicate that the medium influences the intensity of aliphatic protons peaks, as well as may cause a slight deviation in the chemical shift [84,85]. Another important group are the aromatic hydrogens, with a chemical shift between 6.5 and 7.5 ppm. Strangely, the second sample spectra does not develop an intensity band around these chemical shifts, however it is known that the aromatic hydrogens are a constituent of spent caustic [8]. Also, apart from peak intensity increasing, it looks as if acidification created a new peak around 12 ppm for the first spent caustic sample (Figure 2.5 C) and around 9.7 for the second sample (Figure 2.5 D). It appears that with acidification, the intensity

increase in the peak with 12 ppm of chemical shift in one sample and 9.7 ppm in another may be related with carboxylic acids formation (group RCOOH) through the protonation of the carboxylate ion group ($RCOO^-$), due to the acid medium [86]. It could be associated to the same compound formation, nonetheless the aromatic hydrogens in the second sample may cause a resonance that brings this new hydrogen for lower chemical shifts. Although the phenomenon may be similar, the compounds originating chemical shifts variations might derive from different nature structures. Specifically, the peak at 12 ppm (Figure 2.5 C) could be due to a carboxylic acid proton associated to naphthenic compounds, while the peak at 9.7 ppm (Figure 2.5 D) could be associated to a carboxylic acid proton from aromatic compounds [85].

2.4.4.2 FT-IR analysis

Figure 2.6 shows the FT-IR spectra for samples collected in the 17th March and 22nd March in both forms (original and acidified forms).

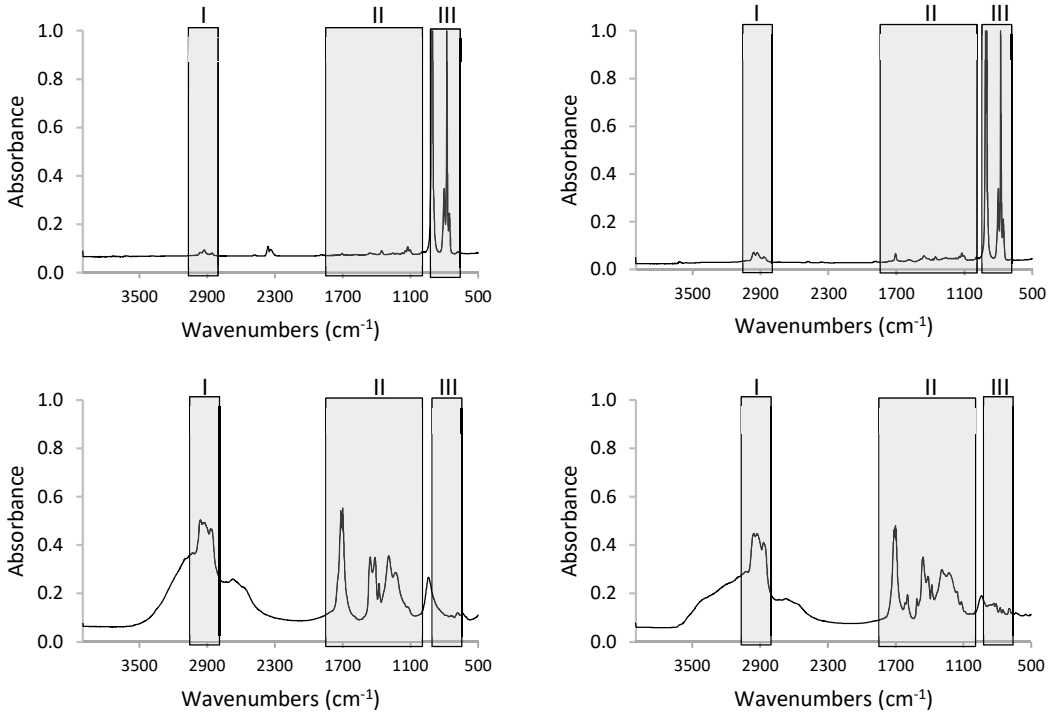

Figure 2.6 - FT-IR spectra of spent caustic samples collected in the 17th March 2018 in original form (A) and acidified form (C) and collected in the 22nd March 2018 in original form (B) and acidified form (D).

Both original and acidified FT-IR spectra appear to be simple, leading to a first hypothesis that the organic structures are low MW compounds. To simplify the analysis, three main regions were identified: 3000 – 2800 cm^{-1} (region I), 1800 – 1000 cm^{-1} (region II) and 900-700 cm^{-1} (region III). Region I contains the characteristics peaks of aliphatic hydrogens, whereas the peaks within region II are characteristic of oxygen-containing functional groups. Furthermore, region III corresponds to characteristic peaks of aromatic structure [87].

Region I

Symmetric and asymmetric C-H stretching occurs in this region, where multiform structural vibrations occur, like CH_2(ring), CH_2(chain), CH_3(end), CH_3(branch) and CH, typical of long chain hydrocarbon-derivative compounds [79]. It can be observed a very low intensity band in this region for original spent caustics (Figure 2.6 A; Figure 2.6 B), but much more intense in acidified forms (Figure 2.6 C; Figure 2.6 D). A broad band at 3380 cm^{-1} is most likely due to the hydroxyl group (OH) present in heteroatom-containing compounds, which are primarily naphthenic acids [69,88].

Region II

Similarly to region I, region II becomes more relevant in acidified forms (Figure 2.6 C; Figure 2.6 D). This region is associated with oxygen-containing functional groups, in more detail, structures C=O and C-O-R groups, being the first mainly associated to esters and carboxylic acids, whereas the second one being associated to phenols, alcohols and ethers [89]. In both samples of spent caustic, a clear increase of oxygen-containing groups occurs with acidification. At 1770 cm^{-1}, the peak may be associated with phenolic esters (RCOOAr). An intense band occurs in acidified forms at 1700 cm^{-1} is definitely related with carboxylic groups (O-C=O) [69,79,86–89]. Between 1700 cm^{-1} and 1650 cm^{-1} several peaks of lower intensity are possibly related with substituted amide (R-CO-NHR) groups [86,87]. The absorptions at 1600 cm^{-1} are due to vibrations of the valence electrons in carbon-carbon (C=C) bonds in the aromatic rings [86,87]. Between 1248 cm^{-1} to 1150 cm^{-1}, the peaks correspond to phenolic hydroxyl group [79]. Not so ever, not all peaks in this region are related with oxygen-containing groups, some of them also correspond to vibrations of the aromatic C=C, $-CH_3$ and $-CH_2-$

groups [69]. Considering only original spent caustic (Figure 2.6 A; Figure 2.6 B), none of the peaks in region II have relevant intensity to be considered.

Region III

This region is much more relevant for original spent caustics, corresponding exclusively to aromatic C-H out of plane deformation bands. These bands constitute a central part of organic structures present in original spent caustics, usually related to substituted and non-substituted aromatic rings, with methyl groups mostly in -meta positions (hence the two major intensity peaks in Figure 2.6 A and Figure 2.6 B) [89,90]. These peaks loose most of their intensity when spent caustic is in acidified form, and together with the contrary observation for region I, it might suggest that several aromatic hydrogens become substituted during acidification by other elements or most likely aliphatic chains (hence the increase of C-H aliphatic peaks).

2.4.4.3 GC-MS analysis

GC is a common and efficient separation technique for complex mixtures and MS is very important as spectroscopic identification technique, therefore it was chosen to identify samples of spent caustic and compare them with final wastewater samples.

Contrary to the previous techniques where only spent caustic was analyzed, here both spent caustic and final wastewater were analyzed in order to conclude more on which type of compounds detected in the final wastewater may derive from spent caustic discharge and cause an increase in polar O&G concentration.

The sample taken on the 17th of March was analyzed together with the respective final wastewater sample (19th of March).

Also, in order to study the effect of low TAN crudes in spent caustic naphthenic acids concentration, a spent caustic sample collected on the 9th of March was analyzed together with a final wastewater sample collected on the 14th of March. The delay between these two samples is higher than 48 h, however for low TAN crudes processing, the variation of polar O&G concentration is very low. Also, it was found that the corresponding spent caustic (from the 12th) derives from the

same production plan as the sample collected on the 9th (Figures A.1 to A.8 presents GC spectra obtained for the analyzed samples).

One method to display the similarities or differences between the mass spectroscopy (MS) signal patterns of the spent caustic and final wastewater samples is to construct certain types of plots such as the plots of double bond equivalents (DBE) versus carbon number. These plots have been useful tools to differentiate complex organic mixtures based on chemical composition [81,91,92]. The aromaticity of an organic compound may be deduced directly from its DBE value according to the following equation:

$$DBE = c - \frac{h}{2} + \frac{n}{2} + 1 \tag{2.6}$$

Where *c*, *h* and *n* are the numbers of carbon, hydrogen and nitrogen atoms, respectively, in the molecular formula [69]. Figure 2.7 exposes DBE calculations for each sample.

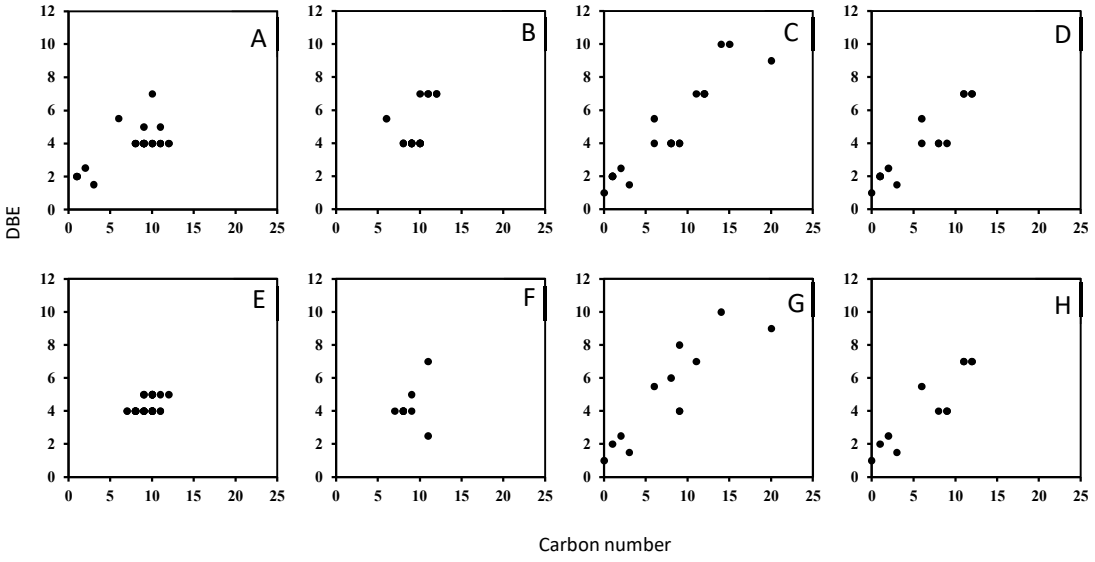

Figure 2.7 - Plot of DBE versus carbon number. Spent caustic collected on 9th March (A - original form; E – acidified form); Spent caustic collected on 17th March (B – original form; F – acidified form); Final wastewater collected on 14th March (C – original form; G – acidified form); Final wastewater collected on 19th March (C – original form; H – acidified form).

From Figure 2.7, it becomes noticeable that a different DBE distribution characterizes spent caustic samples and final wastewaters. Acidification slightly changes the DBE distribution into a

more condensed one, but only for spent caustic. Spent caustics natural pH is so high that chemical modifications occur that changes aromaticity of the compounds, compared with final wastewater [45,93–95]. The number of oxygens is also another metric to evaluate the increasing of functional groups in acidic medium compared with high pH medium. The increase of the average oxygen number according to GC determined structures with MS identification were 51 % between Figure 2.7 A and Figure 2.7 E, 100 % between Figure 2.7 B and Figure 2.7 F, 52 % between Figure 2.7 C and Figure 2.7 G and no increase was verified between Figure 2.7 D and Figure 2.7 H (in this last sample no oxygen containing compounds were identified, contrarily a lot of sulphur and other halogenated elements compounds were identified). The presence of these compounds in much higher concentration than oxygenated organic compounds is justified by the Desalter unit washing routine that is performed on a Friday and whose compounds are detected in the final wastewater by Monday morning in the daily sample collection – 19th March 2018 was a Monday.

All observed species have low MW [20]. Spent caustic original form identified structures present a maximum MW of 178 g/mol. Acidification may in general decrease carbon number due to cleavage reactions, and may increase MW due to the formation of functional groups like carboxylic acids, phenols, etc. [9,46]. Spent caustic acidified form identified structures present a maximum MW of 221 g/mol. This conclusion is different for the final wastewater, where there is absolutely no change in maximum MW of original and acidified forms. In final wastewater sample of 14th March, the highest identified MW compound is composed by a long aliphatic chain with some unsaturated connections and a carboxylic group in one end of that chain. This type of compound may occur at the usual final wastewater pH – around 7. On the other hand, it is not stable at very high pH values like original spent caustic – around 14, due to the functional group stability [96]. After acidification of final wastewater sample this functional group was not affected, maintaining structure at lower pH values. The other final wastewater sample (19th March) identified a cyclic octagon sulphur compound, that does not break under acidic conditions and is also very stable at neutral pH (such specific compound probably derives from desulphurization units wastewaters) [68].

Considering peak integration areas in GC spectra (Figures A.1 to A.8), it becomes possible to evaluate which compounds appear in higher concentrations and are, therefore, more common. Table 2.3 presents all structures that presented a relative percentage higher than 10 % in all samples and their retention time (RT).

Table 2.3 – Identified structures with a relative percentage > 10 % in spent caustic samples collected on 9th March and 17th March and final wastewater samples collected on 14th March and 19th March (original and acidified forms).

Spent caustic 9th March Original form RT: 4.59 min 14.79 %	Spent caustic 9th March Original form RT: 14.41 min 14.29 %	Spent caustic 17th March Original form RT: 10.76 min 15.85 %	Spent caustic 17th March Original form RT: 15.83 min 10.30 %
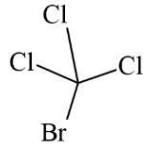	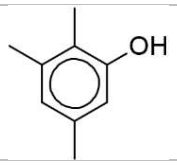	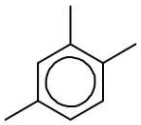	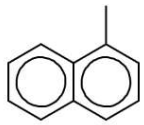
Spent caustic 9th March Acidified form RT: 13.51 min; 13.83 min 19.28 %; 13.19 %		Spent caustic 17th March Acidified form RT: 12.28 min 14.34 %	Spent caustic 17th March Acidified form RT: 13.83 min 11.34 %
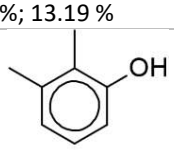		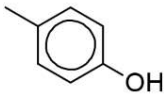	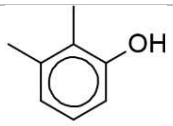
Final wastewater 14th March Original form RT: 4.59 min 54.10 %	Final wastewater 14th March Original form RT: 8.85 min 13.38 %	Final wastewater 19th March Original form RT: 4.59 min 41.42 %	
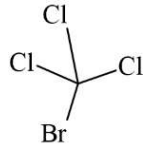	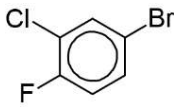	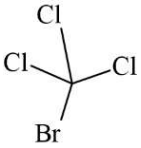	
Final wastewater 14th March Acidified form RT: 4.59 min 51.01 %	Final wastewater 14th March Acidified form RT: 8.84 min 11.89 %	Final wastewater 19th March Acidified form RT: 4.59 min 57.17 %	Final wastewater 19th March Acidified form RT: 8.84 min 13.11 %
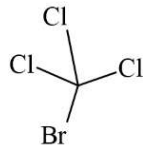	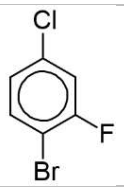	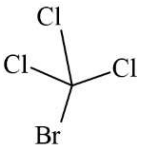	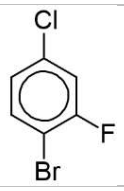

In general, it is possible to observe that spent caustics (original form) contain a lot of aromatic structures, where some of them might even contain functional groups (nonetheless with a very high pH). When it comes to low pH medium, functional groups become much more relevant, being the phenol the most common functional group in acidified spent caustic. An interesting observation is

that low acid crudes processing lead to a spent caustic that naturally has functional groups and halogenated elements detection signal in GC-MS, but contrarily, acid crudes processing lead to spent caustics that tend to have higher MW aromatic structures that in acidic medium will lead to naphthenic acids, carboxylic acids and phenol-derivative compounds [66,83]. These polar compounds will have an effect on polar O&G concentration, according to the SMEWW5520 detection method (liquid-liquid extraction with a non-polar solvent). Because the non-polar solvent interacts with the acidified sample, it will extract all organic family compounds. From all the extracted organic compounds, all that are retained by silica-gel are called polar O&G [97]. Final wastewater compositions are much more constant and suffer less modifications upon acidification, as explained previously. This is confirmed by GC-MS analyses of neutral and acidic pH final wastewater samples.

The aforementioned results show that technologies to treat spent caustic effluents must be suitable to remove low MW organic compounds (as low as 200 Da), usually of aromatic nature and with functional groups such as phenols and naphthenic acids. Also, due to the very high O&G concentrations of these effluents, extremely high organic loads are to be considered. Therefore, treatment technologies based on chemical degradation of organic contaminants such as advanced oxidation processes (AOPs) may be adequate options [21,45,98]. In the case of separation technologies, for example with pressure-driven membrane processes, selected membranes should have an adequate molecular weight cut-off (MWCO), considering the above molecular weights of the molecules to be removed. In this case, nanofiltration (NF) and reverse osmosis (RO) could be interesting options [25,99–101].

2.5 Conclusions

- Among all processed crudes in Sines refinery in 2016 with a TAN higher than 0.1 mg KOH/g, crude oils Azeri Light and CLOV seem to have a greater impact on the increase of polar O&G concentration in the final wastewater (leading to an increase in tariffs due to quality). There is a tendential relation between kerosene cut TAN values and polar O&G concentration in naphthenic spent caustic and final wastewater. Azeri Light and CLOV crude oils processing in Sines refinery lead to an effluent management cost increase of approximately 0.957 €/$ton_{Azeri\ Light}$ and 3.065 €/ton_{CLOV}, respectively.
- Proton NMR, FT-IR and GC-MS analyses suggest functional groups formation upon acidification. Aromatic structures account for a significant part of organic structures that constitute naphthenic spent caustic and that are present in the final wastewater. Naphthenic acids were detected only after acidification due to the carboxylic acid group only being formed in acidic medium. However, the aliphatic part of this structure was detected in the high intensity peaks for -CH_2 and -CH_3 groups in the ^1H NMR spectra, region I of FT-IR and GC-MS (retention time between 10 and 15 min). The maximum identified MW in GC-MS is 221 g/mol in acidified spent caustic, however structures in original spent caustic could be higher due to the acidification reaction. Nevertheless, very low MW is confirmed in polar O&G compounds with pH-sensible organic functional groups. These observations should be considered when choosing treatment technologies that deal with specific compound structures elimination (separation processes, chemical oxidation, etc).
- In view of defining treatment technologies for spent caustic effluents, their main characteristics were studied, being concluded the prevalence of low MW organic compounds, with functional group arrangements such as phenols and naphthenic acids. Even so, the very high organic load and extreme pH of these effluents turns their treatment into a great challenge. Several technologies are proposed for future work, for example AOPs and NF or RO, or a combination of both.

3 Assessment of the potential of nanofiltration polymeric and ceramic membranes to treat refinery spent caustic effluents[†]

[†] To be submitted as**: Rita, A. I.**, Nabais, A. R., Neves, L., Huertas, R., Crespo, J., Santos, M., Madeira, L. M., Sanches, S, *Assessment of the potential of nanofiltration polymeric and ceramic membranes to treat refinery spent caustic effluents*

3.1 Abstract

Spent caustic effluents are very challenging due to their very hazardous nature in terms of toxicity as well as their extreme pH (approximately 12-13). Spent caustic has presented a challenge for wastewater treatment in refineries, due to its composition rich in mercaptans, sulphides and other aromatic compounds, as can be perceived by Chapter 2 in the present thesis. To address such problematic, membrane filtration was studied.

The present study attempts to assess the potential for spent caustic treatment with nanofiltration (NF) polymeric and ceramic membranes, assessing membrane life expectancy. For that, membrane ageing studies in static mode were performed with the polymeric membrane before attempting NF treatment (dynamic studies). A ceramic membrane was also tested for the first time with this type of effluents, only in dynamic mode.

Although the polymeric membrane performance was very good and in accordance with previous studies, its lifespan was very reduced after 6 weeks of contact with spent caustic, greatly compromising its use in an industrial unit. Contrarily to expectations, the ceramic membrane tested was not chemically more resistant than the polymeric one upon direct contact with spent caustic. It was found that the tested ceramic membrane started to lose its retention capacity in less than 1 hour.

Keywords

Naphthenic spent caustic effluent, Nanofiltration, Ageing, Ceramic vs polymeric membranes

3.2 Introduction

Worldwide, attempts have been made to treat complex wastewaters and assess recalcitrant organic compounds separation by membrane filtration. Wastewaters compositions may vary completely, some of them being toxic to human beings and the environment. Most of these wastewaters are produced by heavy chemical industries, such as metallurgic, refineries, paper industry, etc.

In the specific case of refinery wastewaters, the treatment of spent caustic is presently a challenge due to its composition rich in mercaptans, sulphides, aromatic structures with ketones and alcohols, etc. [45]. The mercaptans that are extracted to the caustic solution in the kerosene pre-washing step, along with naphthenic acids and other organosulphur species, constitute naphthenic spent caustic [11–17]. Due to the very high pH of spent caustic, around 13, this wastewater becomes extremely difficult to handle [19,20].

Easy scale-up, low temperature operation and space-efficiency of plants are among some of the advantages of the use of membranes for fluids filtration. However, fouling of the membrane or even complete destruction of its structure are common problems that make membrane selection critical [27]. Ageing studies have been performed to understand membrane degradation and loss of performance with time when exposed to a certain agent under study [27,28,104,29–34,102,103]. Such studies usually assess membrane resistance to cleaning procedures such as oxidant agents as hypochlorite or alkaline agents as NaOH. Most of the ageing studies assess the impact of cleaning agents on membranes to evaluate the membrane integrity over time due to cleanings carried out during short periods of time with a certain frequency. In this context, several characterization techniques are usually applied to address membrane modifications (active layer, cross-section and support layer), such as scanning electron spectroscopy (SEM), energy dispersive spectroscopy (EDS) and Fourier transform infrared spectroscopy (FT-IR) [35].

Nanofiltration (NF) has been applied to treat complex wastewaters with recalcitrant compounds [25,93,105,106]. Several membrane filtration processes have been studied to treat refinery effluents, although usually the studied effluents present milder pH values and organic compounds concentration compared to spent caustic, for example Salahi *et al.* (2010) [99], Abadi *et al.* (2011) [100], Ishak *et al.* (2012) [107], Shariati *et al.* (2011) [108], Zhong *et al.* (2003) [101] and

Zhu *et al.* (2014) [109] only refer to oily wastewaters, which usually mean end-chain wastewater with free and/or emulsified oil particles.

Polymeric membranes are the most common membranes used for NF treatment, however ceramic membranes have also started to be considered as their molecular weight cut-off (MWCO) has been decreasing. A study on chemical cleaning of an Inopor ceramic membrane, similar to the tested membrane on the present study, showed that the alkaline agent NaOH seems to compromise significantly membrane performance [110]. Not many studies exist for low MWCO ceramic membranes addressing membrane performance during ageing studies [111] and/or membrane separation processes such as NF, specially for extreme pH effluents, like spent caustic.

Studies with other matrixes show that, for example in the removal of polycyclic aromatic hydrocarbons (PAHs) from wastewaters, size exclusion may be the primary removal mechanism for ceramic membranes while, for example, hydrophobic interactions played a minor role [37]. Zhao *et al.* [37] studied the impact of organic fouling on ceramic and polymeric membranes, concluding that ceramic membranes present a higher resistance to fouling and could get its permeability restored after chemical cleaning cycles. Given the possible propensity for fouling formation in complexes matrixes with a higher concentration of organics, it seems that ceramic membranes could enable an effective separation. A Koch MPF-34 polymeric membrane and a TiO_2 ceramic membrane supported on Al_2O_3 were used to treat acid-mine waters (pH 1.0) with positive results (maximum concentration factor of 4.19 for the polymeric membrane and 3.29 for the ceramic membrane to achieve 80 % of permeate recovery, which was the maximum recovery tested), however the authors refer a need for lower MWCO ceramic membrane [38]. From the work of López *et al.* (2020) [38], it seems that both ceramic and polymeric membranes tested may be chemically resistant to very low pH values, but no conclusion is made regarding very high pH values. A study performed by Dalwani *et al.* [112] addressed NF performance with a modified polyethersulphone (PES) composite membrane in acidic and alkaline media, observing a stable membrane performance even after prolonged exposure (up to several weeks). The authors reported that especially at strong alkaline conditions, the membrane appeared to have wider pores where they describe the phenomenon as membrane matrix swelling caused by different interactions between the ions in the solution and the resulting membrane charge density at different pH. Santos *et al.* [25] attempted to treat refinery spent caustic with a NF Koch MPF-34 spiral wound configuration polymeric membrane. In such study, very high rejections were obtained for key components of spent caustic effluents (99.9 % for oil and grease and 97.7 %

for chemical oxygen demand (COD)) at the optimal concentration factor of 3. On the other hand, this study did not include testing the membrane on the long term (i.e., assessing retention and permeability profiles with time) and main structure modifications due to high pH exposure time, turning these results only valid for first time application (fresh membrane). Therefore, more studies are necessary about the lifespan of this (and other) membranes and provide feedback for a potential industrial treatment.

The present study attempts to assess the potential for spent caustic treatment with NF polymeric and ceramic membranes. For that, membrane ageing studies in static mode were performed with the polymeric membrane before testing its performance for spent caustic treatment (under dynamic conditions) and results were compared with the work performed by Santos *et al.* (2016) [25], in which the same membrane was used to treat refinery spent caustic. A ceramic membrane was also tested, only in dynamic conditions. To the best of the authors knowledge, previous studies did not evaluate membrane ageing in filtration mode throughout long term operations, also with the particularity of such an aggressive effluent.

3.3 Experimental section

3.3.1 Reagents

H_2SO_4, 95–97 %, was provided by Fluka, Honeywell (USA), NaOH pellets were supplied by PanReac - reagent grade, silica gel (grade 923) was provided by Grace Davidson (USA), tetrachloroethylene was provided by PanReac AppliChem (USA), and $NaHSO_3$ was provided by AnalaR NORMAPUR, VWR (USA).

Cotton filter papers, grade 40, with a diameter of 150 mm and a pore size 8 µm were provided by Whatman, GE (USA). This material was used as part of SMEWW5520 C/F – analysis of oil and grease in wastewater (cf. section 3.3.6.1).

3.3.2 Membranes

Both polymeric and ceramic nanofiltration membranes were assessed in terms of their potential towards naphthenic spent caustic effluents. The commercial proprietary composite polymeric Koch membrane, type flat-sheet (18'x18') SelRO MPF-34 with a MWCO of 200 Da, was

selected based on its stability under acid/base conditions as well as promising results previously obtained [25]. A commercial ceramic NF membrane from Inopor (Germany) with active and support layers composed by titania (TiO_2) and alumina (Al_2O_3), respectively, was also studied. This is a single-channel tubular membrane with a MWCO of 200 Da and a filtration area of 0.011 m^2.

3.3.3 Experimental setup

The assessment of NF membranes potential to treat spent caustic effluents was conducted in a bench scale unit illustrated in Figure 3.1.

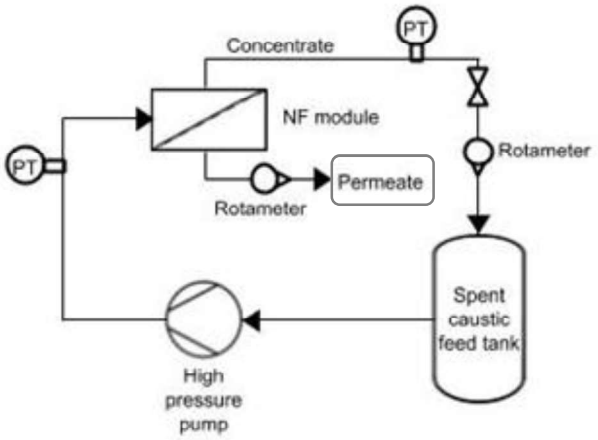

Figure 3.1 - Schematic representation of the experimental setup.

The bench unit consisted of two vessels for the feed and the permeate, a Ifimoto Iberica centrifugal high pressure pump (Figure 3.2) and a manual valve, through which the pressure inside the system could be adjusted. Transmembrane pressure (TMP) was measured with two pressure transducers Aplisens model WW-45 placed before and after the NF module. A pre-treatment of the effluent was ensured with a 80 µm pre-filter, which can retain solid particles that could promote membrane fouling.

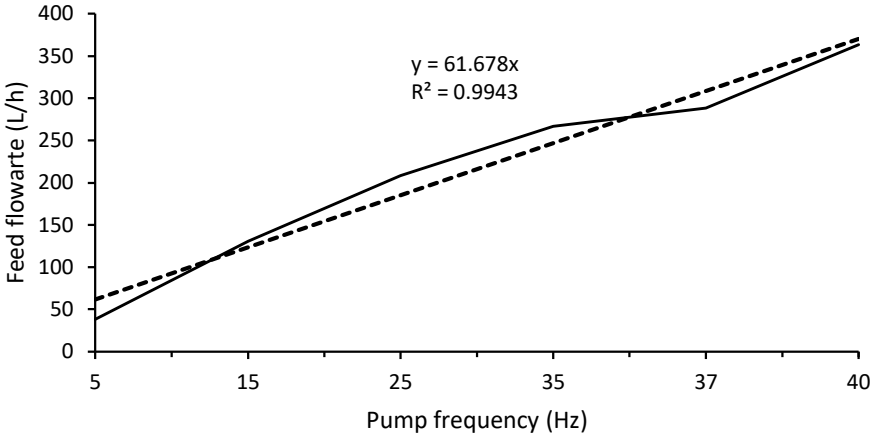

Figure 3.2 - Pump frequency to determine feed flowrate, no applied pressure.

The bench scale unit in this setup is very versatile, as it allows to try different types of membrane configurations and even MWCO ranges. The bench scale in Figure 3.1 may include a crossflow module with the polymeric flat sheet membrane or a tubular module with the ceramic tubular membrane. For the crossflow module, a stainless steel crossflow cell was used with a 15 cm^2 flat-sheet SelRO MPF-34 membrane (Koch, Spain) that was placed between two rectangular cross-section channels (feed and permeate) measuring 150 mm x 10 mm x 1 mm (length x wide x height) each. In the case of the tubular configuration, a stainless steel tubular single-channel housing of 500 mm x 10 mm (length x internal diameter) was used with a 110 cm^2 tubular single-channel ceramic membrane, a TiO_2 with 200 Da (Inopor, Germany).

3.3.4 Ageing experiments

Membrane ageing is typically employed to address membrane degradation, where alterations can be evaluated in both the active layer and the support. Ageing experiments were executed first in static conditions for 12 weeks in duplicate and secondly in dynamic conditions for 6 and 12 weeks (static ageing prior to NF test).

The ageing experiments in static conditions allowed to study dimensions, mass and contact angle and were performed in duplicate with 4 cm^2 pieces (2x2 cm each piece). The 4 cm^2 pieces were individually soaked in the ageing solution (spent caustic effluent no. 1 (Table 3.1)) inside glass

flasks and were kept in the dark and under static conditions for 12 weeks. Dimensions and mass measurements were taken each two weeks, while the contact angle measurements were performed by the end of the 12 weeks immersion. The contact angles of the polymeric membranes were measured to evaluate their hydro-philic/-phobic nature over the soaking time while the dimensions and mass were taken in order to evaluate a possible loss of volume and/or mass (cf. section 3.3.7.1). In order to compare with the pristine membrane, another 4 cm^2 piece was rinsed with distilled (DI) water before analyses.

The ageing experiments in dynamic conditions were performed with two pieces of polymeric membranes with 15 cm^2 that were cut to enable a perfect fitting in the filtration unit for subsequent filtration tests. These membranes were rinsed with DI water to remove all preservatives and then characterized as described in section 3.3.7. After that, the pieces were individually soaked in the ageing solution (spent caustic effluent no. 1 (Table 3.1)) inside glass flasks and were kept in the dark and under static conditions during 6 or 12 weeks. After these periods, the aged membranes were taken, rinsed with DI water and placed in a $NaHSO_3$ solution (5 g/L) for preservation until nanofiltration testes were carried out. Then, the aged membranes and the pristine membrane (used as control, rinsed with DI water before NF test), were submitted to NF tests (described in section 3.3.5), after which were characterized by means of scanning electron microscopy – energy dispersive X-ray spectroscopy (SEM-EDS) and Fourier-transform infrared (FT-IR) spectroscopy, in order to conclude about possible structure modifications caused by changes in the retention capacity and permeability over time, as a mean to simulate long-term industrial treatment processes.

The ceramic membrane was not subjected to ageing tests since modifications on its structure were not expected to occur due to its resistance under extreme pH conditions.

3.3.5 Nanofiltration experiments

The hydraulic permeability for both polymeric and ceramic membranes was determined prior to any experiment. Polymeric membranes were cut in rectangles of 15 cm^2 of filtration area and placed in the crossflow module. The ceramic membrane was directly placed in the Inopor housing. Water permeability was determined by filtering DI water at 10.0 bar, 8.0 bar and 6.0 bar for 2 h (also ensuring compaction of the polymeric membrane for NF tests). Permeate weight was measured

over time using a 250 mL beaker. Temperature throughout the test was monitored with a thermometer (VWR). Temperature and TMP were measured every 15 min during water permeability tests. Permeability, L_P, was calculated as shown in Eq (3.1), where V_P stands for permeate volume, *t* stands for the duration of a permeate sample collection, *A* stands for filtration area and ΔP stands for average working pressure of the NF module. No correction was included for temperature.

$$L_P = \frac{V_P}{t \times A \times \Delta P} \tag{3.1}$$

After hydraulic permeabilities have been determined, the membrane performance was assessed through NF tests. Nanofiltration experiments with polymeric membranes were performed with effluent no. 1 (Table 3.1) and conducted at 10 bar with a cross-flow velocity of 1.22 m/s (equivalent to 2.82 L/min), representing a Re of 2485 (very low flux, almost laminar). Nanofiltration experiments with ceramic membranes were performed with effluent no. 2 (Table 3.1) and conducted at 10 bar with a cross-flow velocity of 1.93 m/s (equivalent to 4.45 L/min), representing a Re of 15134 (which is turbulent).

A pre-treatment was necessary in order to remove particulates and oily droplets that could cause fouling on the membrane. However, the pre-treatment was performed separately from NF tests, where the NF module in the experimental setup (Figure 3.1) was replaced by the pre-filter. A total volume of 100 L of naphthenic spent caustic was pre-filtered before executing NF tests. NF tests were carried out in concentration mode, meaning that the permeate was collected in a different flask and the retentate was recirculated to the feed flask. The NF test was predicted to run until no more permeate would be obtained (it would mean that the system reached saturation and the feed was concentrated to the maximum possible at the tested pressure). Because the flux was so low during NF tests, it was not possible to perform flux intermediate measurements during each test. As so, each test lasted until enough permeate volume was collected to perform all the physico-chemical analyses (around 7 h for pristine polymeric membrane tests, and approximately 1.3 h for each aged membrane). After the conclusion of the NF test, a sequence of basic and acid washings was applied. The NF unit was rinsed first with tap water to remove the working solution, and then

the unit was rinsed with DI water. After that, the basic cleaning focused on feeding the system with a sodium hydroxide solution (5 g/L) recirculated for 15 min. After rinsing the system with DI water, an acid cleaning with a citric acid solution (5 g/L) was carried out for 15 min, followed by a final rinsing with DI water. Hydraulic permeabilities were taken in each step. By the end of the cleaning procedure, the unit was fed with a solution of sodium bissulfite (5 g/L) to preserve the membrane for future use.

In the case of the pristine polymeric membrane, two more NF tests were attempted to test the robustness of the membrane, modifying the pH of the spent caustic stream feeding the NF unit. Spent caustic (effluent no. 1 in Table 3.1) pH was lowered to 10.0 and to 3.0 with H_2SO_4. In the case of pH 3.0, two phases were formed, the phase of interest being the polar one, so only this phase was collected to treat by NF. In the case of ceramic membranes, the 200 Da membrane was tested with the spent caustic at its original pH (effluent no. 2 in Table 3.1).

All samples throughout the study were characterized, as described in the following section, in terms of contaminants concentrations such as COD, O&G (polar and non-polar), phenolic compounds, suphides, pH and conductivity in order to evaluate the retention capacity of the membranes. Before and after NF tests, the polymeric membrane was characterized by SEM-EDS and FT-IR and the ceramic membrane by SEM-EDS (as described in section 3.3.7). Inductively Coupled Plasma Atomic Emission Spectrometry (ICP-AES) was used to determine the concentration of metal elements, titanium and aluminium, in spent caustic solutions (feed, permeates collected during the test, total permeate and retentate), in the NF test carried out with the 200 Da ceramic membrane (see section 3.3.7.4).

3.3.6 Characterization methods

3.3.6.1 Effluents Characterization

COD was measured using the LCK 014 kit (HACH) and a DR 3900 spectrophotometer (HACH) after the digestion of the samples in a HT 200 S digester (HACH LANGE), according to APHA guide [82]. Sulphides and phenolic compounds were determined by spectrophotometry using a DR 3900 spectrophotometer (HACH) as well as the LCK 653 kit and the LCK 346 kit from HACH, respectively. O&G (polar and non-polar) was measured according to the Standard Method SMEWW 5520 C/F [82], after sample dilution to ensure that the concentration would fit into the calibration curve of

the NICOLET 6700 FT-IR. The conductivity was measured using a conductivity meter, model LF 320 (WTW), pH was measured using a pH 1100 L pH meter (VWR) and temperature with an alcohol thermometer (VWR).

3.3.7 Membranes Characterization

3.3.7.1 Dimensions and contact angle

The mass and thickness of the polymeric membranes were monitored with a KERN ABJ-NM/ABS-N analytical balance and a micrometer (Elcometer 124, Elcometer®, UK), respectively.

The contact angles were determined by the sessile drop method, by manually depositing a drop of DI water and spent caustic on the membrane surface. Multiple replicates (9 measurements on 3 different locations of the active layer and support) were performed and the mean angle was determined. All images were acquired by CAM2008 (KSV) software, where the drop shape fitting was executed by mathematical functions.

3.3.7.2 SEM-EDS and Mapping

Scanning electron spectroscopy (SEM) with energy dispersive spectroscopy (EDS) analysis were performed on polymeric membranes, while SEM with elements mapping was performed on the surface of ceramic membranes. The morphology of the support and active layers of the membranes was studied by a Hitachi S-2400 scanning electron microscope. The microscope was equipped with a silicon drift detector (SDD) to characterize the elemental composition of the surface based on the EDS spectroscopy and a digital acquisition system with software Esprit 7.1 to detect Bruker light elements. Prior to SEM-EDS and SEM-Mapping characterizations, membranes were coated with gold to make them electrically conductive.

Two different areas of each membrane were processed using the ImageJ software (http://imagej.nih.gov/ij/) for the × 300 SEM images amplification obtained. The original SEM images composed of 256 grey levels were analysed using ImageJ. The images were spatially scaled, their total membrane surface area was calculated and then, binarized after setting a certain threshold level (149 for pristine polymeric membrane and 255 for aged polymeric membranes). Pore density (number of pores divided by area of membrane), porosity (area of pores divided by

membrane area), total pore area, and the average Feret's diameter (the longest distance between any two points along the selection boundary) were determined using data retrieved by the software.

3.3.7.3 FT-IR

FT-IR coupled to attenuated total reflectance (ATR) was used to analyse and compare the surface chemical structure of membranes on both sides (active and support layers). Bruker Spectrometer IFS 66/S instrument (USA) equipped with an H-ATR and a ZnSe crystal was used as equipment and normalized spectra were recorded with accumulated 60 scans in the range of 4000 to 550 cm^{-1} and with 4 cm^{-1} resolution. All membranes were cleaned with DI water and dried before analysis. Three different random zones were selected for the analysis of each membrane layer to assess potential differences in the chemical structure in different membrane areas.

3.3.7.4 ICP-AES

The equipment used for ICP-AES analyses was a Horiba Jobin Yvon S.A.S., Model Ultima2 (France). This was equipped with a 40.68 Hz RF generator and a Czerny-Turner 1.00 m spectrophotometer. Data acquisition and equipment control were performed with a computer equipped with JY v5.4 software, which allows visualizing all parameters and obtained data on-line. Volume sample was 1 mL per each metallic element, therefore 2 mL.

3.4 Results and Discussion

3.4.1 Effluents

Spent caustic is the solution that results from the kerosene pre-washing step, before the sweetening process, in the kerosene Merox unit of a petroleum refinery. In the specific case of Sines Refinery, in Portugal, this extremely aggressive effluent accounts for 90 % of impact on the final refinery wastewater in terms of polar oil and grease (O&G) [7].

The characteristics of spent caustic vary over time, due to the different crudemix being processed in the refinery and the operating conditions employed. Two different spent caustic effluents were tested due to constraints related with the plant operation procedures: one to assess NF on polymeric membranes (effluent no. 1) and the second collection to assess NF on ceramic

membranes (effluent no. 2). Also, for the polymeric membrane, their robustness was tested at different feed pH. Table 3.1 exhibits their compositions.

Table 3.1 - Characteristics of spent caustic effluents tested.

Effluent no.	**1**	**2**
Date of collection	**January 11th 2019**	**August 10th 2019**
COD (mg O_2/L)	102190	88360
Phenolic compounds (mg/L)	1908	2742
Sulphides (mg/L)	34.9	31.6
Total O&G (mg/L)	18970	17837
Polar O&G (mg/L)	15053	10090
Non-polar O&G (mg/L)	3917	7747
Conductivity (mS/cm)	60.7	61.2
pH (Soresen scale)	13.87	13.85

3.4.2 Koch SelRO polymeric membrane

3.4.2.1 NF tests to evaluate membrane performance

The membrane hydraulic permeability for the polymeric membrane was determined to be 1.81±0.28 $Lh^{-1}bar^{-1}m^{-2}$, at 22±2 ºC. The fabricant of the polymeric membrane, Koch, refers a hydraulic permeability from 1.5 to 2.0 $Lh^{-1}bar^{-1}m^{-2}$, which is in line with the obtained experimental value.

Membrane performance was addressed during ageing for 6 and 12 weeks with spent caustic (effluent no. 1 in Table 3.1). The values of L_P/L_{P0} (hydraulic permeability at a given time normalized by the hydraulic permeability of the pristine membrane) obtained for 6 weeks and 12 weeks were, respectively, 4.46 and 4.62. A considerable increase in the hydraulic permeability of the membrane after soaking in the spent caustic effluent can be observed. It is interesting that the increase in the permeability mainly occurs within the initial period of 6 weeks since similar permeabilities were attained after 6 and 12 weeks of ageing (8.00$\pm$0.31 $Lh^{-1}bar^{-1}m^{-2}$ vs. 8.30$\pm$0.34 $Lh^{-1}bar^{-1}m^{-2}$ after 6 and 12 weeks, respectively). Pure water permeability is an intrinsic membrane characteristic mainly governed by the active layer pore size distribution.

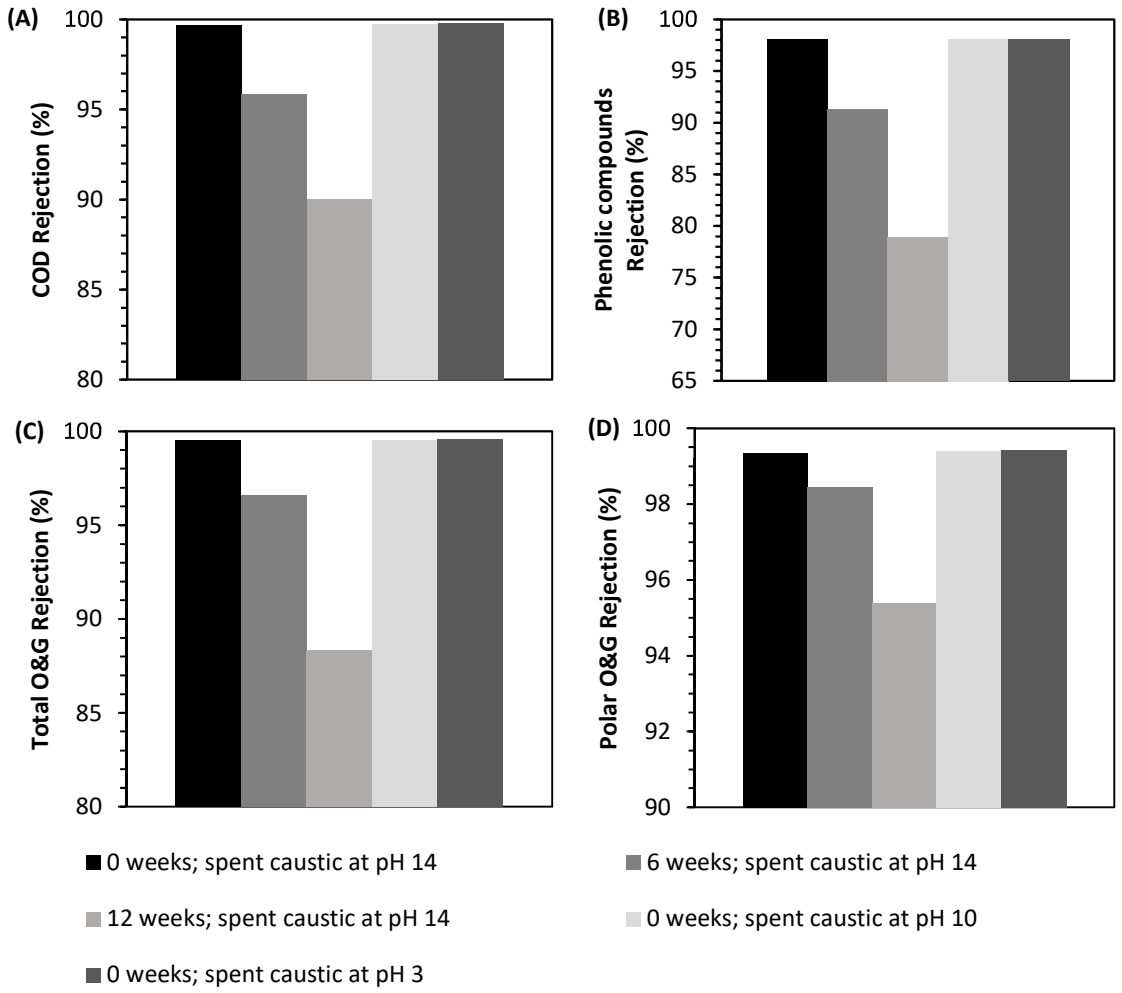

Figure 3.3 - Apparent rejection of contaminants during membrane separation with aged membranes for 0 (pristine membrane), 6 and 12 weeks with spent caustic at pH 14 and pristine membranes with spent caustic at pH 10 and 3. (A) COD, (B) phenolic compounds, (C) total O&G, (D) polar O&G.

Figure 3.3 shows the rejection of contaminants during membrane separation tests. COD removals were very high for the pristine membrane (99.6 %) however a continuous decrease is observed with the ageing time (95.8 % for 6 weeks and 90.0 % for 12 weeks). Considering the first 6 weeks of ageing, COD removal decreased on average 0.63 % per week, but on the second period of 6 weeks, COD removal decreased on average 0.97 % per week. For the aged membranes for 6 and 12 weeks, phenolic compounds removals reached 91.3 % and 78.9 %, respectively, which are much lower than the pristine membrane performance (98.1 %). Sulphide compounds are not presented in Figure 3.3 since their rejection is of 100 % in all samples, which may be related to the natural

degradation of sulphides into the atmosphere, also considering that NF tests occurred during summertime in the open air. O&G removal reached a maximum of 99.5 % for the pristine membrane. Considering aged membranes, the performance on O&G removal decreased also (96.6 % removal for 6 weeks aged membrane and 88.3 % removal for 12 weeks aged membrane). On aged membranes, polar O&G removals reached 98.4 % for 6 weeks and 95.4 % for 12 weeks, respectively (0.15 % average removal per week during the first 6 weeks of ageing and 0.51 % average removal per week during the second 6 weeks of ageing). These results indicate a loss of rejection on polar O&G contaminants on aged membranes, especially for 12 weeks aged membrane. This loss of retention capacity was more relevant during the second 6 weeks of ageing and may be related with the increase of permeability.

As referred previously, the major increase in permeability occurred during the first 6 weeks of ageing, while the highest decreases in the rejection capacities were observed during the second 6 weeks of ageing. The small increase on permeability in the second 6 weeks of ageing seem not to be able to justify the increase of the loss of retention capacity in the same period. It could be related with molecular exclusion mechanisms, as it seems that the membrane pore integrity has been compromised during the ageing period, as reported elsewhere [27–32,34,113,114].

One possible reason to change membrane pore integrity in such a way that compromises permeability and retention capacity could be the very high pH of the spent caustic. Data from FT-IR observations suggest that the active layer is not likely to have been modified since the differences observed are related to the adsorption of organic components that are present in spent caustic. On the other hand, the support layer seems to have been considerably modified, according to the alterations in permeability and retention properties.

Although the membrane is pH-resistant, it could happen that the extreme pH conditions negatively affect the membrane structure. In order to test this, spent caustic pH was decreased from 14 to 10 and 3. The values of L_P/L_{P0} obtained for pH of 14, 10 and 3 were, respectively, 3.04, 2.37 and 2.07. Hydraulic permeability seems to suffer more the higher the pH is, particularly between pH 10 and 14. Figure 3.3 shows the impact of pH on the retention capacity of the polymeric membrane. Retention capacity is nearly independent of the pH value, with all contaminants rejections similar in all experiments. Therefore, it can be concluded that pH manipulation will only cause an alteration in the permeability, not being responsible for retention capacity alterations.

Santos *et al.* [25] attempted to treat naphthenic spent caustic with a Koch NF polymeric SeIRO spiral-wound membrane module. It is suggested that the contaminants present in the spent caustic do not significantly affect the membrane performance. The results obtained corroborate the study of Santos *et al.* [25] for a pristine membrane, however a great loss of performance was observed for aged membranes during the first 6 weeks of ageing in permeability and retention capacity in the second 6 weeks of ageing.

3.4.2.2 Contact angle and thickness

Contact angle highly depends on the surface composition and, to a less extent, on the surface roughness. The contact angle is a measure of the tendency for the water to wet the membrane surface (it can be measured on both sides). For the Koch SeIRO polymeric membrane, the contact angle with DI water on the active and support layers was 30.62º and 36.28º, respectively, showing the hydrophilic nature of the membrane on both sides. Interestingly, the contact angle with spent caustic was approximately ~ 0º on both sides, demonstrating the higher affinity of the membrane to the spent caustic effluent, potentially towards polar organic compounds (with a polarity lower than the water polarity).

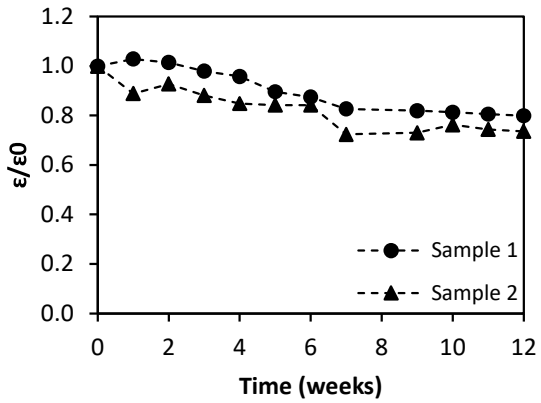

Figure 3.4 - Thickness profile measured for the two immersed polymeric membranes along the 12 weeks of ageing (ε – thickness at any time during the ageing procedure; ε_0 at the beginning of the ageing procedure).

Figure 3.4 presents the thickness evolution during 12 weeks of ageing in duplicate samples. In the present work, both length and width were determined as 2 cm for all sampling points throughout the 12 weeks. Figure 3.4 shows a consistent loss of thickness for the two studied membranes, and therefore a loss of membrane volume is observed during ageing. This observation could be related with modifications on the membrane structure, either on the active layer, support, or both. These results are consistent with permeability and retention properties data obtained and discussed above.

3.4.2.3 SEM-EDS

Active and support layers as well as cross-sections of pristine and aged membranes (for 6 and 12 weeks) were analysed by scanning electron microscopy (SEM). Figure 3.5 shows the results obtained.

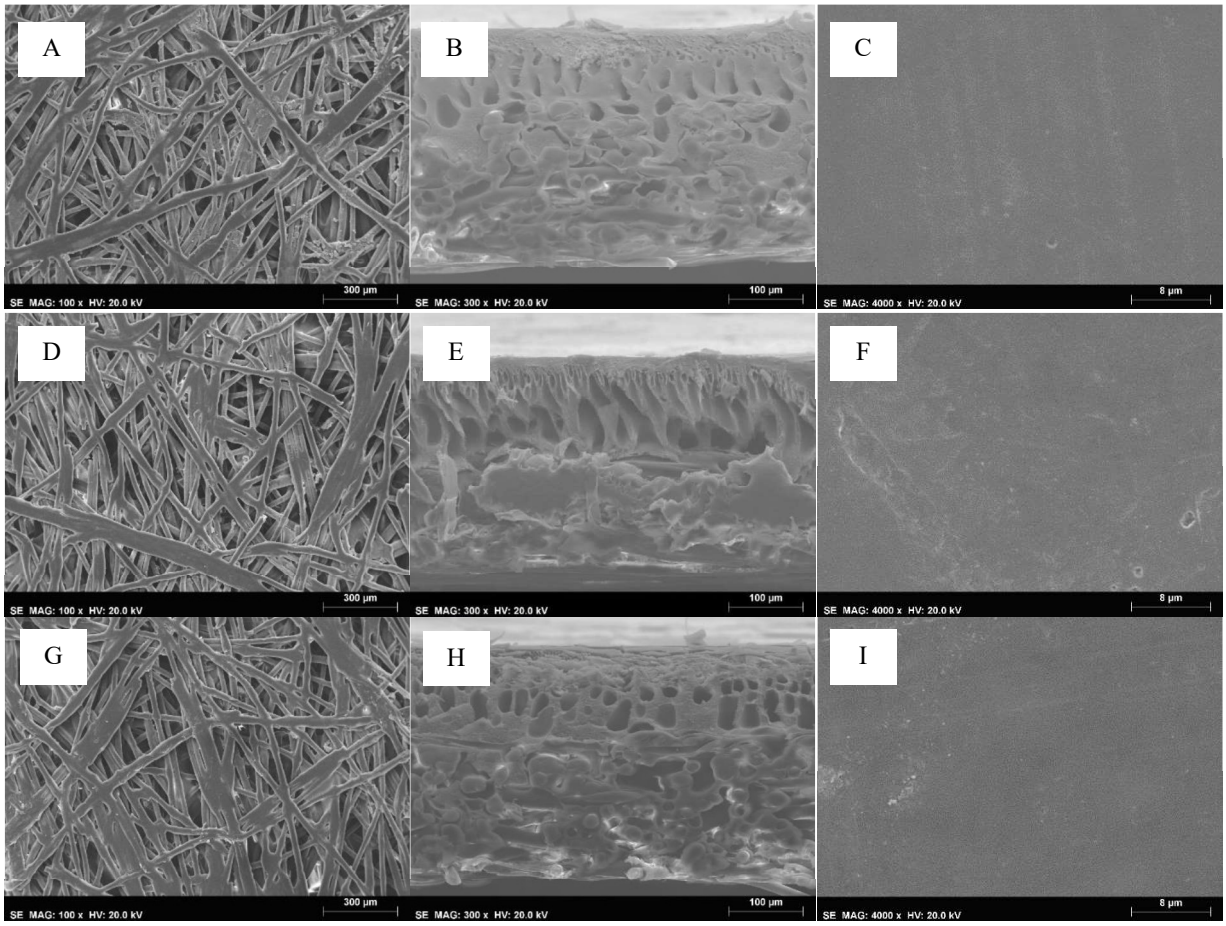

Figure 3.5 - SEM analysis for the polymeric membrane. A – pristine membrane support layer; B – pristine membrane cross section; C – pristine membrane active layer; D – 6 weeks aged membrane support layer; E – 6 weeks aged membrane cross section; F – – 6 weeks aged membrane active layer; G – 12 weeks aged membrane support layer; H – 12 weeks aged membrane cross section; I – 12 weeks aged membrane active layer. Support layer magnification is x100, cross section magnification is x300 and active layer magnification is x4000.

In terms of physical modifications of the membrane structure, it appears that the intermediate structure (right after the active layer in the cross-section view) gets slightly looser with ageing (Figure 3.5 B; E; H), although it is not completely clear. Pore coalescence may be the cause for this observation. The support layer (Figure 3.5 A; D; G), seems unchanged. No conclusions can be withdrawn regarding the active layer since the structure is very compact and SEM maximum magnification does not enable comparisons among the membranes with the required level of detail. On the other hand, variations on permeability and thickness were observed with time, thus making

it impossible to draw a clear conclusion of a connection between membrane structure and function (L_P, rejection capacity) on SEM results alone. To further study membrane structure, FT-IR profiles were collected and are discussed in the next section. Chemical surface composition (EDS) was also studied to determine elementary composition (Table 3.2).

Table 3.2 - EDS analysis of active and support layers of polymeric membranes (pristine, 6 and 12 weeks aged prior to NF test).

Membrane	Active layer			Support layer	
	C (%)	S (%)	O (%)	C (%)	S (%)
Pristine membrane	61.6	19.9	18.5	99.0	1.0
Aged for 6 weeks	64.7	19.0	16.3	99.0	1.0
Aged for 12 weeks	67.7	16.6	15.7	99.3	0.7

It is interesting to observe a continuous increase in the carbon element content with ageing in the active layer while other elements (S and O) are decreasing, which could mean a possible degradation of this layer. On the support, an alteration occurs between 6 and 12 weeks of ageing and is related with a loss of sulphur. Although the membrane composition is not available, SEM-EDS analysis suggest that its composition essentially includes carbon, oxygen and sulphur in the active layer and mostly carbon in the support. Specially for the active layer, which has the selectivity property, several polymers used in NF polymeric membranes contain such composition, for example PES (polyethersulphone) or PS (polysulphone) [115].

Pore density analyses were performed on the pristine membrane, as well as for the 6 and 12 weeks aged membranes, prior to NF tests. A section of each membrane was processed using the ImageJ software for the x300 images magnifications of samples cross-section. The total membrane surface area was calculated, and the images were then binarized. The area measurements obtained, calculated pore density (number of pores divided by area of membrane), porosity (area of pores divided by area of membrane), circularity (Eq (3.2)), and Feret's diameter (the longest distance between any two points along the selection boundary) [116] are presented in Table 3.3.

$$\text{Circularity} = \frac{\text{Area}}{\text{Perimeter}^2} \quad (3.2)$$

Table 3.3 - Pore measurements for pristine membrane, as well as 6 and 12 weeks aged membranes prior to NF test based on the SEM cross-section magnification of x300.

	Control	**Membrane 6 plus treatment**	**Membrane 12 plus treatment**
Porosity (%)	12.098	19.905	27.935
Number of pores	2196	2962	4039
Pore density (μm^{-2})	0.032	0.041	0.063
Minimum Pore Area (μm^2)	0.074	0.074	0.075
Maximum Pore Area (μm^2)	442.449	3821.366	714.915
Total Pore Area (μm^2)	8345.469	14257.465	18022.096
Average Circularity	0.828 ± 0.252	0.878 ± 0.221	0.837 ± 0.252
Average Feret diameter (µm)	1.662 ± 3.745	1.441 ± 4.974	1.503 ± 3.570
Minimum Feret's diameter (µm)	0.384	0.384	0.386
Maximum Feret's diameter (µm)	39.761	141.438	66.347

The results obtained show increasing porosity, number of pores and pore density. Extremely high Feret's diameter [116] values were detected, indicating the highly irregular shape of pores, particularly for the 6 weeks aged membrane. The average circularity value was approximately 0.9 in all the measurements with values obtained that varied between 0.6 and 1 (perfect circles). These results seem to corroborate that the increase of permeability and loss of retention capacity are related with the increase of the number of pores. It must be referred, however, that Table 3.3 only refers to the pores in the support. This is due to the low MWCO of the active layer, where SEM could not show any pores due to the typically very low pore size of NF membranes for SEM analysis. It becomes clear that the pores in the support are of micro scale, even in the pristine membrane.

3.4.2.4 FT-IR

The objective of these studies was to infer on the possible structure alterations that occurred during ageing experiments and after NF tests. The tested membranes are divided as the pristine

membrane without any treatment ("Pristine") and with a NF test ("Pristine + NF test"), the duplicate aged membranes after immersion for 12 weeks ("Membrane 1 + 12 weeks" and "Membrane 2 + 12 weeks") and the aged membranes for 6 and 12 weeks followed by a NF test ("Membrane 6 weeks + NF test" and "Membrane 12 weeks + NF test").

The FT-IR spectra (Figure 3.6) obtained for the active layers for two membranes immersed under the same conditions in the effluent were analysed and compared with the membrane that was not immersed.

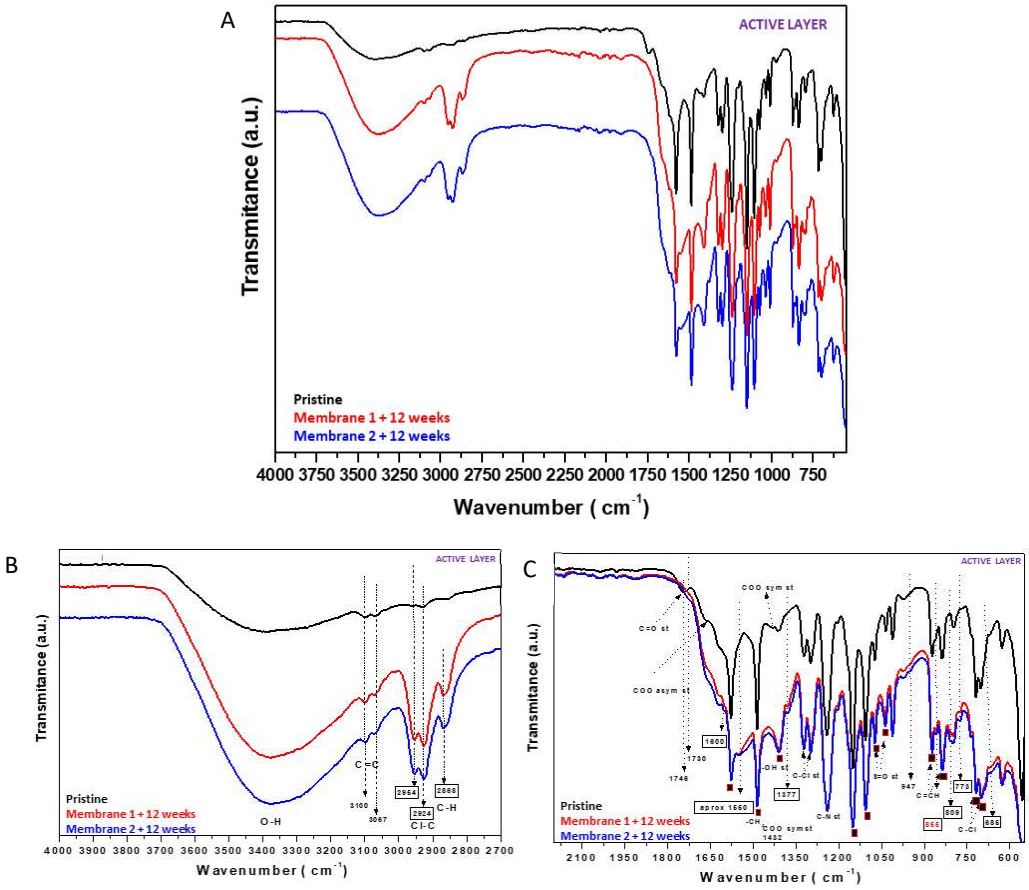

Figure 3.6 - FT-IR spectra of pristine membrane and membrane after 12 weeks immersion in spent caustic active layers (duplicate) (A). FT-IR spectra magnifications in the regions 4000–2700 cm^{-1} (B) and 2200–550 cm^{-1} (C).

Magnification in the region 4000-2700 cm^{-1} (Figure 3.6 B) and the corresponding peaks defining the main chemical bonds in the polymeric structures in the region 2200-550 cm^{-1} (Figure

3.6 C) were highlighted. The assignment for the fingerprint region (1500-550 cm^{-1}) is also summarized in Table 3.4.

Table 3.4 - Assignment for FT-IR fingerprint region (1500-550 cm^{-1}).

Adsorption band (cm^{-1})	**Assignment**
1576	-NCO st (Amide II) [117]
1480	(CH_2)bend [118,119]
1410	O–H st [120]
1299	S=O [121]
1241	C-O-C [122]
1149	C-O st [123]
1109	C-O-O st [123]
1070,1031	S=O st [124]
871,833	C=CH [117]
723, 695	C-Cl st [118,125]

The results obtained by FT-IR for the active layer of 12 weeks aged membranes after immersion (duplicate) were identical but showed some differences compared to the pristine membrane. The pristine membrane spectrum presented a characteristic adsorption band observed at 1746 cm^{-1} due to the stretching vibration of the C=O group. For the 12 weeks aged membranes the peak at 1746 cm^{-1} disappeared. This fact could be attributed to the aminolysis reaction with the urethane groups with ammonia or alkanolamines, present in the effluent and giving as sub-products alcohols and amides [126]. This is in line with the increase of intensity of the band associated to these groups, around 3370 cm^{-1} and 1410 cm^{-1} for -OH bond, as well as the differences in the C=O band in the amide region (around 1690- 1630 cm^{-1}). The increase of the intensity for bands at 2950 $cm^{-1}$and 2924 cm^{-1} in the 12 weeks aged membranes spectra could be attributed to the presence of compounds from the effluent (Figure 2.6 A and C). A broad band appearing at around 1520 cm^{-1} that was associated to the presence of ammonia (NH^{4+}) and salt derivates (-NH^{3+}) (Figure 3.6 C) could be also related to the effluent. Bands at around 1550-1550 cm^{-1} associated with N–O asymmetric stretch, 1377 cm^{-1} symmetric stretch, and 773 cm^{-1} out-of-plane stretch modes for deformation of nitrocompounds (nitrates (NO^{3-}) and nitrites (NO^{2-})) [117] that are present as residues in the aged

membranes (Figure 3.6 C), are also often found in the spectra of other oily effluents [127]. New peaks at 809 cm^{-1} and at 685 cm^{-1} are also associated with the effluent residue.

Bands associated to the C=C bound at 3100 cm^{-1}, 871 cm^{-1} and 833 cm^{-1} (Figure 3.6 B,C) (Table 3.4) were identified in all spectra, where in particular the band at 3100 cm^{-1} may be related to pore hidration. The peak at 1142 cm^{-1} was associated to C-Ost and was also present in all spectra, as well as peak in the range of 800-600 cm^{-1}, also assigned to C=CH stretching vibration [117] and occasionally C-Cl [118,125]. Also a peak at around 1576 cm^{-1} was observed in all spectra and is possibly associated with stretching mode of CNH group, which is often associated to urethane [125]. Peaks at 1665 cm^{-1} and 1435 cm^{-1} were also associated to asymmetric and symmetric vibration of –COO- groups respectively [57,128]. The pristine and both the 12 weeks aged membranes showed characteristic bands around 3370, 3100, 2950-2924 and 2860 cm^{-1} (Figure 3.6 B), associated to stretching vibrations of –OH, =C-H, S=O, and H–C–H bonds, respectively [117], from which the vibration S=O seems to be in accordance with SEM-EDS results.

As a conclusion, the immersion of the membranes does not impact on the main bands associated with the membrane initial structure (O-H, CH_2) and the changes observed in the spectra are likely due to the adsorption of components from the effluent as well as chemical reactions due to the presence of potential additives employed during membrane production.

The impact of filtration in the chemical structure of the membrane was also checked by comparing the pristine membrane before and after the NF test as well as two immersed membranes for 6 and 12 weeks prior to a NF test (Figure 3.7).

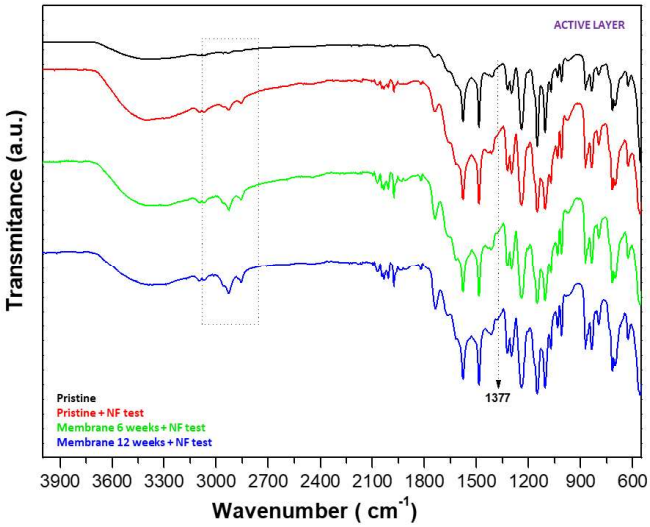

Figure 3.7 - FT-IR spectra of the pristine membrane before and after the NF test as well as aged membranes for 6 and 12 weeks after NF tests (active layers).

For all membranes tested by filtration, the spectra obtained did not show significant differences apart from the new signals detected in the region of 2090-1952 cm^{-1} that could be assigned to isotiocianate bonds (N=C=S st) [117,129] and a new peak at 1819 cm^{-1} (C=O st) associated to acid halide or anhydride, which is an indicator of chemical modifications in the urethane structure. The intensity of the peaks at around 3413 cm^{-1}, around 2960-2854 cm^{-1} (Figure 3.7), and around 1737 cm^{-1} increases as the contact time with the effluent increases. The presence of the bands at 1410 cm^{-1} and 1377 cm^{-1} are probably related to the presence of alcohols and other effluent components, respectively.

The support layers were also analysed by FT-IR, being the results of static ageing for 12 weeks presented in Figure 3.8 and ageing for 6 and 12 weeks prior to NF test presented in Figure 3.9.

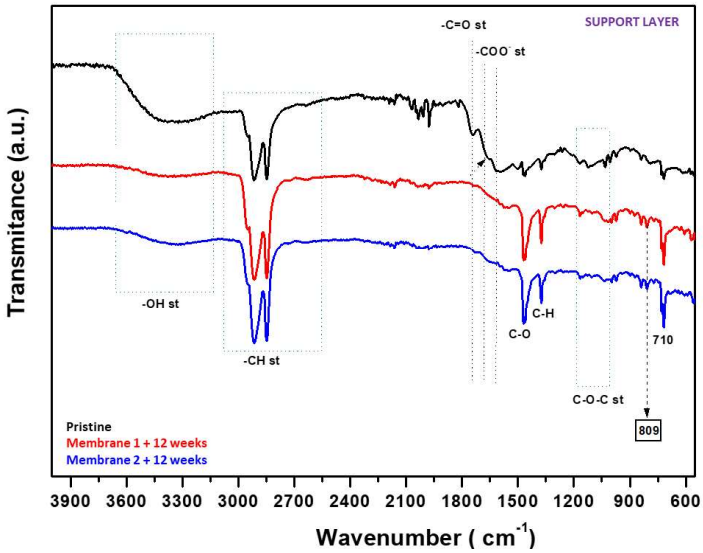

Figure 3.8 - FT-IR spectra of pristine membrane and membrane after 12 weeks immersion in spent caustic support layers (duplicate).

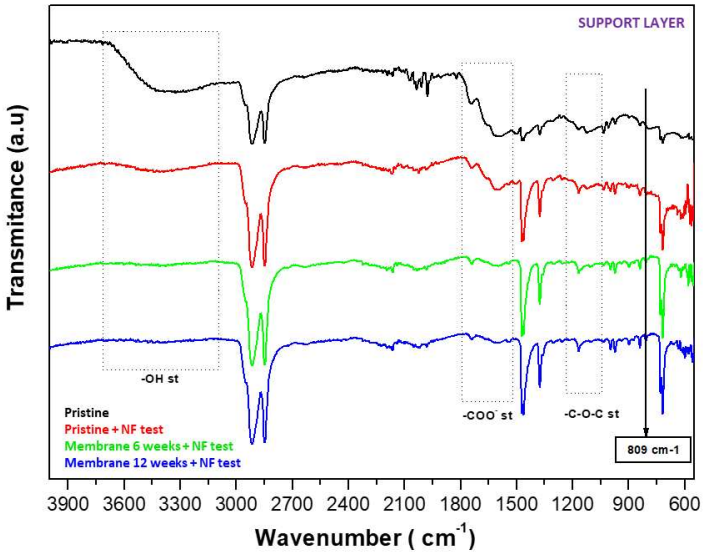

Figure 3.9 - FT-IR spectra of pristine membrane before and after NF test, as well as aged membranes for 6 and 12 weeks after NF tests support layers.

The spectra for membranes immersed (Figure 3.8) showed an evident deacetylation with the loss of –OH, COO- groups and also an important change in the region for C-O bonds (1165-1015 cm^{-1}) groups (Figure 3.8) although the peaks associated to C-H bonds (2985-2800 cm^{-1}) remained in the

structure. These results indicate that the polymeric structure of the support layer might have been considerably damaged. These changes were similar and more evident for the membranes subjected to filtration (Figure 3.9). These changes became more pronounced as the contact time with the effluent increased (Figure 3.9). The peak at 809 cm^{-1} present in both spectra could be also related with the effluent components (Figure 2.6).

Data discussed above suggests that the active layer is not likely to have been modified since the differences observed are related to the adsorption of organic components that are present in spent caustic. On the other hand, the support layer seems to have been considerably modified, in line with the changes observed in the permeability and retentive properties of the membranes, as well as EDS results.

3.4.3 Inopor ceramic membrane

3.4.3.1 Evaluation of membrane performance

Similarly to section 3.4.2, in this one the performance of the ceramic membrane under study was evaluated.

Although compaction is not required for ceramic membranes, this membrane was allowed to compact for half an hour, with DI water. Hydraulic permeability was determined to be 5.61±0.14 $Lh^{-1}bar^{-1}m^{-2}$ at 23±2 ºC. The fabricant of the ceramic membranes, Inopor, refers a hydraulic permeability of 9.0 $Lh^{-1}bar^{-1}m^{-2}$, which is relatively higher than the obtained value but typically ceramic membranes may present a slightly deviation due to the rigid structure.

Tests were performed for a maximum period of 6 hours or until no more permeate flux was observed. Figure 3.10 shows the permeability evolution for the ceramic membrane during the NF test.

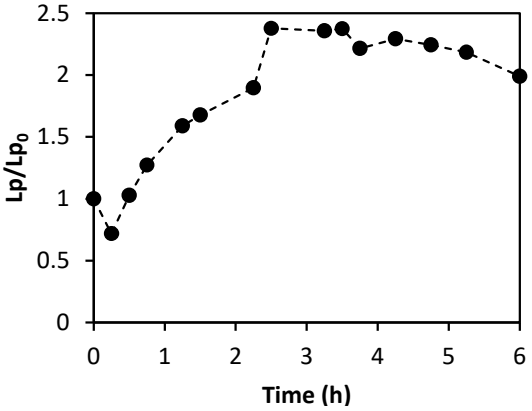

Figure 3.10 - Relative permeability of the 200 Da ceramic membrane throughout the test with spent caustic effluent.

Figure 3.10 shows that permeability increased between 0.5 h and 2.5 h of test, slightly decreasing afterwards for the 200 Da membrane. TiO_2 is a non-toxic material, and according to the manufacturer, very resistant to extreme pH conditions (1-13 between 20 to 40 ºC) [130]. Spent caustic is a difficult wastewater due to extreme pH, around 13 (Table 3.1). Contrary to expectations, the 200 Da ceramic membrane did not resist to spent caustic. At first sight, it appears that during the membrane cleaning with spent caustic alkaline pH (during NF test), the real MWCO of the ceramic membrane was exposed.

The results obtained evidence that the membranes addressed are not suitable to treat the tested spent caustic effluents. After the filtration test, the membrane was rinsed with DI water and L_P was assessed. For the 200 Da membrane, L_P was determined to be 47.72 ± 1.23 $Lh^{-1}bar^{-1}m^{-2}$, at 22 ± 2 ºC. The original hydraulic permeability was determined as 5.61 ± 0.14 $Lh^{-1}bar^{-1}m^{-2}$ at 23 ± 2 ºC, from where it may be observed that L_P increased more than 8 times, not being able to recover the initial permeability.

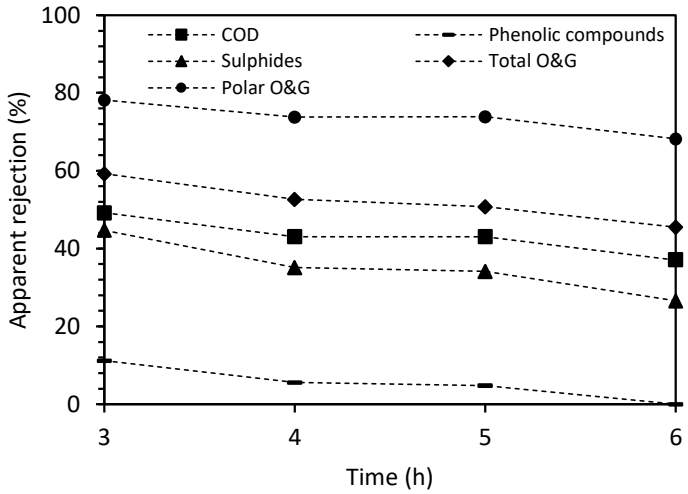

Figure 3.11 - Apparent rejection of contaminants during membrane separation with 200 Da ceramic membrane during the 6 h of test.

Figure 3.11 shows the decrease in the rejection of all contaminants (or lumped parameters) addressed (COD, phenolic compounds, sulphides, total O&G and polar O&G) throughout the 6 hours of test. The loss in retentive properties could be related with changes in the membrane structure. Considering rejection capabilities of the ceramic membrane, phenolic compounds seem to be the contaminants with the lowest rejection, possibly due to their low molecular weight. The comparison of the removals obtained for total O&G and polar O&G suggests that the membrane performed better towards the removal of polar O&G. Some authors argue that NF TiO_2 ceramic membranes possess a tendency to lose rejection when the contaminants are positively charged and maintain high rejection for negatively charged compounds and low molecular weight neutral organics [131]. In a strong alkaline medium, organic compounds with functional groups located at the end of their structures usually are present in their ionic form. Figure 3.11 presents rejections only after 3 h of test, given that the flux was too low to allow for a permeate collection. In order to further study the reason behind the loss of rejection and to confirm if membrane loss of integrity could have occurred, an ICP analysis was performed to the feed, permeate and retentate samples (Table 3.5). Also, SEM –EDS analyses were performed on the membrane to verify the observations above.

Table 3.5 - ICP analysis of feed, retentate and permeate samples after the NF test with the 200 Da membrane.

Sample Name	[Al], mg/L	[Ti], mg/L
Feed (Spent caustic)	2.06	0.02
Retentate	2.07	0.05
Permeate – Total	1.38	0.43
Permeate of 3 h of NF test	1.45	0.50
Permeate of 4 h of NF test	1.37	0.29
Permeate of 5 h of NF test	1.62	0.27
Permeate of 6 h of NF test	1.81	0.28

Table 3.5 shows a similar aluminium concentration in both the feed and retentate, but lower in the permeate samples, therefore showing that there was no release of aluminium from the membrane structure. For the titanium element, concentration was slightly increased in the retentate compared with feed concentration, but increased considerably in the permeate samples leading to an indication of titanium element being released from the membrane structure.

Cross sections, surfaces and elements mapping of the ceramic membrane was analysed by scanning electron microscopy (SEM). Figure 3.12 show the surfaces and cross-section of the membrane, along with their most significant elements mapping. Table 3.6 contains the EDS analysis for the active layer of the ceramic membrane after the NF tests.

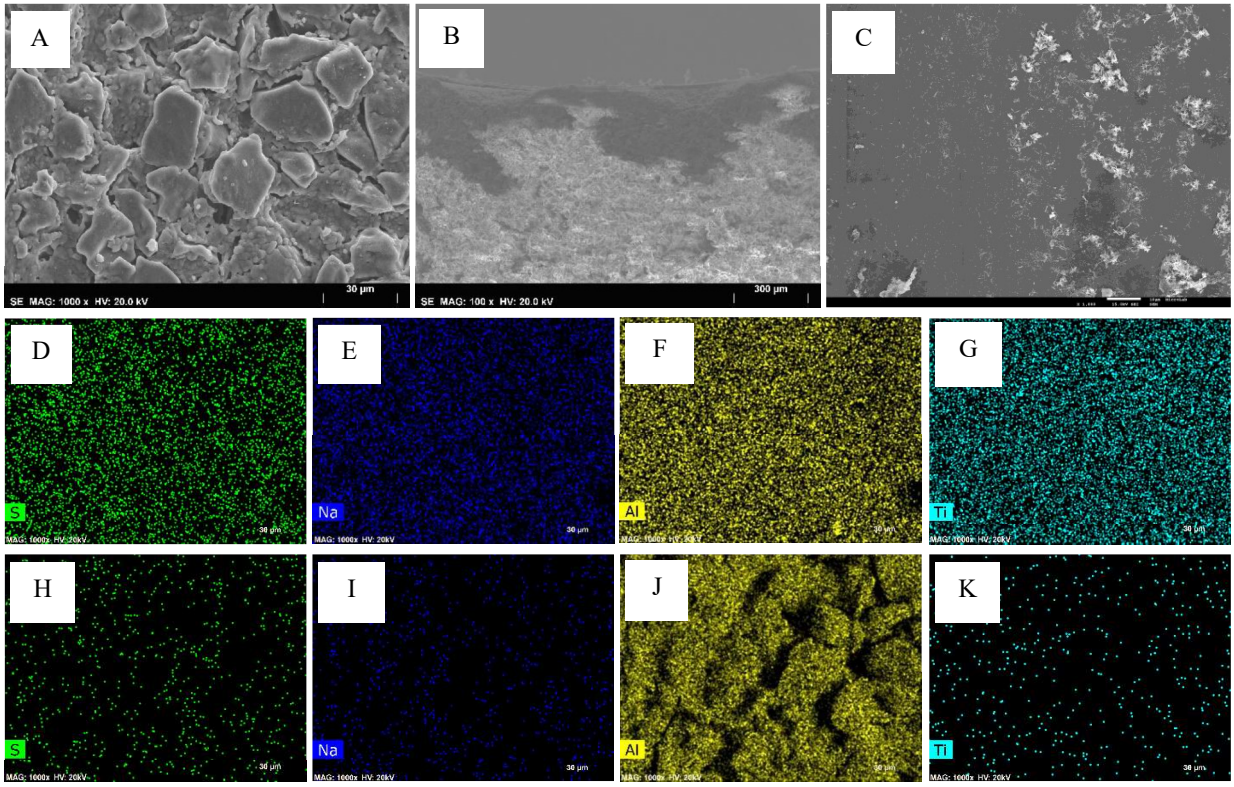

Figure 3.12 - SEM-EDS analysis of the 200 Da ceramic membrane after the NF test as well as the most significant elements mapping on the active layer and support layer after NF test. A – support layer; B – cross-section; C – active layer; D – sulphur element on the active layer; E – sodium element on the active layer; F – aluminium element on the active layer; G – titanium element on the active layer; H – sulphur element on the support layer; I – sodium element on the support layer; J – aluminium element on the support layer; K – titanium element on the support layer. Layer magnifications are x1000 and cross section magnification is x100.

Table 3.6 - EDS analysis of active layer of the ceramic membrane after the NF test (200 Da).

Membrane	O (%)	C (%)	Al (%)	Ti (%)	Zr (%)	Na (%)	S (%)	Fe (%)	Si (%)
200 Da	22.1	10.2	18.0	23.8	10.8	9.9	3.2	1.6	0.4

Although SEM analysis (Figure 3.12) does not appear to evidence damages on the membrane structure (e.g. cracks) or differences in the distribution of the elements over the membrane, the increase in the membrane permeability and the loss of its retention properties is corroborated by ICP observations, which may indicate a desintegration mechanism. Possibly, because the loss of Ti detected by ICP is not so high and/or can be homogeneous throughout membrane area, SEM-EDS images do not show it as ICP analysis. Although the membrane was thoroughly rinsed with DI water after the experiment, the deposition of some salts can be observed in both the active and support

layers. The distribution of some elements originally only present in spent caustic, like sulphur and sodium, were analyzed through mapping. Also, the distribution of the metallic elements that compose the membrane (aluminum and titanium) were analyzed by mapping. The concentration of sulphur and sodium is considerably higher in the selective layer, which might indicate a certain retention for these compounds. The aluminium distribution seems to be similar on both sides of the membrane, but the selective layer composition is only made of TiO_2. Titanium is also present in the support layer, which is not composed by titanium. ICP results indicate a loss of titanium, not aluminium. Nevertheless, the presence of aluminium occurs in both layers, due to a deposition of compounds from the matrix on the active layer, where there is the aluminium element. Possibly the loss of elements observed by ICP has not such expression in Figure 3.12 results, presumably because this loss might not be so relevant. Due to this membrane presenting high rejections, the concentration of elements on the active layer will be higher. On the other hand, the support layer pores are wider, therefore accumulating some elements from the active layer; this could mean that the titanium element released by the active layer loss of integrity will accumulate in the support layer.

3.5 Conclusions

Permeability results of the polymeric membrane showed a very accentuated performance decrease mainly during 6 weeks of ageing, and a smaller loss of permeability in the second 6 weeks period (final permeability was 4.5 times higher than the hydraulic permeability). A great loss in rejection was also noted following the permeability results (between 5 to 20 % less rejection in the analysed contaminants/lumped parameters). SEM analysis show that the cross-section of the membrane suffered visible alterations in pore density, as if the structure loosens up with time in direct contact with spent caustic. Thickness was also decreased during ageing. EDS analyses stand out an increase of the carbon element on the active layer, while FT-IR results suggest that the active layer did not suffer any structural modifications, however it was sensible to adsorption of the organic compounds naturally present in spent caustic. On the other hand, the support layer suffered several alterations that may justify the permeability and selectivity changes observed.

The 200 Da membrane permeability decreased during the first 10 min of test, but after that the membrane started to increase permeability regularly (and lost rejection properties) until 2.5 h of test, contrary to expectations. ICP-AES analysis suggest a destruction mechanism of the membrane, verifying a loss of titanium element during the NF test. This membrane could be further tested in the future with spent caustic modified to lower pH values, given that the original pH of spent caustic is extremely high, and it could help conclude about the full pH spectrum resistance to spent caustic by this new ceramic membrane.

4 Comparison of different strategies to treat challenging refinery spent caustic effluents[‡]

[‡] Published as**: Rita, A. I.**, Rodrigues, C. S. D., Santos, M., Sanches, S., Madeira, L. M. *Comparison of different strategies to treat challenging refinery spent caustic effluents*, Separation and Purification Technology, 253 (2020) 117482.
https://doi.org/10.1016/j.seppur.2020.117482

4.1 Abstract

Worldwide, spent caustic effluents from Merox units are a challenge for refineries given their very hazardous nature in terms of toxicity as well as their extreme pH (approximately 12-13). Although this is a global concern, the spent caustic effluent generated by Galp Refinery located in Sines, the major refinery in Portugal, was used as case study. To tackle this problem, two strategies were addressed in this study to treat spent caustic effluents: (i) neutralization, followed by Fenton oxidation post-treatment (approach 1) and (ii) neutralization, followed by liquid-liquid extraction (approach 2). Approach 1 allowed removals of 70% for total organic carbon (TOC), 80% for chemical oxygen demand (COD) and 95% for polar oil and grease (O&G). The *Vibrio Fischeri* toxicity test showed a considerable decrease in the acute toxicity of the spent caustic effluents after this treatment (approximately 70%). Approach 2 allowed for a mineralization of 97%, COD reduction of 96% and polar O&G removal of 99%. Both sets of technologies permitted a direct discharge of treated spent caustic into the effluent pre-treatment system of the refinery. Since the proposed treatment approaches enable a considerable improvement in the effluent quality and noteworthy annual savings were determined compared with current effluent management strategies (1.39 and 1.58 M € for treat approach 1 and 2, respectively), this study provides useful information for the development of industrial scale plants in petroleum refineries for the treatment of spent caustic effluents.

Keywords

Naphthenic spent caustic effluent, Neutralization, Fenton oxidation, Oil and grease, Toxicity.

4.2 Introduction

Spent caustic is a challenge in refineries worldwide due to its hazardous nature, especially the kerosene Merox spent caustic, which may account for more than 90% of the total contamination generated by refineries in terms of oil and grease [7]. Among refineries, the characteristics of spent caustics may vary greatly. Spent caustic may have different compositions according to the production process. Spent caustic can be sulphidic (ethylene plants or refining liquefied petroleum gas unit), naphthenic (refining jet/kerosene unit) – like the one used herein – or cresylic (refining gasoline unit). In general, sulphidic spent caustics present much lower COD than naphthenic/cresylic spent caustics but contain much higher concentrations of sulphides. Most literature on spent caustic remediation describes experimental work developed with sulphidic spent caustic, not addressing other types of spent caustic. The source of the crude oil, the refining processes employed and the emission regulations all influence the quality and quantity of spent caustic [10].

The UOP Merox process attempts to remove sulphur compounds from crude oil derived products. In the specific case of kerosene, the Merox technology consists of a sweetening reaction, where the remaining mercaptans are converted to disulphides, removing the strong odours and decreasing sulphur concentration in treated kerosene. The water that results from the kerosene pre-washing is called naphthenic spent caustic, hereby simply referred to as spent caustic. The pre-washing step consists of a liquid-liquid extraction process with kerosene and a sodium hydroxide solution, in the presence of an electric field. The mercaptans that are extracted to the caustic solution in the pre-washing, along with naphthenic acids and other organosulphur species, constitute naphthenic spent caustic. Then, the oxidation reaction occurs by means of a catalyst at room temperature, consuming atmospheric oxygen according to the following reactions (R corresponds to a generic group) [18]:

$$RSH + NaOH \rightarrow RSNa + H_2O \quad (4.1)$$

$$RSNa + \frac{1}{4}O_2 + \frac{1}{2}H_2O \rightarrow RSSR + NaOH \quad (4.2)$$

Hydrogen sulfide (H_2S) and carbon dioxide (CO_2), which are also present in the medium to be oxidized, react with the caustic soda according to the following competitive reactions:

$$H_2S + 2NaOH \rightarrow Na_2S + 2H_2O \quad (4.3)$$

$$CO_2 + 2NaOH \rightarrow Na_2CO_3 + H_2O \quad (4.4)$$

Spent caustic is a very complex matrix of organic oxygenated contaminants and mercaptans. Phenolic derivatives, monoaromatic and polycyclic aromatic compounds,

cycloalkanes, ethers, ketones and some esters are often found in caustic refinery effluents. Several authors have proposed characterization methods to study complex aqueous matrixes and extract information that helps describing and identifying families of compounds [11–17]. Naphthenic spent caustic may contain as much as 30000 ppm of polar oil and grease (O&G) and presents very high chemical oxygen demand (COD) (as much as 140000 ppm) [18]. Moreover, it usually presents a very high concentration of naphthenic acids (2 – 10 wt. %) that promote foam formation, sulphides (> 0.1 wt. %) and NaOH (1 – 4 wt. %). Spent caustic has an average pH around 13 and is a highly odorous waste due to its composition, rich in mercaptans, sulphides and some volatile organics, which inhibit biological treatment [19,20].

Spent caustic can be disposed of by incineration, though this is done less and less due to the generation of greenhouse gases and toxins. It can also be recycled upstream to the desalter unit, diluted with different types of water or neutralized with acid effluents. Another typical strategy is the direct injection into the atmospheric distillation unit although a maximum percentage of 7% is allowed [20]. Recycling spent caustic upstream to the desalter unit can be only a limited solution because of the detrimental alkalinization of the crude (generation of emulsions). Spent caustic has often been discharged, after dilution with the effluents from other processes, directly into the general effluent treatment system or into cooling water in an open system. However, this has led to more specific and more costly wastewater treatment [20,132], given the increasingly stringent regulations for wastewater quality. Treating the effluents directly at the source using effluent specific treatments would be more cost-effective and could enable valorization of resources within the process.

A traditional and efficient treatment for such an alkaline effluent is neutralization. Sulphuric acid (H_2SO_4) is usually the most used acid. Considering the advantage of heating the spent caustic during neutralization, the products are released as acid gases while naphthenic acids are sprung as an oily layer or can be processed or incinerated in a sulphur improvement unit. At industrial scale, this process is already implemented in some refineries for the neutralization of effluents prior to discharge into wastewater treatment systems. Eq (4.6) to (4.9) describe the main steps involved in the neutralization of typical salts and/or other organic compounds (thus the R for a generic group) that are usually present in spent caustic effluents [9].

$$2NaOH + H_2SO_4 \rightarrow Na_2SO_4 + 2H_2O \quad (4.5)$$

$$2Na_2S + H_2SO_4 \rightarrow Na_2SO_4 + 2NaHS \quad (4.6)$$

$$2Na_2CO_3 + H_2SO_4 \rightarrow Na_2SO_4 + 2NaHCO_3 \quad (4.7)$$

$$2NaSR + H_2SO_4 \rightarrow Na_2SO_4 + 2RSH \quad (4.8)$$

$$2NaOR + H_2SO_4 \rightarrow Na_2SO_4 + 2ROH \quad (4.9)$$

Acid neutralization consists on a reconversion of the acid components, separating them into an oily phase, instead of degrading them [9,20]. Seyedin and Hassanzadeganroudsari [9] reported an efficient removal of COD (70%) by neutralization, depending on the operating conditions. However, because of volatile organic compounds (VOCs) and hydrogen sulfide (H_2S) release, neutralization cannot be considered as a single treatment [46,47], thus, its combination with other processes is required.

Fenton is a promising advanced oxidation process (AOP), developed upon the pioneering work of H. J. Fenton [133], wherein wastewater pollutants react with the hydroxyl radicals generated by hydrogen peroxide (H_2O_2) in a non-pressurized reactor, at low to moderate temperature and pressure conditions, in the presence of a low-cost catalyst (e.g., iron sulphate (Fe_2SO_4)), yielding carbon dioxide and oxidation products [51,95,134]. As referred, the oxidation species generated in the reaction are hydroxyl radicals ($HO^{\bullet}$), which exhibit a very high oxidation potential, 2.80 V [134,135]. The main reactions involved are presented below, where Eq (4.10) depicts the hydroxyl radicals generation and Eq (4.11) the ferrous iron (catalyst) regeneration [50]:

$$Fe^{2+} + H_2O_2 \rightarrow Fe^{3+} + OH^- + HO^{\bullet} \quad (4.10)$$

$$Fe^{3+} + H_2O_2 \rightarrow Fe^{2+} + H^+ + HO^{\bullet}{}_2 \quad (4.11)$$

Eq (4.11) describes the limiting step given that its associated rate constant is very low, around 0.02-0.01 $M^{-1}s^{-1}$ [50]. Therefore, it becomes essential to increase the efficiency of the process through the increase of H_2O_2 and Fe^{2+} concentrations. However, such high concentrations may lead to the inhibition of the reaction due to radical scavenging effects as described in Eq (4.12) and (4.13):

$$H_2O_2 + HO^{\bullet} \rightarrow HO^{\bullet}{}_2 + H_2 \quad (4.12)$$

$$Fe^{2+} + HO^{\bullet} \rightarrow Fe^{3+} + OH^- \quad (4.13)$$

Another important factor that affects Fenton's process efficiency is the pH. The optimal pH values range from 2.5 to 4.5 [51]. For higher pH values, Fe^{3+} reacts with OH^-, leading to the formation of a precipitate ($Fe(OH)_3$) as well as the inhibition of Fe^{2+} regeneration; still, at higher pHs hydrogen peroxide will decompose into water and oxygen, instead of generating hydroxyl radicals [39]. On the other hand, at very acidic conditions the reaction between ferrous ion and

hydrogen peroxide becomes too slow, apart from the fact that hydrogen peroxide reacts preferably with the H^+ species. Temperature usually has positive effect on Fenton processes since it increases the rate of degradation reactions. On the contrary, special attention must be given to the H_2O_2 decomposition with increasing temperature, losing capacity to turn into $HO^\bullet$ radicals [136].

The use of hydrogen peroxide (in Fenton process) deserves special care, due to the fact that it is corrosive and can be degraded with heat, if excessive temperatures are reached. Hydrogen peroxide is hazardous in terms of handling at industrial scale, however it is used in a regular basis at Sines Refinery as an oxidizing agent to treat the final wastewater. The operators handle the product with care because the dosing system is manual, the hoses material usually is PVC and the effluent basins are made of concrete.

The Fenton process may be applied as a pre- or post-treatment, depending on the nature of the effluents. Although it is mostly applied as a post-treatment, it can be a useful pre-treatment when a reduction in the effluent toxicity is required, for example prior to a biological stage [94]. To that end, Alnaizy [19] reported high COD removal from refinery spent caustic effluent using the Fenton processes (approximately 95%) and reported that the treatment is less expensive than other classic treatments. A new study topic for Fenton processes are alkaline Fenton oxidation studies, in order to avoid the need for neutralization. However, low efficiency in COD removal (43%) and dissolved organic matter removal (86%) are reported compared to neutral and acid pH conditions [46,52]. Other types of AOPs, such as the combination of hydrodynamic cavitation (HC) and Fenton process, have demonstrated high efficiency in oxidation of hardly degradable organic contaminants. On the other hand, it seems that for example phenol oxidation is still low compared with other higher molecular weight contaminants, denoting a bottleneck of this technology concerning smaller organic molecules [53,57]. In the recent years, AOPs based on persulphates have also demonstrated potential to oxidize organic pollutants, both in terms of technology and investment. Persulphates (PS)- and peroxymonosulphates (PMS)-based AOPs are in science very similar to Fenton, but here the oxidation species is the sulphate radical, which exhibits a high oxidation potential. New developments have been made in order to optimize catalytic activity, as there are several choices for the catalyst [54,55]. In general, and in accordance with the technologies tested in the present work, the green nature of these technologies and their performances turn them attractive to oxidize organic pollutants in different industrial wastewaters [56,58]. On the other hand, and according to several authors [e.g. [56]], the oxidation potential of hydroxyl radicals is

higher than sulphate radicals, which could mean that although hydroxyl radicals need a lower pH medium to enhance activity, the expected degradation of COD and other organic contaminants would be higher. Other technologies such as photocatalytic AOPs have demonstrated to be successful in organic contaminants oxidation at basic pH conditions, however their application is more complex and implies additional separation steps to remove/recover the catalyst [54,137]. Another promising trend in research to oxidize organic contaminants of industrial effluents at basic pH conditions is hydrodynamic and acoustic cavitation processes coupled with AOPs (ozonation, H_2O_2 oxidation, Peroxone, UV-C, and others). Recent studies have demonstrated that COD removal is still low/moderate (in the range of 40-50 %) but the potential is high, due to smaller process costs and avoidance of dangerous reactions (for example neutralization); however, by-products formation is still a matter to be addressed concerning acoustic and hydrodynamic cavitation coupled with AOPs [56,58].

Liquid-liquid extraction (LLE) consists on a classical chemical process, based on mass transfer concepts where a solvent extracts the contaminants from the effluent, allowing to treat spent caustic effluents [65]. Although LLE may lead to the generation of more effluent, its combination with oxidation technologies such as AOPs was previously shown to enable very high removals of organics such as aromatic compounds (around 99%) [63]. Sabri *et al.* [64] assessed the treatment of spent caustic combining LLE with ionic liquids and obtained an extremely high removal of COD (99.8%). LLE has also been considered an efficient extraction process for the removal of other organic contaminants such as phenols from spent caustic [65].

In this study, the treatment of spent caustic from a Merox unit will be evaluated, following two approaches: (i) neutralization, followed by Fenton oxidation (approach 1) and (ii) neutralization, followed by liquid-liquid extraction (approach 2). The main objective aims at reducing the organic load of the effluent and its subsequent negative impact after discharge in the quality of the refinery global effluent (final wastewater) and respective treatment costs. Galp Refinery located in Sines, Portugal, will be used as a case study. So far, only a few research studies have delivered results to tackle this problem since these are really challenging effluents. To the best of authors' knowledge, this study conveys for the first time the comparison of the two treatment strategies evaluated and delivers the economic savings that refineries may achieve through their implementation, which is of the outmost interest for worldwide refineries in light of current and future more stringent legislation.

4.3 Materials and Methods

4.3.1 Reagents

H_2O_2, 35 wt. %, was supplied by *Solvay (Brussels, Belgium)*. $FeSO_4.7H_2O$ (99.5 %) was provided by *AnalaR NORMAPUR, VWR (USA)*. H_2SO_4, 95–97 %, was provided by *Fluka, Honeywell (USA)*. HCl, 37 %, was provided by *Chem-Lab (Belgium)*. NaOH, 48 wt. %, was supplied by *Ercros (Spain)*. Na_2SO_4 was supplied by *Labchem (USA)*. Silica gel (grade 923) was provided by *Grace Davidson (USA)*. Tetrachloroethylene was provided by *PanReac AppliChem (USA)*. Na_2SO_3 was provided by *AnalaR NORMAPUR, VWR (USA)*. Potassium titanium (IV) oxalate was provided by *Sigma-Aldrich*.

Cotton filter papers, grade 40, with a diameter of 150 mm and a pore size 8 µm were provided by *Whatman, GE (USA)*. This material was used as part of SMEWW5520 C/F – analysis of oil and grease in wastewater.

Kerosene, used as the solvent for liquid-liquid extraction, was supplied by Sines refinery since it is a final product of the Merox process, the same unit that produces the naphthenic spent caustic effluent. Therefore, its use in real practice allows a higher integration considering process logistics.

4.3.2 Characterization of the effluents

Galp refinery located in Sines, Portugal, has a nominal processing capacity of 220,000 barrels of oil per day and produces about 350 m^3/h of industrial effluent. Although only 2 m^3 of spent caustic are produced per hour in the kerosene Merox unit, this effluent stream is responsible for more than 90% of the total contamination in terms of O&G, particularly polar O&G, in the final wastewater. The characteristics of the spent caustic effluent fluctuate over time according with the nature of the processed crude oils. Therefore, the suitability of the technologies tested in this study towards the treatment of naphthenic spent caustic effluents with different compositions was addressed by collecting the effluents in the kerosene Merox unit pre-washing column outlet during the petroleum refining process at different dates. Their average composition was obtained using the methods described in section 4.3.3.4 and are shown in Table 4.1.

Table 4.1 - Characterization of spent caustic effluents tested at lab scale (effluents 1, 2 and 3) and pilot scale (effluents 4 and 5).

Effluent n.o.	**1**	**2**	**3**	**4**	**5**
Date of collection	June 22nd 2018	December 17th 2018	January 11th 2019	February 22nd 2019	April 1st 2019
TOC (mg C/L)	20417	21846	21968	12010	24552
COD (mg O_2/L)	84570	81160	102190	40780	96980
Phenolic compounds (mg/L)	2500	2201	1908	3358	2900
Sulphides (mg/L)	29.9	27.2	34.9	16.7	63.2
Sulphates (mg/L)	11	10	9	10	10
Total O&G (mg/L)	15255	14719	18970	4044	16544
Polar O&G (mg/L)	13061	12043	15053	3475	13260
Non-polar O&G (mg/L)	2194	2676	3917	570	3284
Conductivity (mS/cm)	73.3	88.2	60.7	90.8	80.0
pH (Sorensen scale)	13.79	13.86	13.87	13.65	13.67

When spent caustic effluents are discharged into the effluent pre-treatment system of refineries, a dilution effect occurs due to their mixture with the other effluents (e.g.: desalter effluent, sour waters, etc.). Therefore, the concentration of the contaminants may decrease as much as 150 times (scenario in Sines refinery). This dilution effect will be taken into consideration when evaluating the performance of each treatment.

4.3.3 Optimization of treatment technologies

4.3.3.1 Neutralization (lab scale)

The lab scale neutralization tests consisted of slowly adding H_2SO_4 (96%) to 100 mL of stirred spent caustic with pH control between 2 and 10. To study the performance of neutralization to decrease polar O&G concentration, the following pH values were selected: 3 and 5, as they appear to be optimal for further studies if Fenton oxidation is considered afterwards [51]. Neutralization tests were performed using different spent caustic effluents: 1-3 (Table 4.1).

4.3.3.2 Fenton Oxidation (lab scale)

Fenton oxidation was addressed as a post-treatment in order to further decrease COD and polar O&G concentration after neutralization at lab scale, following the procedure described in section 4.3.3.1. In order to optimize the process, different conditions were tested using the

same effluent (effluent 3, Table 4.1). Several runs were carried out by varying the concentrations of oxidant and catalyst (one at a time), as shown in Table 4.2.

Table 4.2 - Fenton oxidation conditions.

	Test	$[H_2O_2]$ (g/L)	Fe^{2+}:H_2O_2 (molar ratio)
Phase 1: Oxidant optimization	**1**	5.4	1:5
	2	7.2	1:5
	3	10.8	1:5
	4	21.6	1:5
Phase 2: Catalyst optimization	**5**	10.8	1:10
	6	10.8	3:1
	7	10.8	No catalyst

The strategy followed was to first evaluate the impact of the oxidant concentration and then evaluate the impact of the catalyst concentration through the variation of Fe^{2+}:H_2O_2 molar ratio, applying the previously optimized oxidant concentration. The oxidant stoichiometric concentration – $[H_2O_2]_{ST}$ (10.8 g/L) was calculated according to the COD of the effluent obtained after neutralization (in g O_2/L), as described in Eq (4.14), which is based on the stoichiometry of the hydrogen peroxide decomposition into water and oxygen;

$$[H_2O_2]_{ST} \Big/ MM(H_2O_2) = 2 \times \left[COD \Big/ MM(O_2) \right] \quad (4.14)$$

where *MM* (*i*) stands for the molar mass of species *i*.

Besides the stoichiometric concentration, the oxidant concentrations tested were 1.5 and 2 times lower as well as 2 times higher the stoichiometric value to cover a wide range of concentration. In fact, low concentrations of oxidant decrease the operating costs, but typically values above the stoichiometric one are required [135] due to scavenging/parallel reactions like the one shown in Eq (4.12). Regarding the Fe^{2+}:H_2O_2 molar ratio, the tested catalyst concentration ratio was 5 and 10 times lower and 3 times higher the oxidant optimized concentration, apart from an additional test without catalyst addition.

Oxidation tests were carried out in a 250 mL flask, which was equipped with a laboratory condenser to confine the gaseous products and guarantee no release to the atmosphere, with a potential loss of mass. Continuous stirring was provided during each test using a magnetic stirrer and a stirring plate (VELP SCIENTIFICA, model AREX DIGITAL). All tests were performed at room temperature and at pH 3.0 $\pm$ 0.5, during 120 min and at a stirring speed of 200 rpm.

Temperature was monitored throughout the experiments, while the pH was set at 3.0 due to being inside the optimal range [39,51].

In each test, samples were collected throughout time for TOC and COD monitoring. Three samples of 10 mL were collected to measure COD at times 0, 5 and 120 min. Eight samples of 5 mL each were collected to measure TOC at times 0, 5, 10, 15, 30, 45, 90 and 120 min. In the end of the experiments, residual H_2O_2 was readily measured, and the remaining effluent was preserved in the dark at 4 ºC to measure O&G, conductivity, sulphides, phenolic compounds, pH and sludge concentration (this last parameter was only considered in the test performed under the optimized conditions).

In order to stop the reaction and carry out TOC analysis, Na_2SO_3 (which instantaneously consumes residual H_2O_2) was added to the sampling flasks at a concentration 5 times higher than the stoichiometric concentration to ensure the degradation of all the H_2O_2 added. To stop the reaction and further carry out COD analysis, pH was increased, leading to a quick stop of the catalyst activity, since Fe^{2+} form is converted into Fe^{3+} at basic pH and precipitates as $Fe(OH)_3$. Moreover, H_2O_2 decomposition into H_2O and O_2 is accelerated under basic conditions.

4.3.3.3 Neutralization and liquid-liquid extraction (pilot scale)

Having learned from the optimization of neutralization at lab scale (section 4.3.3.1), a treatment consisting in neutralization followed by liquid-liquid extraction was addressed at pilot scale to evaluate this technology under more realistic conditions, using a pilot unit (*Idratech, Srl*; Figure 4.1).

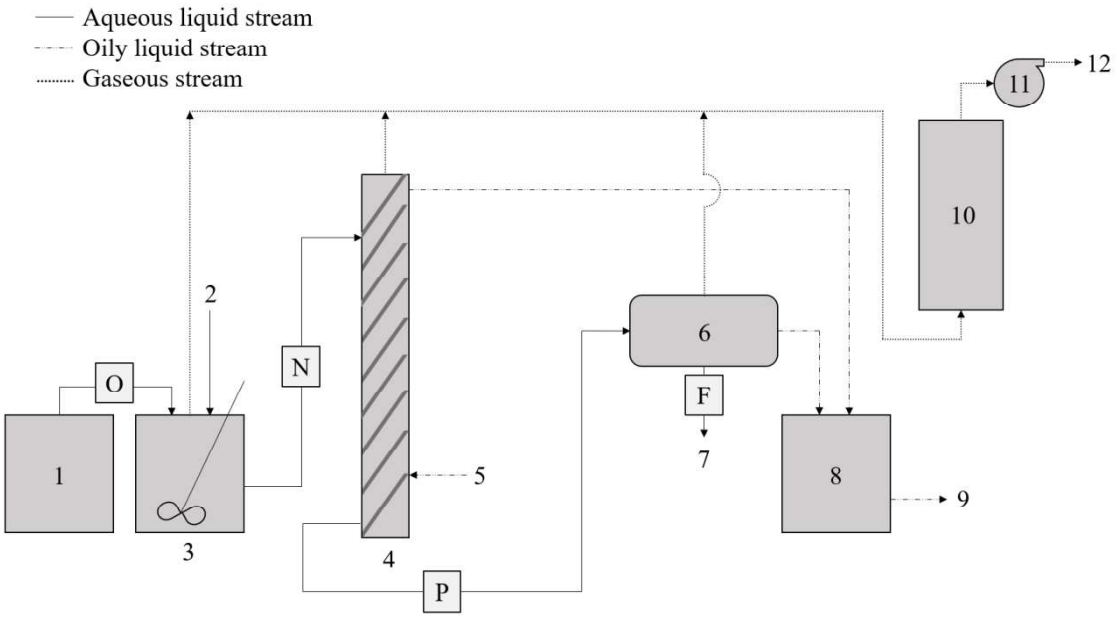

Figure 4.1 - Schematic diagram of the pilot scale unit set-up. 1 – spent caustic tank; 2 – concentrated H2SO4, 96%; 3 – neutralization tank; 4 – liquid-liquid extraction column; 5 – fresh kerosene; 6 – deoiling system; 7 – treated effluent; 8 – slops/exhausted kerosene reception tank; 9 – slops to be reintroduced in the process; 10 – activated carbon column; 11 – blower; 12 – clean gaseous stream. Points for sample collection: O – original spent caustic; N – neutralized spent caustic; P – pre deoiling; F – treated effluent).

The basis and concept of this treatment are conveniently described in patent n. US 7,160,458 B2, 2007 [138] and are briefly described below.

Neutralization takes place in tank 3 where the addition of sulphuric acid promotes the adjustment of pH and the conversion of organic compounds from the ionic to the non-ionic form - e.g. acids, aldehydes, etc. (Eq 4.6 – 4.9). This chemical transformation leads to the formation of two phases: a polar phase and an organic phase that contains the organic compounds originally present in spent caustic. The organic phase is very rich in oxygenated and sulphur compounds so it can be managed as a slop stream. Pezzeta *et al.* [138] refer the destination of this organic stream as a crude, gas oil or gasoline reservoir, specifically if this unit is incorporated in a petrochemical complex, the exhausted kerosene can be reused in other units of the latter. Slops are liquid waste produced in several refining operations that can be reintroduced in the process given their high content in hydrocarbons. Slops are not compatible with product specifications but are compatible with fresh oil (therefore slops can be reprocessed). As such, the resulting organic phase becomes very valuable as it is possible to refine along with fresh crude oil. The sampling point of neutralized spent caustic is located right after tank 3 (point of collection *N* in). The liquid outcome of tank 3 gets into column 4 to be washed with kerosene

(stream 5), which will extract the organic phase formed during neutralization. The liquid-liquid extraction takes place in column 4. Kerosene from the Merox unit where spent caustic is generated was added to the extraction column to be used as the extraction solvent. After this process, the organic phase leaves the column by the top along with the kerosene and both are forwarded to the slops reception tank (tank 8), as exhausted kerosene.

A common practice in refineries is to introduce phenolic water into the desalter unit to extract phenolic compounds to crude oil and then thermally degrade them in the atmospheric distillation unit (especially in the top levels). By the end, the small fraction of phenolics that remain after distillation present higher boiling points and leave in heavier cuts, which will be submitted to thermal and catalytic cracking processes. A similar study has been performed by Hoffmann *et al.* [65], where phenolic compounds in caustic wastewaters are extracted to crude oil in a storage tank, however it is referred the desalter unit as a possible alternative. The same logic can be applied to the organic contaminants concentrated into the oily layer that is extracted to kerosene, producing the exhausted kerosene.

The polar phase leaves column 4 by the bottom (point of collection *P* in Figure 4.1) and passes through a deoiling system (drum 6), which consists of a phase separator equipped with a plastic floatable accessory with a rugged and lumpy structure that guarantees a very efficient phase separation and, consequently, the recovery of all possible organic products (the remaining organic traces that are still present in the polar phase). The collected organic phase traces are forwarded to the slops tank (tank 8). The resulting polar phase from the deoiling system is the treated effluent (stream 7). The gaseous streams containing hazardous components produced in each step of the treatment (e.g. H_2S) are recovered, pass through an activated carbon filter for cleaning (column 10) and are then, released into the atmosphere using a blower.

The pilot unit comprises three feed pumps: one for spent caustic (from tank 1 to tank 3), other for H_2SO_4 (to be introduced in tank 3) and the other to feed the column with fresh kerosene (column 4). The unit contains two flow meters, one for spent caustic and the other for fresh kerosene. The unit comprises a 40 cm pH meter probe that is introduced in tank 3 to allow a continuous monitoring of pH during neutralization. The unit operates at normal temperature and pressure.

Samples of 1 L were collected in glass bottles from the four collection points depicted in Figure 4.1: *O*, *N*, *P* and *F*. Collection point “O” refers to “original effluent”, “N” refers to “after neutralization”, “P” refers to “pre deoiling system” and “F” refers to “final/treated effluent”. They were collected exactly 2 hours after setting the operating conditions of the system in each

test. The following parameters were then determined to evaluate the process performance: COD, phenolic compounds, O&G and sulphides. pH and conductivity were measured in each sample, right after collection.

In this study, operating conditions were optimized in view of the maximum removal of contaminants, considering (i) the lowest acid consumption, this is, the highest possible pH during neutralization as well as (ii) the most suitable ratio between spent caustic and kerosene flow rates (L/h) getting into the liquid-liquid extraction column, allowing for a minimum kerosene consumption. A first set of seven tests were carried out for this purpose using effluent 4 (Table 4.1) and a second set of three tests with effluent 5 (Table 4.1), according to Table 4.3.

Table 4.3 - Operating conditions tested in the neutralization and LLE unit.

Effluent 4		
Test	**Neutralized spent caustic pH**	**Ratio of spent caustic:fresh kerosene flow rates**
1	5 - 6	150:20
2*	5 - 6	150:20
3	5 - 6	120:20
4	5 - 6	200:20
5	< 4	270:20
6	< 4	250:20
7	< 4	120:20
Effluent 5		
Test	**Neutralized spent caustic pH**	**Ratio of spent caustic:fresh kerosene flow rates**
1	2	160:20
2	4	240:30
3	4	100:20

*Test 2 was performed with diluted spent caustic (1:2) with water before neutralization to assess the impact of the concentration of the components on the process performance.

The runs using effluent 4 were proposed in order to test a broad range of pH, as well as flow ratios between spent caustic and fresh kerosene. Aiming at acid consumption minimization, only pH 2 and 4 were tested in subsequent tests using effluent 5. The selection of the tested flow ratios was based on the minimization of fresh kerosene consumption. Flow rates of spent caustic and kerosene are provided in L/h.

4.3.3.4 Analytical Methods

Samples collected for COD analysis after Fenton reaction were pre-treated by adding a solution of NaOH (25 %) to increase the pH up to 11. After the catalyst precipitation, the supernatant was collected and its pH was corrected to neutral by means of the addition of a H_2SO_4 solution (5 M). COD was measured using the LCK 014 kit (HACH) and a DR 3900 spectrophotometer (HACH) after the digestion of the samples in a HT 200 S digester (HACH LANGE).

The quantification of residual H_2O_2 was performed as described by Sellers (1980) [139], using an UV-Vis spectrophotometer, model Evolution 300 (Thermo Scientific).

Samples for TOC analyses after neutralization, Fenton reaction and LLE extraction were prepared by collecting the supernatant of each sample after the settling of sludge formed with excess of Na_2SO_3 and diluting the supernatant 200 times with Mili-Q water to ensure that the TOC concentration would fit within the calibration curve of the TOC equipment. TOC was then measured in a TOC-V Series TOC Analyzer (Shimadzu). Sulphides, sulphates and phenolic compounds were determined by spectrophotometry using a DR 3900 spectrophotometer (HACH LANGE) as well as the LCK 653 kit, SulfaVer® 4 and LCK 346 kit from HACH, respectively. Oil and grease (polar and non-polar) was measured according to the Standard Method SMEWW5520 C/F [82], after sample dilution to ensure that the concentration would fit into the calibration curve of the NICOLET 6700 FT-IR. The conductivity was measured using a conductivity meter model LF 320 (WTW) while pH was measured using a pH 1100 L pH meter (VWR) and temperature with an alcohol thermometer (VWR). Reaction glass flasks (250 mL) were used for Fenton experiments (VWR), as well as a magnetic stirring plate (VELP SCIENTIFICA).

In order to assess biodegradability and toxicity, the residual H_2O_2 in the oxidized spent caustic sample (effluent 3, Table 4.1) was firstly removed by adding a 25 % NaOH solution until pH of 12, rest for a 24 hour period and then the addition of a 5 M H_2SO_4 solution until final pH of 7 - 8.

Biodegradability was assessed by respirometry, measuring the oxygen uptake rate (*k*) at 20 ºC. First, the samples were inoculated with biomass from the activated sludge tank of a WWTP treating refinery effluent, and the concentration of dissolved oxygen was recorded for 30 min, using an YSI Model 5300 B biological oxygen monitor. The specific uptake rate of dissolved oxygen (*k'*) was calculated by dividing the decay rate of the dissolved oxygen (mgO_2/L.h) by the volatile suspended solids concentration after the addition of the inoculum (625-725 mg/L).

The toxicity of the effluent was evaluated after correcting the pH of all the samples to 7 - 8 using H_2SO_4 (5 M) (in the case of original spent caustic) and NaOH (25%) (in the case of Fenton reactions), through the inhibition of *Vibrio fischeri* in accordance to the standard DIN/EN/ISO 11348-3, i.e., assessing the bioluminescence after contact times (between the samples and the bacteria) of 5, 15, and 30 min, at 15 ºC, in a Microtox Modern Water model 500 equipment.

All analytical determinations were carried out in duplicate, and the coefficient of variation was less than 8.0 % for TOC, 9.0 % for COD, 10.0 % for phenolic compounds, 3.0 % for sulphides and 6.0 % for O&G (total and polar). In Fenton experiments, the coefficient of variation was less than 12.0 % for temperature and 10.0 % for pH.

4.4 Results and Discussion

4.4.1 Neutralization (Lab Scale)

Neutralization with mineral acids as a chemical treatment is a well known and classic process for several types of effluents [6]. During the acidification process, sulphuric acid is added to the spent caustic, producing the release of sulphides and mercaptans in the form of acid gases (H_2S) and VOCs. The naphthenic acids, a major compound class that is formed from the sodium salts that exist originally in the spent caustic, are expected to be concentrated in an oily layer after neutralization, giving origin to two phases: an organic phase and an aqueous phase [9,95]. Neutralization was therefore tested to evaluate its effectiveness towards the removal of polar O&G in naphthenic spent caustic effluents (in other words polar O&G concentration in the polar phase, given that treated spent caustic is based on the polar phase that is formed during neutralization).

The three naphthenic spent caustic effluents collected to address neutralization in this study (effluents 1, 2 and 3 in) were obtained from acid crude oils processing, the main factor responsible for the increase in the concentration of polar O&G in the naphthenic spent caustic. These samples were collected at different dates to address the robustness and versatility of this treatment process towards spent caustic matrices with different compositions. Since the optimum pH range for Fenton oxidation is between 2.5 and 4.5 [134], neutralization tests were carried out at pH 3 and 5 aiming at applying a Fenton's process afterwards to improve the quality of the effluent.

Although several attempts were carried out to analyse the composition of the organic phase (e.g. COD, TOC), it was not possible to adapt for this purpose the conventional methods described for the analysis of aqueous solutions given the oily nature of these phase samples. However, it was possible to quantify O&G (both polar and non-polar) in this phase since a non-polar solvent is used in the analysis. Figure 4.2 presents the recovery of O&G in organic phases after neutralization at pH 3 and 5.

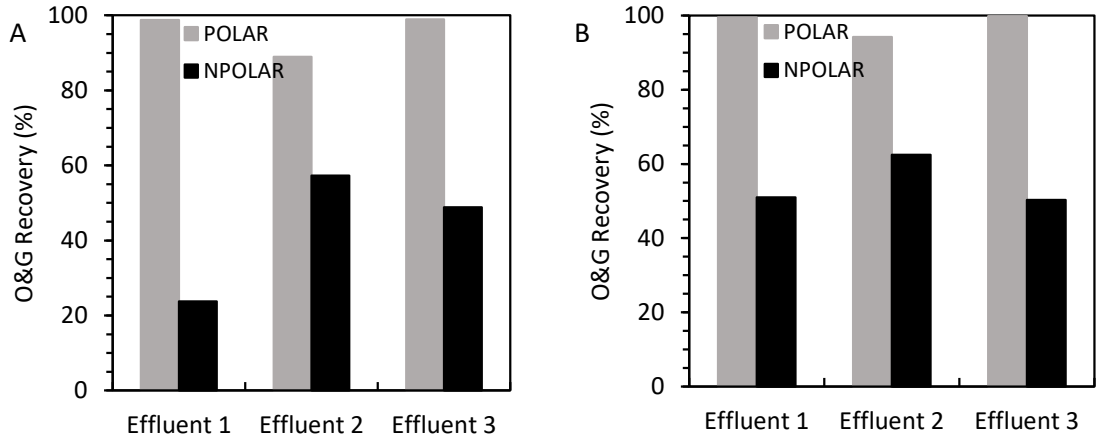

Figure 4.2 - O&G recovery in organic phases after neutralization: (A) pH 3; (B) pH 5. The composition of effluents 1, 2 and 3 is detailed in Table 4.1.

O&G contaminants were similarly extracted to the organic phase during neutralization at both pHs tested, regardless of the different characteristics of the initial effluents (Table 4.1). Given the aqueous nature of the polar phases, their composition in terms of TOC, COD, O&G, phenolic compounds and sulphides could be attained. Moreover, the decay of TOC throughout time was monitored during neutralization, as shown in Figure 4.3.

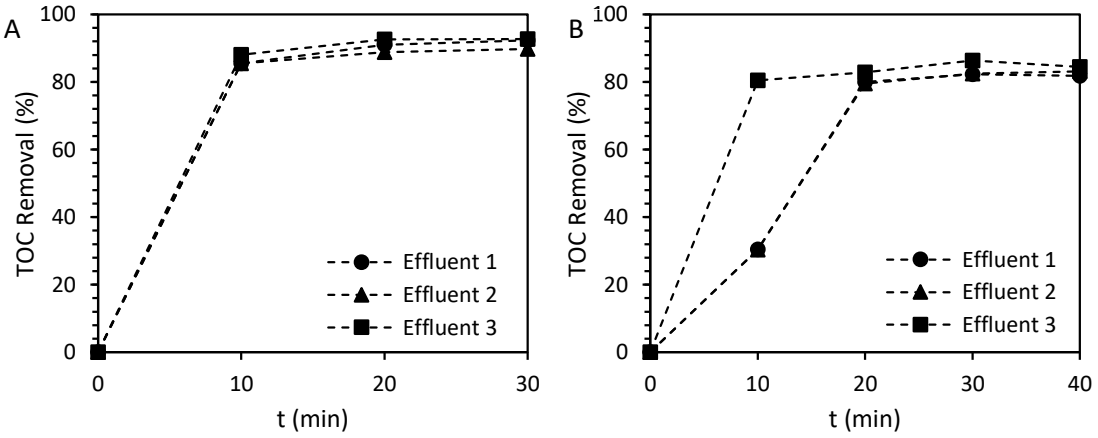

Figure 4.3 - TOC removals during neutralization for the polar phases at pH 3 (A) and pH 5 (B). The composition of effluents 1, 2 and 3 is detailed in Table 4.1.

As illustrated in Figure 4.3, TOC stabilization is usually achieved within approximately 10 min, apart from effluents 1 and 2 at pH 5, for which lower TOC removals were achieved at 10 min (approximately 30 %) and a longer period was required to attain a stable TOC removal (20 min). Therefore, the composition of the effluents seems to impact the efficiency of neutralization. Furthermore, although high TOC and COD removals were obtained in the end of the experiment at both pHs (88 - 93 % TOC removal at pH 3 and 75 - 84 % TOC removal at pH 5; 86 – 95 % COD removal at pH 3 and 85 - 90 % COD removal at pH 5), neutralization patterns seem to be pH dependent since lower pHs favour TOC removal. Neutralization was proved to have better performance at lower pH values, however there is an optimal value, different for each spent caustic. This means the removals (in terms of COD and TOC) differ from one effluent to the other. Another consideration is related with the nature of spent caustic itself. Different naphthenic spent caustics are obtained every day in a refinery, which depends on the production plan operating conditions and the crude oils to be processed. Crude oils with a total acid number higher than 0.10 mg KOH/g seem to produce more concentrated spent caustics, therefore producing very different TOC and COD values depending on the collection date. Still, it should be considered that COD is sensitive also to inorganic compounds susceptible of being oxidized, not only to the organic ones as TOC.

To further assess neutralization efficiency towards the removal of TOC, COD, O&G, phenolic compounds and sulphides, polar phases were analysed (Figure 4.4).

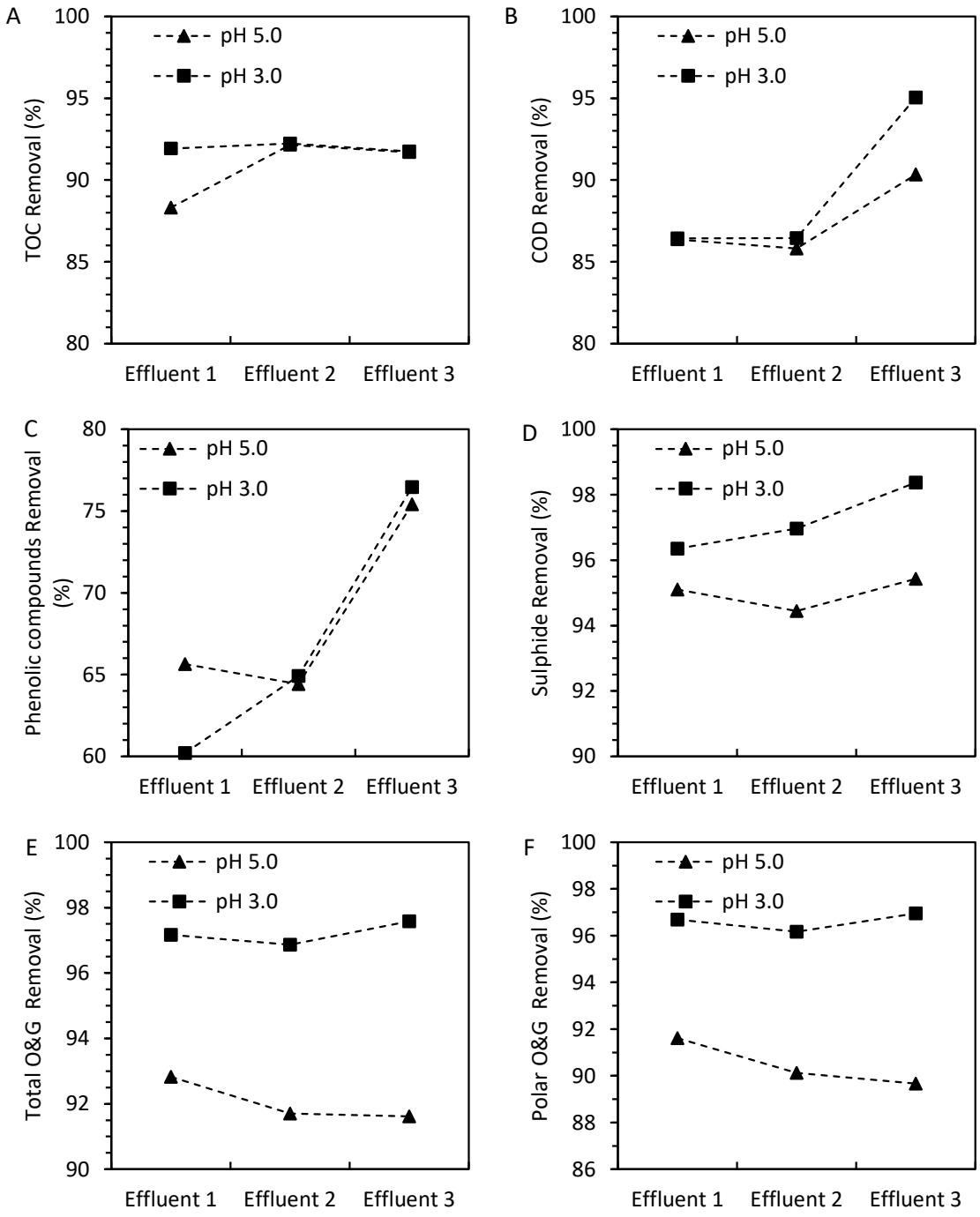

Figure 4.4 - Removals from polar phases after neutralization at pHs 3 and 5: (A) TOC; (B) COD; (C) phenolic compounds; (D) sulphide ; (E) total O&G; (F) polar O&G . The compositions of effluents 1, 2 and 3 are detailed in Table 4.1.

Figure 4.4 shows that neutralization was very effective to remove organic contaminants in the polar phase. In general, it could be pointed out that pH 3 favours organics removals, especially sulphides and polar O&G. Furthermore, the highest removals were obtained for

effluent 3, which is the effluent with the highest concentration of organics (higher COD and polar O&G).

Sulphate removal is not shown in Figure 4.4 because a high concentration of sulphate was generated as a result of sulphuric acid addition (as confirmed after carrying out the same neutralization procedure using chloridric acid instead, without any sulphate formation – data not shown). Due to the dilution effect observed in the effluent pre-treatment system, the concentration of sulphate is decreased by approximately 150 times, leaving behind any environmental problem that could arise. Besides, it appears to not be so environmentally concerning as the other contaminants [95].

These results corroborate previous studies [19] in terms of VOCs and H_2S release during neutralization. The addition of the acid is likely to promote the release of VOCs and H_2S into the gaseous phase while the organic contaminants that are not volatile are extracted into the organic phase (Eq 4.5 - 4.9). At high pH values, all components are present in their ionic form, preventing liquid-liquid extraction to separate non-polar from polar species. The acidification of the medium enables the conversion of several ionic species to their non-ionic form. Consequently, H_2S is emitted given that it is one of the ionic species that are sensitive to temperature increase during acidification and it is one of the products of neutralization of mercaptans. In terms of environmental regulations, H_2S is a very controlled air pollution substance causing bad odours, thus, a careful destination must be planned for this contaminant.

Table 4.4 presents the final concentrations obtained for the treated effluents by neutralization. These results do not include the dilution effect that occurs within Sines refinery treatment system. When defined, the discharge limits set by the municipal wastewater treatment plant (that avoid penalties related with the discharge of effluents with low quality from Sines refinery) are also presented for comparison.

Table 4.4 - Concentration of the contaminants in the polar phases after neutralization of the effluents 1, 2 and 3 at pHs 3 and 5. The column on the right shows the maximum limits for wastewater discharge imposed to Sines refinery by the WWTP.

	Effluent 1		**Effluent 2**		**Effluent 3**		**Discharge Limits [4]**
pH after neutralization	**3**	**5**	**3**	**5**	**3**	**5**	
TOC (mg C/L)	1651	2385	1698	1715	1813	1823	Not monitored
COD (mg O_2/L)	11470	11530	11002	11521	5060	9880	150
Phenolic compounds (mg/L)	995	859	772	783	449	469	5
Sulphides (mg/L)	1.1	1.5	0.8	1.5	0.6	1.6	2
Sulphates (g/L)	25	25	23	23	27	21	Not monitored
Total O&G (mg/L)	432	1095	462	1221	459	1591	5
Polar O&G (mg/L)	432	1095	462	1189	459	1556	Not monitored
Non-polar O&G (mg/L)	0	0	0	32	0	35	Not monitored
Conductivity (mS/cm)	35.3	35.4	34.2	34	33.1	32.5	Not monitored

Comparing the obtained final concentrations with the discharge limits depicted in Table 4.4 and the dilution effect that occurs, where the concentrations are approximately 150 times more diluted, it can be concluded that further treatment is still required to improve the quality of the neutralized effluent since it presents an impact of 60% (w/w) in the final effluent in terms of polar O&G. Given that the maximum O&G concentration discharge is 5 mg/L, the direct discharge into the local municipal wastewater treatment plant is still limited.

4.4.1.1 Fenton Oxidation (Lab Scale)

Process optimization

Fenton oxidation was tested as a polishing treatment of the neutralized effluent (polar phase). In order to proceed with the optimization of the operating conditions of Fenton oxidation, a single effluent was selected - effluent 3 (). This selection was based on its higher concentration in organics, namely COD and polar O&G. The strategy for Fenton optimization included both the oxidant (Phase 1) and the catalyst (Phase 2, using the optimum oxidant concentration) concentrations, as shown in Table 4.2. To determine the optimum oxidant concentration, TOC removals were obtained, together with pH and temperature profiles (Figure 4.5).

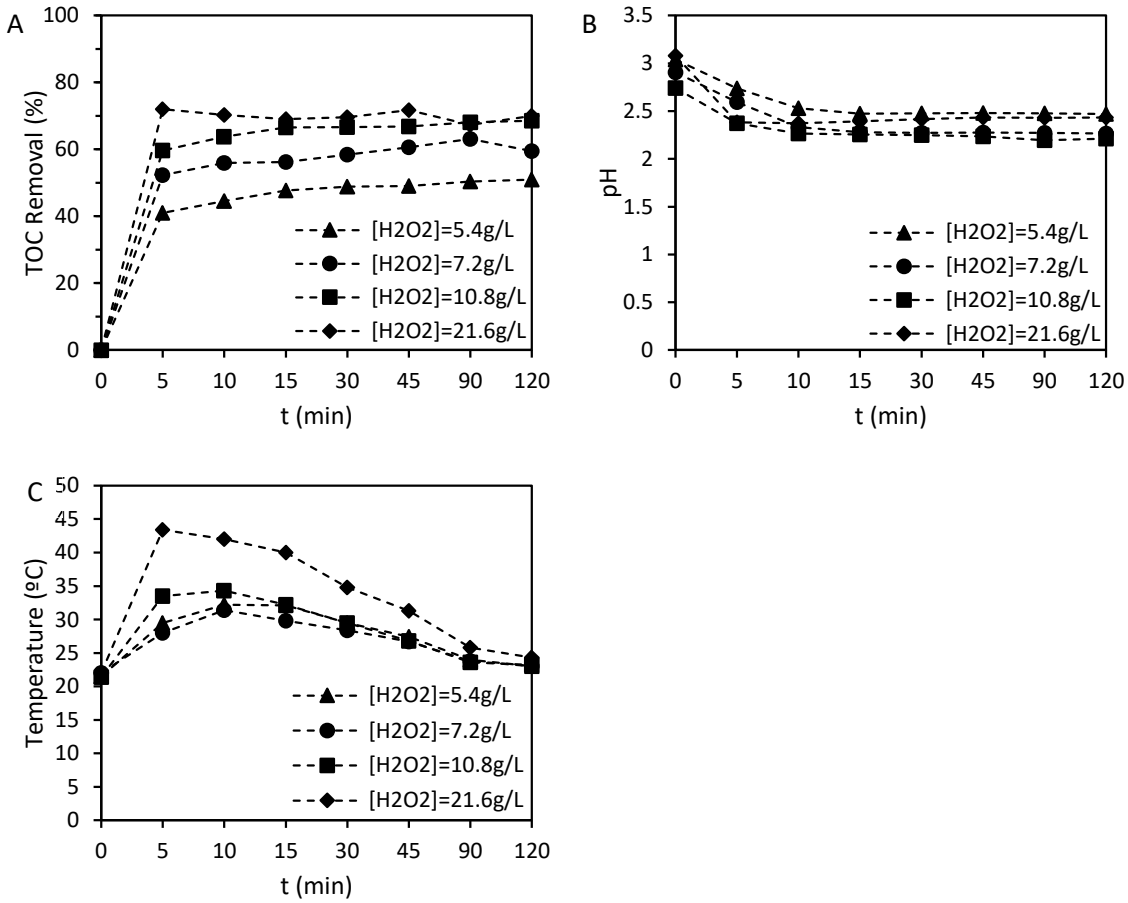

Figure 4.5 - Profiles of (A) TOC removal, (B) pH and (C) temperature during oxidation tests performed for the optimization of the oxidant concentration (Fe^{2+}:H_2O_2 = 1:5). Operating conditions are detailed in Table 4.2.

Hydrogen peroxide is the responsible for the formation of $HO^{\bullet}$ radicals. It is interesting to observe in Figure 4.5 A that the trend of TOC removal is similar for all the conditions tested: a sharp increase is observed within the initial 5 min period, then between 5 and 15 min an increase still occurs but gradual and after, a plateau is reached. Furthermore, TOC removal increases with the concentration of oxidant applied since as the oxidant concentration increases, the reaction gets faster and oxidation occurs mostly within 5-15 min of reaction (51 – 70 % TOC removal). However, final overall mineralization is similar (approximately 70 %) in tests 3 and 4 (oxidant concentration of 10.8 and 21.6 g/L respectively, as shown in Table 4.2), which can be related with the well-known scavenging effect of the radicals due to the excess of oxidant (Eq 4.12). Globally, considering neutralization and Fenton oxidation, maximum TOC and COD removals were 97 % and 99 %. Therefore, the optimum concentration of oxidant is the stoichiometric one, in this case, 10.8 g/L. Noor *et al.*, (2011) [95] obtained an optimal oxidant amount for a stoichiometric H_2O_2/COD of 1.1. Sheu *et al.*, (2001) [94] report the same result for optimum

oxidant amount (H_2O_2/COD of 1.1). In the present work, where a completely different spent caustic is treated, best results were found for the stoichiometric ratio, i.e. H_2O_2/COD ratio of 1. The pH profile depicted in Figure 4.5 B is typical of Fenton oxidation, showing a higher pH decay during the highest TOC removal increase in the first 5 min, which is probably related with the formation of carboxylic acids during the oxidation of organic matter [19].

Temperature profiles depicted in Figure 4.5 C show that there is a tendency for a temperature increase with increasing oxidant concentration in the beginning of the oxidation process, particularly for the highest concentrations (10.8 and 21.6 g/L). The maximum temperature increase (approximately 25 ºC) was determined for test 4 (Table 4.2) within a very short period of time. Generally, the maximum temperature values and the maximum pH were attained at similar times. Such behavior is related with the strong organic load of the effluent and the exothermicity of the oxidation reactions, as also observed by other authors [135]. In this study, H_2O_2 is used to oxidize the polar phase formed after neutralization of spent caustic. Given that the temperature of the polar phase did not in any occasion increase beyond 30 ºC and that the breaking down of H_2O_2 into water and oxygen occurs between 40-50 ºC [136], the performance of Fenton process, under the conditions employed, should not be compromised by H_2O_2 degradation due to heat.

The optimization of the catalyst (Fe^{2+}) concentration plays an important role in the Fenton process by promoting the decomposition of the H_2O_2 molecules to form the $HO^{\bullet}$ species [134]. In Table 4.2, test 6 did not allow the collection of the sample to measure COD because the formation of sludge was much higher than the total volume of the sample. Figure 4.6 presents TOC removals as well pH and temperature profiles obtained for phase 2 of optimization, regarding the catalyst concentration.

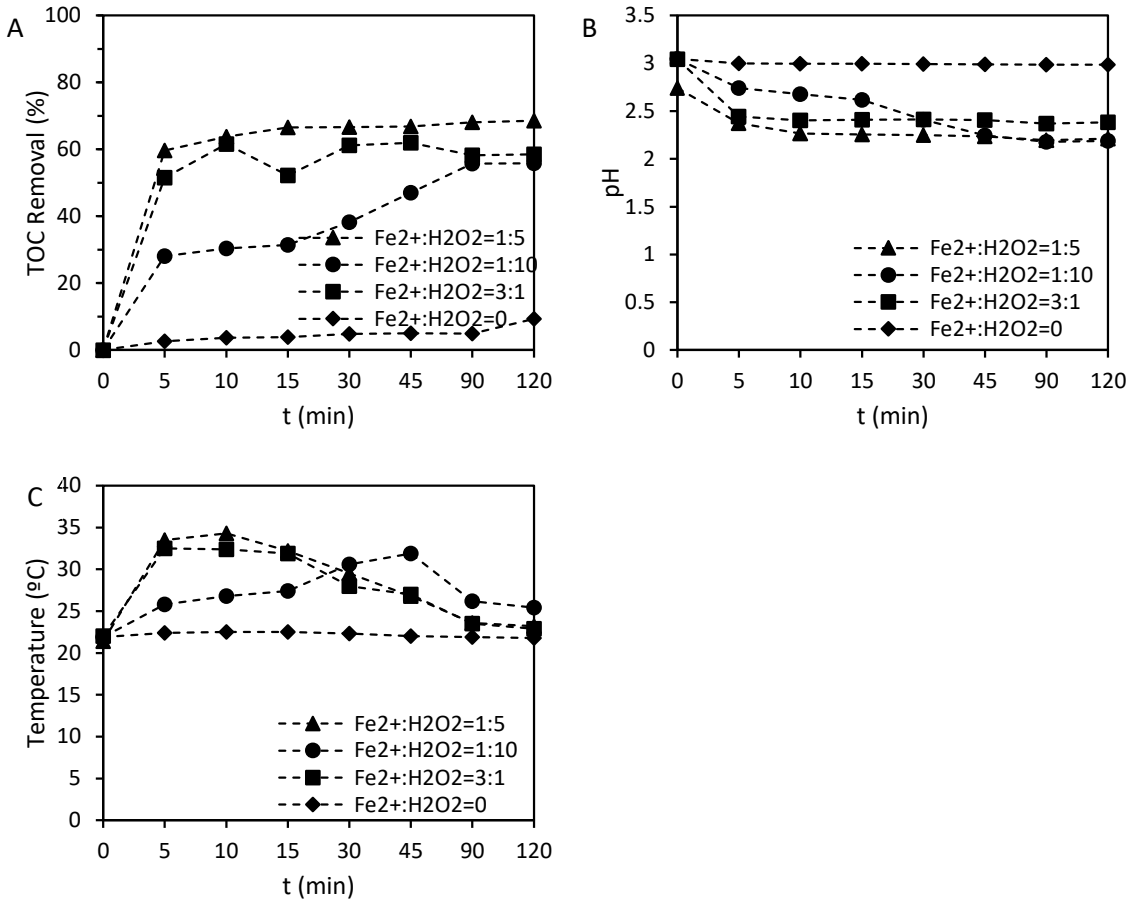

Figure 4.6 - TOC removal during oxidation tests performed for the optimization of catalyst concentration ($[H_2O_2]$ = 10.8 g/L). (A) TOC removal; (B) pH profile; (C) Temperature profile. Operating conditions are detailed in Table 4.2.

When no catalyst was applied (test 7; Table 4.2), the degradation observed (9 %) was very low due to the weak oxidation potential of hydrogen peroxide in the absence of a catalyst (Figure 4.6 A). In this case, as expected, pH and temperature remained almost unchanged (Figure 4.6 B and C). Figure 4.6 A shows that using half of the concentration of the catalyst applied in phase 1 (test 5 - Fe^{2+}:H_2O_2 - 1:10; Table 4.2) results in a lower TOC removal (56 %) compared with the initially tested catalyst concentration (test 3 - Fe^{2+}:H_2O_2 - 1:5; Table 4.2) (70 %). A catalyst concentration three times higher (test 6 - Fe^{2+}:H_2O_2 - 3:1; Table 4.2) is not better either, probably because this concentration is excessive and, thus, likely to inhibit oxidation reactions due to radical scavenging reactions between the catalyst in excess and the hydroxyl radicals (Eq 4.13) [135]. Interestingly, the temperature profiles obtained in both optimization phases (Figure 4.5 C and Figure 4.6) are very similar, being none pronounced and in shorter times for higher catalyst dose.

Overall, both Figure 4.5 and Figure 4.6 show good TOC removals (70 % and 59 % maximum removal of TOC during oxidant and catalyst optimization stages, respectively). Furthermore, it is interesting to observe that only approximately 10 min were required to achieve 95 % of the maximum TOC removals obtained in all tests.

Considering all the results obtained during both optimization phases, the optimum conditions for the Fenton treatment of the spent caustic effluents tested are: 10.8 g/L of H_2O_2 and a Fe^{2+}:H_2O_2 molar ratio of 1:5. A residual concentration of H_2O_2 of 0.0034 M was obtained. The composition of the effluent treated by neutralization followed by Fenton oxidation, both at the optimized conditions attained in this study, as well as the final removals obtained, are depicted in Table 4.5.

Table 4.5 - Characterization of the final treated effluent after neutralization and Fenton oxidation. The column on the right shows the maximum limits for wastewater discharge imposed to Sines refinery by the WWTP. LOD – limit of detection.

	Removal (%)	**Concentration in the treated effluent**	**Concentration in the treated effluent after dilution effect**	**Discharge Limits [4]**
TOC (mg C/L)	69	571	-	Not monitored
COD (mg O_2/L)	80	994	< LOD	150
Phenolic compounds (mg/L)	95	23.6	0.2	5
Sulphides (mg/L)	100	0.04	< LOD	2
Sulphates (mg/L)	0	27000	-	Not monitored
Total O&G (mg/L)	95	25	0.2	5
Polar O&G (mg/L)	95	25	-	Not monitored
Non-Polar O&G (mg/L)	100	0	-	Not monitored

Generally, very high removals were obtained for the chemical-physical parameters addressed. Except for TOC (69 %), removals higher than 80 % were determined for all the other parameters. Comparing the composition of the effluent with the target limits and still considering the dilution effect of 150 times, it is possible to conclude that the parameters of the treated effluent are within the Sines Refinery imposed discharge limits.

The final effluent presented a darker coloration compared with the initial one as a result of the oxidation reactions. Concurrent with this observation, sludge was formed (6.4 g/L) due to the precipitation of iron, concurrent with a previous study [140]. When Fenton process is considered, metallic sludge is produced. Several destinations with different costs may be considered but one of the most common practices nowadays is to treat it and recover the iron

to be reused as catalyst [140]. Alternatively, one could consider in future work the so-called heterogenous Fenton process, wherein the active phase (iron species) are fixed in a solid matrix support (e.g. zeolite, activated carbon, clay, etc.) [141,142], thus considerably decreasing or avoiding the presence of the metal in the final effluents.

Biodegradability and Toxicity assessment

Biodegradability and toxicity through inhibition of *Vibrio Fischeri* were assessed for the treatment comprising neutralization and Fenton oxidation of effluent 3 (composition presented in Table 4.1). The selection of effluent 3, as mentioned previously, was based on its higher concentration in organics, namely COD and polar O&G. The following samples were analyzed: original spent caustic, neutralized spent caustic (only polar phase) and oxidized spent caustic (after Fenton oxidation), on Table 4.6.

Table 4.6 - Biodegradability and toxicity results for original spent caustic (effluent 3), neutralized spent caustic (only polar phase) and oxidized spent caustic (after Fenton oxidation).

	Biodegradability (mg O_2/(gSSV.h))	Inhibition of *Vibrio Fischeri* 5 min (%)	Inhibition of *Vibrio Fischeri* 15 min (%)	Inhibition of *Vibrio Fischeri* 30 min (%)
Original spent caustic	< 0.002	100	100	100
Neutralized spent caustic	5	61	64	71
Oxidized spent caustic	16	19	24	28

Biodegradability and toxicity tests aimed at evaluating the potential of the final effluent to be further treated by conventional treatments applied in wastewater treatment plants, which often includes a biological process as secondary treatment. Table 4.6 shows a considerable increase in the biodegradability of the effluent after neutralization (from a value lower than 0.002 to 5 mg O_2/(gSSV.h)), and particularly after Fenton oxidation (to 16 mg O_2/(gSSV.h)). This trend has been previously reported by other authors. As an example, Rodrigues *et al.* [136] observed an increase in biodegradability from lower than 0.2 to 16.5 O_2/(gSSV.h) using Fenton process coupled with coagulation/flocculation to remove organic loads from dyes. The results obtained in the present study indicate that the technologies optimized in this study improved the potential for further treatment in wastewater treatment plants.

Toxicity tests provide useful and complementary information for removal profiles since TOC removal was not complete and molecules with higher toxicity than the ones that were degraded may be generated. Table 4.6 shows a huge decrease in the toxicity of the effluent, particularly after Fenton oxidation, suggesting that the contaminants are transformed into less toxic ones during the treatment. Data obtained is in line with previous studies: Rodrigues *et al.* [136] reported a decrease in toxicity through a decrease in *Vibrio Fischeri* inhibition from 94-97 to 24-35 % at 60 min, while Rueda-Márquez *et al.* [143] obtained a decrease from 40 to 15 % with the application of H_2O_2 photolysis and catalytic wet peroxide oxidation to a refinery wastewater. Therefore, after neutralization and Fenton oxidation, the effluent becomes more amenable for direct discharge into the effluent pre-treatment system and, consequently, for discharge into the municipal wastewater treatment plant.

4.4.2 Neutralization followed by liquid-liquid extraction (Pilot Scale)

Neutralization was found to be a key process in the treatment of spent caustic effluents in this study due to their extremely high pH. Therefore, it was decided to test this process at pilot scale. Given the efficiency of liquid-liquid extraction towards oily effluents [64], the combination of neutralization with liquid-liquid extraction was assessed and compared with neutralization followed by Fenton oxidation. The pilot unit configuration enabled the collection of samples throughout the process to evaluate the efficiency of each treatment stage: after neutralization, after liquid-liquid extraction, and after deoiling (Figure 4.1).

The impact on treatment performance of operating conditions such as the pH of the neutralized spent caustic and the ratio between the flow rates of neutralized spent caustic and fresh kerosene getting into the extraction column was addressed. The ratio between flow rates can vary greatly, thus, requiring optimization to increase the extraction of the organic phase to the non-polar solvent (fresh kerosene). Two sets of tests were carried out to evaluate the potential of this treatment approach towards spent caustic effluents with very different compositions in terms of polar O&G (the main contaminant of interest) – effluents 4 and 5 (Table 4.1). Effluent 4 presents a lower concentration of polar O&G and was used in the first set of tests (it is a spent caustic that derives from crude oils with total acid numbers lower than 0.10 mg KOH/g, so the original COD, TOC and O&G concentrations are much smaller than other effluents in the present work). In the second set of tests, an effluent with a much higher concentration of polar O&G (effluent 5) was studied (which derives from acid crude oils, in opposition to effluent 4). It must be noted effluent 5 represents the most common average spent caustic composition

that causes relevant impact on the final wastewater in terms of polar O&G contamination. Therefore, final conclusions on process efficiency for this treatment should focus essentially on effluent 5 treatment results.

All samples collected after each stage of the process were characterized in terms of TOC, COD, sulphides, phenolic compounds and O&G (polar and non-polar) to determine their removal in each stage (Figure 4.7).

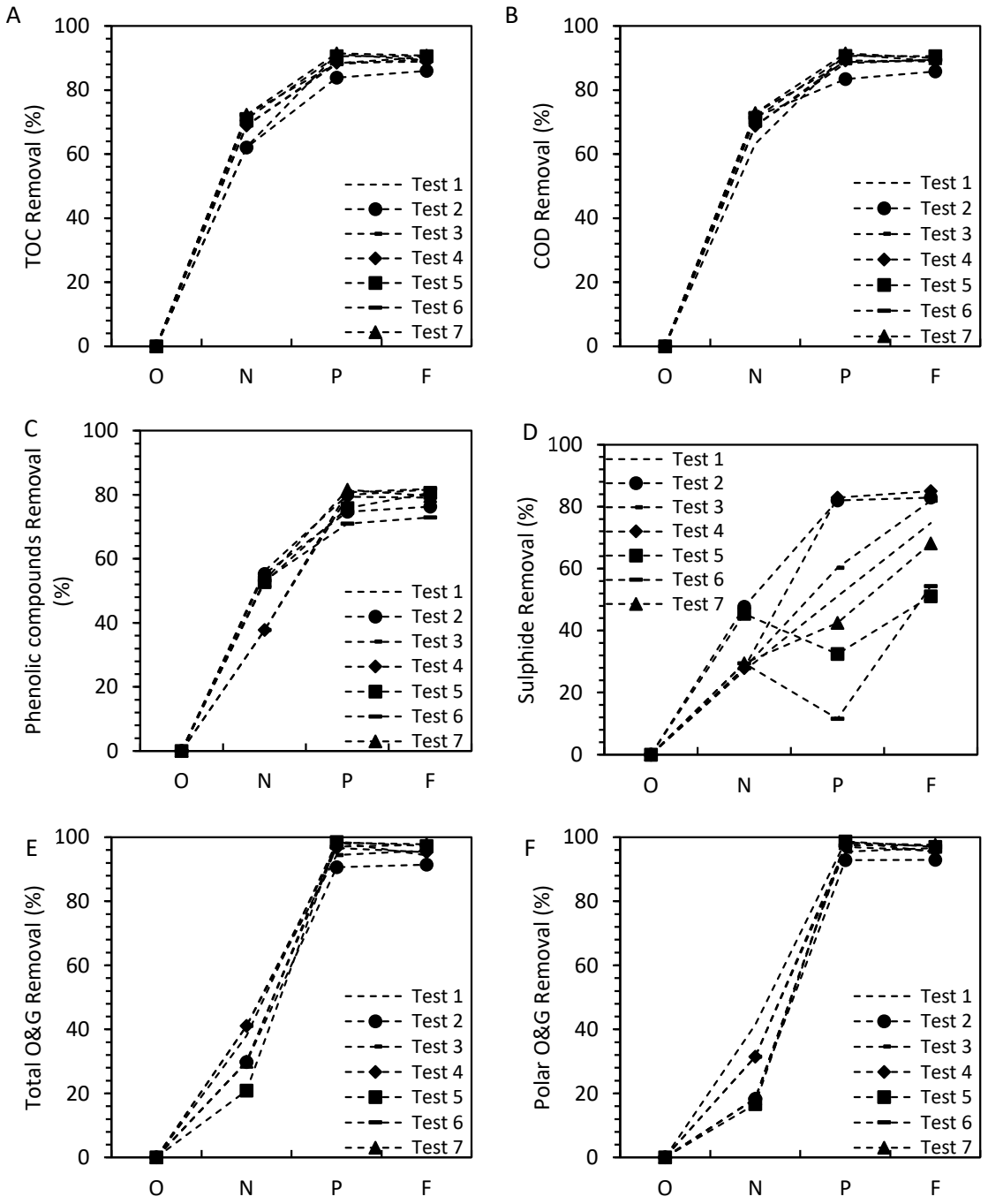

Figure 4.7 - Removal of contaminants during neutralization, liquid-liquid extraction and after deoiling at pilot scale for Effluent 4: (A) TOC, (B) COD, (C) phenolic compounds, (D) sulphide, (E) total O&G, (F) polar O&G. O – original effluent; N – neutralized effluent; P –pre deoiling effluent; F – final effluent/after deoiling. R means the ratio between spent caustic and fresh kerosene (in L/h) entering the liquid-liquid extraction column. * feed was diluted with water 1:2. To see the composition of the original effluents as well as the detailed operating conditions tested, please refer to and Table 4.3.

The removal of TOC and COD in the different stages of the treatment follow the same trend as pH and the flow ratios are changed (Figure 4.7 A and B). Similarly to lab scale experiments conducted in this study, it is clear that neutralization is responsible for a high percentage of TOC (62 – 72 %) and COD (63 – 73 %) removals. Liquid-liquid extraction also enables further interesting removal values for these parameters (84 – 91 % and 83 – 91 % for TOC and COD, respectively).

A similar trend was also obtained for the removal of phenolic compounds (Figure 4.7 C) despite the lower removals achieved (38 – 56 % and 60 – 82 % after neutralization and after deoiling, respectively). For the removal of phenolic compounds, as for sulphides (Figure 4.7 D), higher pHs and kerosene flow rates (120:20 and 200:20 L/h) were preferable. However, the removal of sulphides appears to be much more dependent on operating conditions (Figure 4.7 D). Surprisingly, an increase in the concentration of sulphides was observed after the deoiling stage at a lower pH (pH < 4) and the highest spent caustic flow rate (250:20 and 270:20 L/h), which may be caused by the increased concentration of disulphides in the kerosene (the column has more kerosene if the flow ratio admits a higher flow of kerosene per m^3 of spent caustic), as they can interfere with the sulphides detection method. Regarding O&G (Figure 4.7 E and F), extremely high removals (94 – 98 %) were obtained almost independently of the operating conditions, although lower removals were obtained after neutralization for the following conditions: very low pHs (pH < 4) and higher spent caustic flow rates (270:20 L/h). In fact, the removal of O&G is very dependent on the pH [9], particularly polar O&G, which is composed by aromatic structures that are prone to hydrolysis in the presence of an acid [96]. The very similar trends of total and polar O&G depicted in Figure 4.7 E and F further confirm the removal of polar components by this treatment, along with the complete removal of non-polar O&G. It is also noteworthy that all treated effluent samples collected after all tests presented almost no odor compared to the initial or neutralized spent caustic effluents due to the mercaptans presence. This is due to a high concentration of volatile gases and mercaptans that are released into the gas phase [9,95], proving the remarkable efficiency on removing odours.

In many processes, water is added to dilute the feed in order to decrease its aggressiveness towards the piping due to the high concentration on corrosive components [20]. To evaluate the impact of dilution in the process efficiency, a test was conducted using the diluted effluent (1:2). For the diluted effluent, lower removals were generally obtained compared with the original effluent, showing that there is no advantage in diluting. In fact,

diluting the effluent would represent an extra cost related with water consumption and energy costs since a much larger volume of effluent would be treated.

Considering all the removals attained by neutralization followed by liquid-liquid extraction as well as the target concentration values (Table 4.4), the most suitable operating conditions for this treatment are: pH 4 and flow ratio of 270:20 as spent caustic to fresh kerosene. A second set of tests was then conducted at lower pHs to address the treatment efficiency towards a more concentrated spent caustic effluent (on polar O&G). Figure 4.8 shows the removal of TOC, COD, phenolic compounds, sulphides, and O&G (total and polar) under the different operating conditions tested for effluent 5 (Table 4.1).

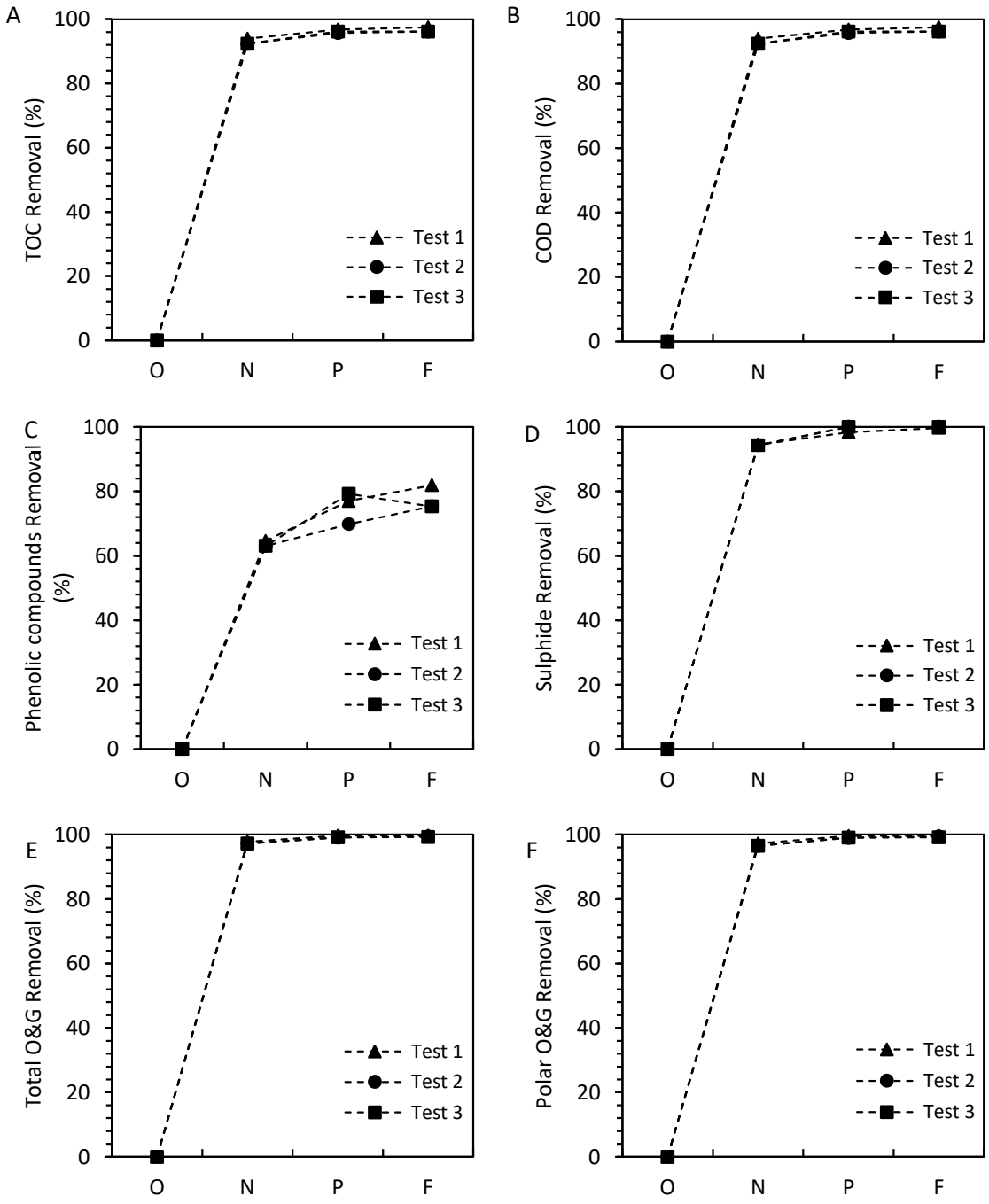

Figure 4.8 - Removal of contaminants during neutralization, liquid-liquid extraction and after deoiling at pilot scale for Effluent 5. (A) TOC, (B) COD, (C) phenolic compounds, (D) sulphide, (E) total O&G, (F) polar O&G. O – original effluent; N – neutralized effluent; P –pre deoiling effluent; F – final effluent/after deoiling. R is the ratio between spent caustic and fresh kerosene (in L/h) getting into the liquid-liquid extraction column. To see the composition of the original effluents as well as the detailed operating conditions tested, please refer to and Table 4.3.

TOC and COD (Figure 4.8 A and B, respectively) were almost completely removed after neutralization (92 – 94 %), independently of the conditions tested. For the final effluent, removals reached 98% for both parameters (the detection limit of the COD analytical method is 16.7 mg/L). Globally, considering neutralization and LLE, maximum TOC and COD removals were 96 % each. A similar trend was also observed for the removal of sulphides (Figure 4.8 D) as well as total and polar O&G (Figure 4.8 E and F). In the case of sulphides, their concentrations were determined to be below the detection limit of the analytical method (0.006 mg/L) in the final treated effluent (Figure 4.8 D). Regarding O&G, both total and polar, removals of approximately 99% were attained (the detection limit of the O&G analytical method is 0.2 mg/L) (Figure 4.8 E and F). Only phenolic compounds were removed at lower percentages: 63 – 65 % and 75 – 82 % for the neutralized and final treated effluent, respectively, showing that the pH did not impact process efficiency and the flows ratio had just a small effect. In fact, when the removals for the final effluent are compared for the highest pH (pH 4), the same removals were attained for both flow ratios assessed (R 240:30 and R 100:20), thus, lower values of kerosene flow rate are enough to attain the same efficiency. As such, a ratio of 8 is enough to ensure the complete treatment of spent caustic, i.e., for each 1000 L of spent caustic, around 125 L of kerosene were consumed in the liquid-liquid extraction and the optimum pH was 4. As said previously, the main conclusions to take about process efficiency of treatment approach 2 are based on effluent 5 (Table 4.1) treatment results, as shown in Table 4.7.

Table 4.7 - Characterization of the final treated effluent 5 after neutralization and liquid-liquid extraction. The column on the right shows the maximum limits for wastewater discharge imposed to Sines refinery by the WWTP.

	Removal (%)	**Concentration in the treated effluent**	**Concentration in the treated effluent after dilution effect**	**Discharge Limits [4]**
TOC (mg C/L)	96	942	-	Not monitored
COD (mg O_2/L)	96	3719	25	150
Phenolic compounds (mg/L)	82	522	3.5	5
Sulphides (mg/L)	100	0.04	< LOD	2
Sulphates (mg/L)	0	37000	-	Not monitored
Total O&G (mg/L)	99	99	0.7	5
Polar O&G (mg/L)	99	99	-	Not monitored
Non-Polar O&G (mg/L)	100	0	-	Not monitored

Considering the dilution of 150 times when spent caustic is discharged into the effluent pre-treatment system of the refinery after neutralization and liquid-liquid extraction, it can be concluded that the resulting final effluent to be sent to the municipal wastewater treatment plant is within the imposed discharge limits.

In sum, neutralization coupled with Fenton oxidation or LLE treat spent caustic effectively, assuring acceptable results in terms of legislation and final wastewater quality in terms of organic contaminants removals, after the dilution effect. A final decision over the most suitable technology combination depends on an economic analysis, based essentially on products costs.

4.4.3 Economic evaluation of Operating Expenses (OPEX)

A simple and preliminary economic analysis was conducted in terms of the OPEX costs related with the consumption of chemicals for the industrial scale treatment of spent caustic applying the technologies addressed in this study (neutralization followed by Fenton oxidation and neutralization followed by liquid-liquid extraction), considering the optimum conditions determined as well as the real spent caustic flow rates in Sines refinery. Only OPEX (not CAPEX) costs were accounted to give a notion of how much could be saved annually instead of paying extra costs for low quality wastewater discharge to the WWTP. The objective is to estimate the potential of these target treatment approaches for spent caustic if they are implemented. For the sake of a unit installation design, a detailed CAPEX analysis would be mandatory but such an extensive analysis is beyond the scope of the present study. For neutralization followed by liquid-liquid extraction, only sulphuric acid is employed while for neutralization followed by Fenton oxidation, iron sulphate and hydrogen peroxide are also used. Although kerosene is also used in liquid-liquid extraction as the extraction solvent, it is produced in Sines refinery and may, thus, be forwarded directly to the process. When it reaches saturation, the exhausted kerosene is managed as slop, to be reintroduced into the refinery process. So, technically, there are no losses in product, nor an additional need to buy an organic solvent. Therefore, kerosene is considered to be costless and given that it is reprocessed, it may present a gain to the refinery in terms of raw material consumption.

Table 4.8 summarize the OPEX costs determined for each technology, showing that the treatment comprising neutralization and liquid-liquid extraction would be less expensive than the treatment consisting of neutralization followed by Fenton oxidation (102.200 € vs 314.484 € - annual costs, which correspond to 5.8 vs. 18.0 €/m^3, for an effluent with a COD of almost 97 000 mg O_2/L). The costs presented were determined based on the chemicals costs and their

required amounts to treat the naphthenic spent caustic effluents produced throughout a year (365 days), considering a production flow rate of 2 m^3/h. Product costs were based on prices charged to Sines refinery by suppliers in 2019.

Table 4.8 - Predicted annual OPEX costs considering market values in 2019.

	Neutralization + Fenton (€)	**Neutralization + Fenton (€/m^3)**	**Neutralization + Liquid-liquid extraction (€)**	**Neutralization + Liquid-liquid extraction (€/m^3)**
H_2SO_4 (96 %)	122.640	7.0	102.200	5.8
$FeSO_4.7H_2O$ (99.5 %)	143.138	8.2	---	---
H_2O_2 (35 %)	48.706	2.8	---	---
Total	314.484	18.0	102.200	5.8

Chemicals costs: H_2SO_4 (96 %) = 0.233 €/L; $FeSO_4.7H_2O$ = 0.851 €/kg; H_2O_2 (35 %) = 0.112 €/L.

Considering the quality of the final effluent of the refinery in case spent caustic is treated by these processes, charges applied by the municipal wastewater treatment would be approximately 1.62 M € per year. The applied charge is the same for both technologies because the quality of the respective treated effluents is similar. Since the costs related with the discharge of the effluent in the municipal wastewater treatment plant were approximately 3.30 M € in 2019, considerable savings of 1.39 M € (neutralization and Fenton oxidation) and 1.58 M € (neutralization and liquid-liquid extraction) would be possible for Galp if such technologies could be implemented.

4.5 Conclusions

Neutralization of spent caustic was found to be an essential process in spent caustic treatment and management. pH is an important operating parameter, impacting on the removal of many contaminants (e.g. COD, O&G, phenolic compounds and sulphides).

Both Fenton oxidation and liquid-liquid extraction as post-treatments of neutralization enabled a considerable improvement of the quality of the effluent, constituting suitable treatments with substantial economic savings in terms of OPEX costs related with the current charges of discharge into the municipal wastewater treatment. In this view, the combination of neutralization with liquid-liquid extraction was found particularly attractive (savings of 1.39 M € for neutralization and Fenton oxidation and 1.58 M € for neutralization and liquid-liquid extraction, respectively). Liquid-liquid extraction was the technology that delivered a treated effluent with the highest removals (96 % for COD and 99 % for polar O&G).

Although Fenton oxidation proved to be a suitable technology to treat spent caustic because considerably high removals were achieved for COD (80%) and polar O&G (95%), further research on valorisation of the sludge produced during the process due to the high ferrous concentration could be interesting in future studies.

The results obtained in the present work may be useful for the development/optimization of industrial scale plants in petroleum refineries for the treatment of Merox spent caustic effluents, providing effective treatment alternatives and lower costs related with effluent management. However, a more realistic economic evaluation should be carried out, accounting with security and environmental/social problems. In this context, materials that can contact with corrosive species such as H_2S (e.g. inox) as well as suitable systems for their removal from gaseous streams should be selected to comply with EU legislation.

5 Conclusions and Future Work

5.1 Conclusions

The strategy followed in the present work focused on treating spent caustic, aiming to decrease its impact on the polar O&G concentration in the final wastewater, reducing therefore the taxation for Sines refinery low quality effluent discharges into the RM WWTP. In order to comply with the defined objective, attempts were made to study and develop target compound removal technologies to treat spent caustic at its source. Proton NMR, FT-IR and GC-MS analyses suggest the formation of functional groups when pH decreases, constituting the polar O&G class of compounds. Aromatic structures account for a significant part of the organic structures that constitute naphthenic spent caustic and that are present in the final wastewater. Naphthenic acids were detected at lower pH values due to the hydrolysis reactions that occur in the functional groups in their ionic form at spent caustic natural pH. The average molecular weight in the identified structures is low and the strong alkaline medium keeps most of terminal organic functional groups in their ionic form. There is a strong presence of sulphides and mercaptan-derivative compounds, which together with pH turn this effluent a true challenge for wastewater treatment. Nevertheless, as this effluent accounts for more than 90 % of polar O&G contamination in the final wastewater at Sines refinery [7], its treatment directly at the source using effluent-specific technologies would be more cost-effective and could enable valorisation of resources within the process.

Among all processed crudes in Sines refinery in 2016 with a TAN higher than 0.1 mg KOH/g, crude oils Azeri Light and CLOV seem to cause a greater impact on the increase of polar O&G concentration in the final wastewater. There is an apparent proportional relation between kerosene cut TAN values and polar O&G concentration in naphthenic spent caustic and final wastewater. Azeri Light and CLOV crude oils processing in Sines refinery led to an effluent management cost increase of approximately 0.957 €/$ton_{Azeri\ Light}$ and 3.065 €/ton_{CLOV}, respectively. This result helped in defining polar O&G contamination occurrences in the wastewater treatment circuit, which helped in predicting collecting samples of spent caustic/final wastewater with high O&G concentrations. Also, it allowed defining a specific scheme of treatment in the refinery wastewater circuit if any of these crudes were planned to be processed.

A target-compound treatment that was attempted was separation by membrane processes. In particular, nanofiltration is known to be able to remove low molecular weight organic molecules like hydrocarbons and phenolic compounds. Due to the high pH, alkaline-resistant membranes were tested, namely a 200 Da polymeric membrane (Koch) and a 200 Da ceramic membrane (Inopor). The polymeric membrane presented higher resistance than the ceramic membrane, however it did not present interesting results for considering a possible treatment optimization. The ceramic membrane presented very low lifespan, with permeability increasing regularly until 2.5 h of test. Contrary to expectations, neither of the tested membranes presented attractive results for industrial spent caustic treatment, due to very quick losses of retention properties; still, analyses by ^{1}H NMR, GC-MS and FT-IR corroborate deterioration in both membranes.

Another treatment was based exclusively on chemical combined technologies. Neutralization was found to be a relevant first step in combined technologies, as it allows decreasing the pH and extracting most of the high organic load into an organic phase (at least 85 % COD extraction for pH equal or lower than 5), that can be easily separated. Two strategies were studied: (i) neutralization followed by Fenton oxidation post-treatment (approach 1) and (ii) neutralization followed by liquid-liquid extraction (approach 2). Approach 1 (tested at lab scale) allowed to remove 95 % of polar O&G, with a 70% decrease in the acute toxicity after treatment. Approach 2 (tested at pilot scale) allowed to remove 99 % of polar O&G. Both Fenton oxidation and liquid-liquid extraction enabled, as post-treatments of neutralization, a considerable improvement of the effluent quality, constituting suitable treatments with substantial economic savings in terms of OPEX costs (as compared to the current charges for discharge into the municipal wastewater treatment plant). In this view, the combination of neutralization with liquid-liquid extraction was found particularly attractive (savings of 1.39 M € for neutralization and Fenton oxidation and 1.58 M € for neutralization and liquid-liquid extraction). At first, approach 2 did not seem interesting enough because it could produce another effluent, however in the refinery context it was found that the produced oily phase is compatible with kerosene and, therefore, kerosene could be used as the organic extraction solvent. The contaminated kerosene can be introduced in the refinery distillation process. This study had such success that an internal Sines refinery project was initiated to apply this technology and the interconnections between products, pipping and recirculation to treat naphthenic spent caustic, instead of discharging it directly into the wastewater circuit, were assembled.

5.2 Future Work

The results obtained in the present work may be useful for the development/optimization of industrial scale plants in petroleum refineries for the treatment of Merox spent caustic effluents, providing effective treatment alternatives and lower costs related with effluent management.

Characterization studies are always an important task, particularly in refinery products. These studies should be further explored and carried out in the future, as a much more detailed project, due to its high interest for optimizing studies of refinery Merox processes. For example optimizing the extraction method and study in more detail the chemical transformations, or instead of a qualitative analysis, it would be very interesting to attempt a quantification of the identified compound-families, as it could present basis to optimize fresh caustic consumption in the Merox process according to the processed crude oils, for example. Although environmental regulation has been applied in many countries to control wastewater quality, organic compounds removals to upgrade the quality of the produced effluents still presents a major operational and economic challenge for the petroleum refining industry.

In spite of the obtained results, membrane separation processes should continue to be studied, but in future work a chemical pre-treatment should be included in order to decrease the effluent pH. Membrane processes per se demonstrated to be insufficient to treat spent caustic with the tested operating conditions, however possibly with more tests in different conditions (initial pH, cleaning procedure, pressure variation, etc.), more conclusions could be drawn regarding these membranes performance. Combined processes having membrane separation as final treatment may pose an elegant and interesting alternative. An attempt was performed by studying neutralization and NF in a combined process, however the results were too incomplete to draw any conclusion, therefore, more work would be interesting with the 200 Da ceramic membrane. In order to increase permeability and to have a higher performance for a possible industrial scale up and considering energy consumption decrease, a higher MWCO ceramic membrane could be also tested in the future, for example, the 450 Da Inopor ceramic membrane. Other polymeric NF membranes in the market would be interesting to study, as long as they are guaranteed to resist extreme pHs.

Although Fenton oxidation proved to be a suitable technology to treat spent caustic because considerably high removals were achieved for COD (80%) and polar O&G (95%), further research on valorisation/reuse of the sludge produced during the process due to the high ferrous concentration could be interesting. Another alternative would be to attempt treating the

wastewater in the equalization basin, given the proven success of Fenton oxidation for petroleum refinery wastewater, and no extreme neutralization would be necessary, since the pH of equalized effluent in Sines refinery varies between 5 and 7. A complete economic analysis of the best presented technology option would be very interesting in the future, as many refineries could gain insight of real market values to treat such an aggressive effluent.

References

[1] Galp, 40 Anos Refinaria de Sines, (2020). https://www.galp.com/corp/pt/sobre-nos/a-galp/feiras-e-eventos/40-anos-refinaria-de-sines (accessed November 15, 2020).

[2] L.C. Barros, M.J. Franco, A.P. Mano, TRATAMENTO DE ÁGUAS RESIDUAIS EM REFINARIAS. Enquadramento Geral, 7º Congr. Da Água. (2004).

[3] C.M.E. Santo, A Indústria de Refinação de Petróleo: Características e Tratamento das Águas Residuais, E-LP Eng. Technol. J. (2010) 21–46.

[4] Águas de Santo André, REGULAMENTO DE RECOLHA E TRATAMENTO DE ÁGUA RESIDUAL INDUSTRIAL DO SISTEMA DE SANTO ANDRÉ - RARISA, (2007).

[5] B. Santos, Optimization of Wastewater Quality in the Sines Refinery, Universidade Nova de Lisboa, 2015.

[6] E. Metcalf, H. Eddy, Wastewater engineering: treatment and reuse, 4th Editio, McGraw Hill, 2003. https://doi.org/10.1016/0309-1708(80)90067-6.

[7] B. Santos, C.F. Galinha, J.G. Crespo, M.A. Santos, S. Velizarov, Prediction of polar oil and grease contamination levels in refinery wastewater through multivariate statistical modeling, Sep. Purif. Technol. 119 (2013) 51–57. https://doi.org/10.1016/j.seppur.2013.09.009.

[8] R.W. Harber, Implementing an effective caustic management program within the petroleum refinery, (1986) 38.

[9] S. Seyedin, M. Hassanzadeganroudsari, Evaluation of the Different Methods of Spent Caustic Treatment, Int. J. Adv. Res. Sci. Eng. Technol. 5 (2018) 5275–5283.

[10] C.E. Ellis, Wet air oxidation of refinery spent caustic, Environ. Prog. 17 (1998) 28–30. https://doi.org/10.1002/ep.670170116.

[11] G. Boczkaj, P. Makoś, A. Przyjazny, Application of dispersive liquid–liquid microextraction and gas chromatography with mass spectrometry for the determination of oxygenated volatile organic compounds in effluents from the production of petroleum bitumen, J. Sep. Sci. 39 (2016) 2604–2615. https://doi.org/10.1002/jssc.201501355.

[12] P. Makoś, A. Przyjazny, G. Boczkaj, Methods of assaying volatile oxygenated organic compounds in effluent samples by gas chromatography—A review, J. Chromatogr. A. 1592 (2019) 143–160. https://doi.org/10.1016/j.chroma.2019.01.045.

[13] G. Boczkaj, P. Makoś, A. Fernandes, A. Przyjazny, New procedure for the control of the treatment of industrial effluents to remove volatile organosulfur compounds, J. Sep. Sci. 39 (2016) 3946–3956. https://doi.org/10.1002/jssc.201600608.

[14] G. Boczkaj, P. Makoś, A. Fernandes, A. Przyjazny, New procedure for the examination of the degradation of volatile organonitrogen compounds during the treatment of industrial effluents, J. Sep. Sci. 40 (2017) 1301–1309. https://doi.org/10.1002/jssc.201601237.

[15] P. Makoś, A. Fernandes, G. Boczkaj, Method for the determination of carboxylic acids in industrial effluents using dispersive liquid-liquid microextraction with injection port

derivatization gas chromatography–mass spectrometry, J. Chromatogr. A. 1517 (2017) 26–34. https://doi.org/10.1016/j.chroma.2017.08.045.

[16] P. Makoś, A. Fernandes, A. Przyjazny, G. Boczkaj, Sample preparation procedure using extraction and derivatization of carboxylic acids from aqueous samples by means of deep eutectic solvents for gas chromatographic-mass spectrometric analysis, J. Chromatogr. A. 1555 (2018) 10–19. https://doi.org/10.1016/j.chroma.2018.04.054.

[17] P. Makoś, A. Fernandes, G. Boczkaj, Method for the simultaneous determination of monoaromatic and polycyclic aromatic hydrocarbons in industrial effluents using dispersive liquid–liquid microextraction with gas chromatography–mass spectrometry, J. Sep. Sci. 41 (2018) 2360–2367. https://doi.org/10.1002/jssc.201701464.

[18] E. Pino-Cortés, S. Montalvo, C. Huiliñir, F. Cubillos, J. Gacitúa, Characteristics and Treatment of Wastewater from the Mercaptan Oxidation Process: A Comprehensive Review, Processes. 8 (2020) 425. https://doi.org/10.3390/pr8040425.

[19] R. Alnaizy, Economic Analysis for Wet Oxidation Process for the Treatment of Mixed Refinery Spent Caustic, Environ. Prog. 27 (2008) 295–301. https://doi.org/10.1002/ep.

[20] J. Berne, F. and Cordonnier, Industrial Water Treatment - Refining, Petrochemical and Gas Processing Techniques, (1995) 37.

[21] M. Noor, A. Hassan, Z.Z. Noor, A. Aris, Performance of fenton oxidation towards sulfide removal for spent caustic remediation, 2011 Natl. Postgrad. Conf. - Energy Sustain. Explor. Innov. Minds, NPC 2011. (2011) 1–6. https://doi.org/10.1109/NatPC.2011.6136279.

[22] B. Van der Bruggen, M. Mänttäri, M. Nyström, Drawbacks of applying nanofiltration and how to avoid them: A review, Sep. Purif. Technol. 63 (2008) 251–263. https://doi.org/10.1016/j.seppur.2008.05.010.

[23] Aquarden Technologies ApS, Membrane filtration usage in waste water treatment, (2013). https://www.brostroems.com/technology/membrane-filtration/.

[24] S. Sanches, A. Penetra, A. Rodrigues, E. Ferreira, V. V. Cardoso, M.J. Benoliel, M.T. Barreto Crespo, V.J. Pereira, J.G. Crespo, Nanofiltration of hormones and pesticides in different real drinking water sources, Sep. Purif. Technol. 94 (2012) 44–53. https://doi.org/10.1016/j.seppur.2012.04.003.

[25] B. Santos, J.G. Crespo, M.A. Santos, S. Velizarov, Oil refinery hazardous effluents minimization by membrane filtration: An on-site pilot plant study, J. Environ. Manage. Article in (2016) 1–8. https://doi.org/10.1016/j.jenvman.2016.07.027.

[26] S. Judd, The MBR Book - Principles and Applications of Membrane Bioreactors in Water and Wastewater Treatment, Elsevier, 2006.

[27] L. Benavente, C. Coetsier, A. Venault, Y. Chang, C. Causserand, P. Bacchin, P. Aimar, FTIR mapping as a simple and powerful approach to study membrane coating and fouling, J. Memb. Sci. 520 (2016) 477–489. https://doi.org/10.1016/j.memsci.2016.07.061.

[28] F.E. Antón, J.R. Álvarez, S. Luque, Cleaning and ageing of ultrafiltration membranes, Procedia Eng. 44 (2012) 689. https://doi.org/10.1016/j.proeng.2012.08.531.

[29] E. Antón, J.R. Álvarez, L. Palacio, P. Prádanos, A. Hernández, A. Pihlajamäki, S. Luque, Ageing of polyethersulfone ultrafiltration membranes under long-term exposures to alkaline and acidic cleaning solutions, Chem. Eng. Sci. 134 (2015) 178–195. https://doi.org/10.1016/j.ces.2015.04.023.

[30] A. Ettori, E. Gaudichet-Maurin, J.C. Schrotter, P. Aimar, C. Causserand, Permeability and chemical analysis of aromatic polyamide based membranes exposed to sodium hypochlorite, J. Memb. Sci. 375 (2011) 220–230. https://doi.org/10.1016/j.memsci.2011.03.044.

[31] A. Ettori, E. Gaudichet-Maurin, P. Aimar, C. Causserand, Pilot scale study of chlorination-induced transport property changes of a seawater reverse osmosis membrane, Desalination. 311 (2013) 24–30. https://doi.org/10.1016/j.desal.2012.11.004.

[32] M. El Mansour, A. Ettori, S. Luque, J.R. Alvarez, C. Causserand, P. Aimar, Accelerated ageing of crosslinked polyamide membranes, Procedia Eng. 44 (2012) 789. https://doi.org/10.1016/j.proeng.2012.08.571.

[33] B. Pellegrin, R. Prulho, A. Rivaton, S. Therias, J.L. Gardette, E. Gaudichet-Maurin, C. Causserand, Hypochlorite Cleaning of Polyethersulfone/Polyvinylpyrrolidone Ultrafiltration Membranes: Impact on Performances, Procedia Eng. 44 (2012) 472–475. https://doi.org/10.1016/j.proeng.2012.08.454.

[34] B. Pellegrin, R. Prulho, A. Rivaton, S. Thérias, J.L. Gardette, E. Gaudichet-Maurin, C. Causserand, Multi-scale analysis of hypochlorite induced PES/PVP ultrafiltration membranes degradation, J. Memb. Sci. 447 (2013) 287–296. https://doi.org/10.1016/j.memsci.2013.07.026.

[35] C. Causserand, B. Pellegrin, J.C. Rouch, Effects of sodium hypochlorite exposure mode on PES/PVP ultrafiltration membrane degradation, Water Res. 85 (2015) 316–326. https://doi.org/10.1016/j.watres.2015.08.028.

[36] N.N. Li, A.G. Fane, W.S. Winston Ho, T. Matsuura, Advanced Membrane Technology and Applications, John Wiley & Sons, Inc., 2008. https://doi.org/10.1002/9780470276280.ch6.

[37] Y. ying Zhao, X. mao Wang, H. wei Yang, Y. feng F. Xie, Effects of organic fouling and cleaning on the retention of pharmaceutically active compounds by ceramic nanofiltration membranes, J. Memb. Sci. 563 (2018) 734–742. https://doi.org/10.1016/j.memsci.2018.06.047.

[38] J. López, M. Reig, X. Vecino, O. Gibert, J.L. Cortina, Comparison of acid-resistant ceramic and polymeric nanofiltration membranes for acid mine waters treatment, Chem. Eng. J. 382 (2020) 122786. https://doi.org/10.1016/j.cej.2019.122786.

[39] E. Neyens, J. Baeyens, A review of classic Fenton's peroxidation as an advanced oxidation technique, J. Hazard. Mater. 98 (2003) 33–50. https://doi.org/10.1016/S0304-3894(02)00282-0.

[40] J.P. Chen, L. Wang, Characterization of a Ca-alginate based ion-exchange resin and its applications in lead, copper, and zinc removal, Sep. Sci. Technol. 36 (2001) 3617–3637. https://doi.org/10.1081/SS-100108352.

[41] J.P. Chen, H. Yu, Lead removal from synthetic wastewater by crystallization in a fluidized-bed reactor, J. Environ. Sci. Heal. - Part A Toxic/Hazardous Subst. Environ. Eng. 35 (2000) 817–835. https://doi.org/10.1080/10934520009377005.

[42] M.L. Davis, D.A. Cornwell, Introduction to Environmental Engineering, McGraw-Hill, New York, 1998.

[43] F.N. Kemmer, The Nalco Water Handbook, McGraw-Hill, New York, 1998.

[44] R.K. Goel, J.R. V. Flora, J.P. Chen, Flow Equalization and Neutralization, in: Physicochem. Treat. Process. Handb. Environ. Eng., Humana Press, 2005: pp. 21–45.

https://doi.org/10.1385/1-59259-820-x:021.

[45] A.I. Rita, C.S.D. Rodrigues, M. Santos, S. Sanches, L.M. Madeira, Comparison of different strategies to treat challenging refinery spent caustic effluents, Sep. Purif. Technol. 253 (2020) 117482. https://doi.org/10.1016/j.seppur.2020.117482.

[46] A. Fernandes, P. Makoś, J.A. Khan, G. Boczkaj, Pilot scale degradation study of 16 selected volatile organic compounds by hydroxyl and sulfate radical based advanced oxidation processes, J. Clean. Prod. 208 (2019) 54–64. https://doi.org/10.1016/j.jclepro.2018.10.081.

[47] M. Gągol, R.D.C. Soltani, A. Przyjazny, G. Boczkaj, Effective degradation of sulfide ions and organic sulfides in cavitation-based advanced oxidation processes (AOPs), Ultrason. Sonochem. 58 (2019). https://doi.org/10.1016/j.ultsonch.2019.05.027.

[48] P. Stepnowski, E.M. Siedlecka, P. Behrend, B. Jastorff, Enhanced photo-degradation of contaminants in petroleum refinery wastewater, Water Res. 36 (2002) 2167–2172. https://doi.org/10.1016/S0043-1354(01)00450-X.

[49] C.S.D. Rodrigues, L.M. Madeira, R.A.R. Boaventura, Optimization and Economic Analysis of Textile Wastewater Treatment by Photo-Fenton Process under Artificial and Simulated Solar Radiation, Ind. Eng. Chem. Res. 52 (2013) 13313 – 13324. https://doi.org/10.1021/ie401301h.

[50] A. Rubio-Clemente, R.A. Torres-Palma, G.A. Peñuela, Removal of polycyclic aromatic hydrocarbons in aqueous environment by chemical treatments: A review, Sci. Total Environ. 478 (2014) 201–225. https://doi.org/10.1016/j.scitotenv.2013.12.126.

[51] A.M.F.M. Guedes, L.M.P. Madeira, R.A.R. Boaventura, C.A. V Costa, Fenton oxidation of cork cooking wastewater - Overall kinetic analysis, Water Res. 37 (2003) 3061–3069. https://doi.org/10.1016/S0043-1354(03)00178-7.

[52] G. Boczkaj, A. Fernandes, Wastewater treatment by means of advanced oxidation processes at basic pH conditions: A review, Chem. Eng. J. 320 (2017) 608–633. https://doi.org/10.1016/j.cej.2017.03.084.

[53] M. Gągol, A. Przyjazny, G. Boczkaj, Wastewater treatment by means of advanced oxidation processes based on cavitation – A review, Chem. Eng. J. 338 (2018) 599–627. https://doi.org/10.1016/j.cej.2018.01.049.

[54] A. Fernandes, P. Makoś, Z. Wang, G. Boczkaj, Synergistic effect of TiO2 photocatalytic advanced oxidation processes in the treatment of refinery effluents, Chem. Eng. J. 391 (2019). https://doi.org/10.1016/j.cej.2019.123488.

[55] A. Fernandes, M. Gągol, P. Makoś, J.A. Khan, G. Boczkaj, Integrated photocatalytic advanced oxidation system (TiO2/UV/O3/H2O2)for degradation of volatile organic compounds, Sep. Purif. Technol. (2019) 1–14. https://doi.org/10.1016/j.seppur.2019.05.012.

[56] M. Gągol, A. Przyjazny, G. Boczkaj, Effective method of treatment of industrial effluents under basic pH conditions using acoustic cavitation – A comprehensive comparison with hydrodynamic cavitation processes, Chem. Eng. Process. - Process Intensif. 128 (2018) 103–113. https://doi.org/10.1016/j.cep.2018.04.010.

[57] J.A. Khan, M. Sayed, N.S. Shah, S. Khan, Y. Zhang, G. Boczkaj, H.M. Khan, D.D. Dionysiou, Synthesis of eosin modified TiO2 film with co-exposed {001} and {101} facets for photocatalytic degradation of para-aminobenzoic acid and solar H2 production, Appl. Catal. B Environ. 265 (2020) 118557. https://doi.org/10.1016/j.apcatb.2019.118557.

[58] G. Boczkaj, M. Gągol, M. Klein, A. Przyjazny, Effective method of treatment of effluents from production of bitumens under basic pH conditions using hydrodynamic cavitation aided by external oxidants, Ultrason. Sonochem. 40 (2018) 969–979. https://doi.org/10.1016/j.ultsonch.2017.08.032.

[59] L. Yan, H. Ma, B. Wang, W. Mao, Y. Chen, Advanced purification of petroleum refinery wastewater by catalytic vacuum distillation, J. Hazard. Mater. 178 (2010) 1120–1124. https://doi.org/10.1016/j.jhazmat.2010.01.104.

[60] E.A. Taiwo, J.A. Otolorin, Oil recovery from petroleum sludge by solvent extraction, Pet. Sci. Technol. 27 (2009) 836–844. https://doi.org/10.1080/10916460802455582.

[61] G. Hu, J. Li, H. Hou, A combination of solvent extraction and freeze thaw for oil recovery from petroleum refinery wastewater treatment pond sludge, J. Hazard. Mater. 283 (2015) 832–840. https://doi.org/10.1016/j.jhazmat.2014.10.028.

[62] S.M.V. Mendoza, E.A. Moreno, C.A.G. Fajardo, R.F. Medina, Liquid-liquid continuous extraction and fractional distillation for the removal of organic compounds from the wastewater of the oil industry, Water (Switzerland). 11 (2019) 1–16. https://doi.org/10.3390/w11071452.

[63] B. Valley, B. Jing, M. Ferreira, Y. Zhu, Rapid and efficient coacervate extraction of cationic industrial dyes from wastewater, ACS Appl. Mater. Interfaces. 11 (2019) 7472–7478. https://doi.org/10.1021/acsami.8b21674.

[64] M.A. Sabri, T.H. Ibrahim, M.I. Khamis, P. Nancarrow, M.F. Hassan, Spent caustic treatment using hydrophobic room temperatures ionic liquids, J. Ind. Eng. Chem. 65 (2018) 325–333. https://doi.org/10.1016/j.jiec.2018.05.002.

[65] A.C. Hoffmann, S.S. Pletten, M. Mania, A study of transfer rates of phenols from caustic to crude oil, Sep. Purif. Technol. (2019) 515–519. https://doi.org/10.1016/j.seppur.2018.11.058.

[66] J.G. Speight, High Acid Crudes, 2014. https://doi.org/10.1016/B978-0-12-800630-6.00004-6.

[67] M.P. Barrow, J. V. Headley, K.M. Peru, P.J. Derrick, Data visualization for the characterization of naphthenic acids within petroleum samples, Energy and Fuels. 23 (2009) 2592–2599. https://doi.org/10.1021/ef800985z.

[68] J. Speight, The Chemistry and Technology of Petroleum, Fourth Edition, 20064186 (2006). https://doi.org/10.1201/9781420008388.

[69] K.A.P. Colati, G.P. Dalmaschio, E.V.R. De Castro, A.O. Gomes, B.G. Vaz, W. Romão, Monitoring the liquid/liquid extraction of naphthenic acids in brazilian crude oil using electrospray ionization FT-ICR mass spectrometry (ESI FT-ICR MS), Fuel. 108 (2013) 647–655. https://doi.org/10.1016/j.fuel.2013.02.007.

[70] M. Castillo, D. Barceló, Characterisation of organic pollutants in textile wastewaters and landfill leachate by using toxicity-based fractionation methods followed by liquid and gas chromatography coupled to mass spectrometric detection, Anal. Chim. Acta. 426 (2001) 253–264. https://doi.org/10.1016/S0003-2670(00)00828-X.

[71] Y. Li, C. Xu, K.H. Chung, Q. Shi, Molecular Characterization of Dissolved Organic Matter and Its Sub-fractions in Refinery Process Water by FT-ICR MS, Energy & Fuels. 29 (2015) 2923 – 2930. https://doi.org/10.1021/acs.energyfuels.5b00333.

[72] L. Lingbo, Y. Song, H. Congbi, S. Guangbo, Comprehensive characterization of oil refinery effluent-derived humic substances using various spectroscopic approaches,

Chemosphere. 60 (2005) 467–476. https://doi.org/10.1016/j.chemosphere.2005.01.012.

[73] A.U. Israel, I.B. Obot, S.A. Umoren, V. Mkpenie, G.A. Ebong, Effluents and solid waste analysis in a petrochemical company - A case study of Eleme Petrochemical Company Ltd, Port Harcourt, Nigeria, E-Journal Chem. 5 (2008) 74–80. https://doi.org/10.1155/2008/805957.

[74] L.H. Keith, Chemical characterization of industrial wastewaters by gas chromatography-mass spectrometry, Sci. Total Environ. 3 (1974) 87–102. https://doi.org/10.1016/0048-9697(74)90041-2.

[75] I. Michael-Kordatou, C. Michael, X. Duan, X. He, D.D. Dionysiou, M.A. Mills, D. Fatta-Kassinos, Dissolved effluent organic matter: Characteristics and potential implications in wastewater treatment and reuse applications, Water Res. 77 (2015) 213–248. https://doi.org/10.1016/j.watres.2015.03.011.

[76] M. Castillo, Characterization of organic pollutants in industrial effluents by high-temperature gas chromatography–mass spectrometry, TrAC Trends Anal. Chem. 18 (1999) 26–36. https://doi.org/10.1016/S0165-9936(98)00066-1.

[77] H. Ma, H.E. Allen, Y. Yin, Characterization of isolated fractions of dissolved organic matter from natural waters and a wastewater effluent, Water Res. 35 (2001) 985–996. https://doi.org/10.1016/S0043-1354(00)00350-X.

[78] M. Gonsior, M. Zwartjes, W.J. Cooper, W. Song, K.P. Ishida, L.Y. Tseng, M.K. Jeung, D. Rosso, N. Hertkorn, P. Schmitt-Kopplin, Molecular characterization of effluent organic matter identified by ultrahigh resolution mass spectrometry, Water Res. 45 (2011) 2943–2953. https://doi.org/10.1016/j.watres.2011.03.016.

[79] X. Wang, J. Wang, K. Li, H. Zhang, M. Yang, Molecular characterization of effluent organic matter in secondary effluent and reclaimed water: Comparison to natural organic matter in source water, J. Environ. Sci. (China). 63 (2018) 140–146. https://doi.org/10.1016/j.jes.2017.03.020.

[80] A. Imai, T. Fukushima, K. Matsushige, Y.-H. Kim, K. Choi, Characterization of dissolved organic matter in effluents from wastewater treatment plants, Water Res. 36 (2002) 859–870. https://doi.org/10.1016/S0043-1354(01)00283-4.

[81] G.P. Dalmaschio, M.M. Malacarne, V.M.D.L. De Almeida, T.M.C. Pereira, A.O. Gomes, E.V.R. De Castro, S.J. Greco, B.G. Vaz, W. Romão, Characterization of polar compounds in a true boiling point distillation system using electrospray ionization FT-ICR mass spectrometry, Fuel. 115 (2014) 190–202. https://doi.org/10.1016/j.fuel.2013.07.008.

[82] APHA, AWWA, WEF, Standard methods for the examination of water and wastewater, Am. Public Heal. Assoc. Washington, DC, USA. (2005) 1–2671. https://doi.org/30M11/98.

[83] M.M. Ramirez-Corredores, Acidity in Crude Oils: Naphthenic Acids and Naphthenates, in: M.M. Ramirez-Corredores (Ed.), Sci. Technol. Unconv. Oils, 2007: pp. 295–385. https://doi.org/https://doi.org/10.1016/B978-0-12-801225-3.00004-8.

[84] S. Mori, S.M. Eleff, U. Pilatus, N. Mori, P.C.M. Van Zijl, Proton NMR spectroscopy of solvent-saturable resonances: A new approach to study pH effects in situ, Magn. Reson. Med. 40 (1998) 36–42. https://doi.org/10.1002/mrm.1910400105.

[85] M. Balci, Basic 1H-13C-NMR Spectroscopy, 2005.

[86] M. Badertscher, P. Bühlmann, E. Pretsch, Structure Determination of Organic Compounds, Springer, Berlin, Heidelberg, n.d.

https://doi.org/https://doi.org/10.1007/978-3-540-93810-1.

[87] L. V. Castro, F. Vazquez, Fractionation and characterization of mexican crude oils, Energy and Fuels. 23 (2009) 1603–1609. https://doi.org/10.1021/ef8008508.

[88] J.S. Watson, D.M. Jones, R.P.J. Swannell, A.C.T. Van Duin, Formation of carboxylic acids during aerobic biodegradation of crude oil and evidence of microbial oxidation of hopanes, Org. Geochem. 33 (2002) 1153–1169. https://doi.org/10.1016/S0146-6380(02)00086-4.

[89] J. Coates, Encyclopedia of Analytical Chemistry -Interpretation of Infrared Spectra, A Practical Approach, Encycl. Anal. Chem. (2004) 1–23. http://www3.uma.pt/jrodrigues/disciplinas/QINO-II/Teorica/IR.pdf.

[90] T.S. Wang, J.M. Sanders, An infrared study of the out-of-plane C-H bending vibrations of monosubstituted naphthalenes, Spectrochim. Acta. 15 (1959) 1118–1124. https://doi.org/10.1016/s0371-1951(59)80414-8.

[91] C.A. Hughey, C.L. Hendrickson, R.P. Rodgers, A.G. Marshall, K. Qian, Kendrick mass defect spectrum: A compact visual analysis for ultrahigh-resolution broadband mass spectra, Anal. Chem. 73 (2001) 4676–4681. https://doi.org/10.1021/ac010560w.

[92] D.W. Krevelen, Graphical-statistical method for the study of structure and reaction processes of coal, Fuel. 29 (1961) 269–283.

[93] Z. Alipour, A. Azari, COD removal from industrial spent caustic wastewater: A review, J. Environ. Chem. Eng. 8 (2020) 103678. https://doi.org/10.1016/j.jece.2020.103678.

[94] S.H. Sheu, H.S. Weng, Treatment of olefin plant spent caustic by combination of neutralization and fenton reaction, Water Res. 35 (2001) 2017–2021. https://doi.org/10.1016/S0043-1354(00)00466-8.

[95] M. Noor, A. Hassan, Z.Z. Noor, A. Aris, Performance of fenton oxidation towards sulfide removal for spent caustic remediation, 2011 Natl. Postgrad. Conf. - Energy Sustain. Explor. Innov. Minds, NPC 2011. (2011). https://doi.org/10.1109/NatPC.2011.6136279.

[96] G.D. Cooper, B. Williams, Hydrolysis of Simple Aromatic Esters and Carbonates, J. Org. Chem. 27 (1962) 3717–3720. https://doi.org/10.1021/jo01057a529.

[97] B. Ahrland, S. Grenthe, I. Norén, The Ion Exchange Properties of Silica Gel, Acta Chem. Scand. 1 (1960) 1059–1076.

[98] A.E. Papadopoulos, D. Fatta, M. Loizidou, S.H. Sheu, H.S. Weng, M. Noor, A. Hassan, Z.Z. Noor, A. Aris, Treatment of olefin plant spent caustic by combination of neutralization and fenton reaction, Water Res. 35 (2011) 2017–2021. https://doi.org/10.1016/j.jhazmat.2007.04.083.

[99] A. Salahi, T. Mohammadi, F. Rekabdar, H. Mahdavi, REVERSE OSMOSIS OF REFINERY OILY WASTEWATER EFFLUENTS, J. Environ. Heal. Sci. Eng. 7 (2010) 413–422.

[100] S.R.H. Abadi, M.R. Sebzari, M. Hemati, F. Rekabdar, T. Mohammadi, Ceramic membrane performance in microfiltration of oily wastewater, Desalination. 265 (2011) 222–228. https://doi.org/10.1016/j.desal.2010.07.055.

[101] J. Zhong, X. Sun, C. Wang, Treatment of oily wastewater produced from refinery processes using flocculation and ceramic membrane filtration, Sep. Purif. Technol. 32 (2003) 93–98. https://doi.org/10.1016/S1383-5866(03)00067-4.

[102] L. Cui, Z. Feng, C. Goodwin, W. Gao, B.Q. Liao, Structure and properties of membrane at different ages in drinking water treatment, Desalin. Water Treat. 74 (2017) 44–52.

https://doi.org/10.5004/dwt.2017.20735.

[103] M.C. Fraga, S. Sanches, V.J. Pereira, J.G. Crespo, L. Yuan, J. Marcher, M.M. de Yuso, E. Rodríguez-Castellón, J. Benavente, Morphological, chemical surface and filtration characterization of a new silicon carbide membrane, J. Eur. Ceram. Soc. 37 (2017) 899–905. https://doi.org/10.1016/j.jeurceramsoc.2016.10.007.

[104] B. Pellegrin, F. Mezzari, Y. Hanafi, A. Szymczyk, J.C. Remigy, C. Causserand, Filtration performance and pore size distribution of hypochlorite aged PES/PVP ultrafiltration membranes, J. Memb. Sci. 474 (2015) 175–186. https://doi.org/10.1016/j.memsci.2014.09.028.

[105] S. Sanches, A. Penetra, A. Rodrigues, E. Ferreira, V. V. Cardoso, M.J. Benoliel, M.T. Barreto Crespo, V.J. Pereira, J.G. Crespo, Nanofiltration of hormones and pesticides in different real drinking water sources, Sep. Purif. Technol. 94 (2012) 44–53. https://doi.org/10.1016/j.seppur.2012.04.003.

[106] S. Sanches, A. Penetra, C. Granado, V. V. Cardoso, E. Ferreira, M.J. Benoliei, M.T.B. Crespo, V.J. Pereira, J.G. Crespo, Removal of pesticides and polycyclic aromatic hydrocarbons from different drinking water sources by nanofiltration, Desalin. Water Treat. 27 (2011) 141–149. https://doi.org/10/5004/dwt.2011.2087.

[107] S. Ishak, A. Malakahmad, M.H. Isa, Refinery wastewater biological treatment: A short review, J. Sci. Ind. Res. 71 (2012) 251–256.

[108] S.R.P. Shariati, B. Bonakdarpour, N. Zare, F.Z. Ashtiani, The effect of hydraulic retention time on the performance and fouling characteristics of membrane sequencing batch reactors used for the treatment of synthetic petroleum refinery wastewater, Bioresour. Technol. 102 (2011) 7692–7699. https://doi.org/10.1016/j.biortech.2011.05.065.

[109] Y. Zhu, D. Wang, L. Jiang, J. Jin, Recent progress in developing advanced membranes for emulsified oil/water separation, NPG Asia Mater. 6 (2014). https://doi.org/10.1038/am.2014.23.

[110] J. Li, Chemical Stability of Ceramic Membrane, TU Delft, 2016.

[111] T.Y. Chiu, Effect of ageing on the microfiltration performance of ceramic membranes, Sep. Purif. Technol. 83 (2011) 106–113. https://doi.org/10.1016/j.seppur.2011.09.022.

[112] M. Dalwani, G. Bargeman, S.S. Hosseiny, M. Boerrigter, M. Wessling, N.E. Benes, Sulfonated poly(ether ether ketone) based composite membranes for nanofiltration of acidic and alkaline media, J. Memb. Sci. 381 (2011) 81–89. https://doi.org/10.1016/j.memsci.2011.07.018.

[113] B. Pellegrin, R. Prulho, A. Rivaton, S. Therias, J.L. Gardette, E. Gaudichet-Maurin, C. Causserand, Hypochlorite cleaning of polyethersulfone / polyvinylpyrrolidone ultrafiltration membranes: Impact on performances, Procedia Eng. 44 (2012) 472–475. https://doi.org/10.1016/j.proeng.2012.08.454.

[114] C. Causserand, B. Pellegrin, J.C. Rouch, Effects of sodium hypochlorite exposure mode on PES/PVP ultrafiltration membrane degradation, Water Res. 85 (2015) 316–326. https://doi.org/10.1016/j.watres.2015.08.028.

[115] M.R.S. Sousa, J. Lora-García, M.F. López-Pérez, M. Heran, Identification of foulants on polyethersulfone membranes used to remove colloids and dissolved matter from paper mill treated effluent, Water (Switzerland). 12 (2020). https://doi.org/10.3390/w12020365.

[116] W.H. Alton, Ferret diameter, Nature. 162 (1948) 329–330.

https://doi.org/10.1038/162329b0.

[117] E. Pretsch, T. Clerc, J. Seibl, W. Simon, Tables of Spectral Data for Structure Determination of Organic Compounds, 2nd ed., Springer-Verlag Berlin Heidelberg, 1989. https://doi.org/10.1007/978-3-662-10207-7.

[118] M. Kazemnejadi, A. Shakeri, M. Nikookar, R. Shademani, M. Mohammadi, Selective and metal-free epoxidation of terminal alkenes by heterogeneous polydioxirane in mild conditions, R. Soc. Open Sci. 5 (2018). https://doi.org/10.1098/rsos.171541.

[119] N. Ghaemi, S.S. Madaeni, A. Alizadeh, P. Daraei, M.M.S. Badieh, M. Falsafi, V. Vatanpour, Fabrication and modification of polysulfone nanofiltration membrane using organic acids: Morphology, characterization and performance in removal of xenobiotics, Sep. Purif. Technol. 96 (2012) 214–228. https://doi.org/10.1016/j.seppur.2012.06.008.

[120] M.N. Chai, M.I.N. Isa, The Oleic Acid Composition Effect on the Carboxymethyl Cellulose Based Biopolymer Electrolyte, J. Cryst. Process Technol. 03 (2013) 1–4. https://doi.org/10.4236/jcpt.2013.31001.

[121] N. Nasrollahi, S. Aber, V. Vatanpour, N.M. Mahmoodi, Development of hydrophilic microporous PES ultrafiltration membrane containing CuO nanoparticles with improved antifouling and separation performance, Elsevier B.V., 2019. https://doi.org/10.1016/j.matchemphys.2018.10.032.

[122] S. Amiri, A. Asghari, V. Vatanpour, M. Rajabi, Fabrication and characterization of a novel polyvinyl alcohol-graphene oxide-sodium alginate nanocomposite hydrogel blended PES nanofiltration membrane for improved water purification, Sep. Purif. Technol. 250 (2020) 117216. https://doi.org/10.1016/j.seppur.2020.117216.

[123] Z.P. Zhang, M.Z. Rong, M.Q. Zhang, C. Yuan, Alkoxyamine with reduced homolysis temperature and its application in repeated autonomous self-healing of stiff polymers, Polym. Chem. 4 (2013) 4648–4654. https://doi.org/10.1039/c3py00679d.

[124] B. Smith, Infrared Spectral Interpretation - A systematic approach, 1st ed., CRC Press, 1999. https://doi.org/https://doi.org/10.1201/9780203750841.

[125] N. Wang, A. Raza, Y. Si, J. Yu, G. Sun, B. Ding, Tortuously structured polyvinyl chloride/polyurethane fibrous membranes for high-efficiency fine particulate filtration, J. Colloid Interface Sci. 398 (2013) 240–246. https://doi.org/10.1016/j.jcis.2013.02.019.

[126] G.H. Bhuvaneswari., Degradability of Polymers, in: M.G.T. Sabu Thomas, Ajay Vasudeo Rane, Krishnan Kanny, Abitha V.K. (Ed.), Recycl. Polyurethane Foam., 2018: pp. 29–44. https://doi.org/https://doi.org/10.1016/B978-0-323-51133-9.00003-6.

[127] I. Radelyuk, K. Tussupova, K. Zhapargazinova, M. Yelubay, M. Persson, Pitfalls of wastewater treatment in oil refinery enterprises in Kazakhstan-a system approach, Sustain. 11 (2019) 1–20. https://doi.org/10.3390/su11061618.

[128] F. Cheng, J. He, T. Yan, C. Liu, X. Wei, J. Li, Y. Huang, Antibacterial and hemostatic composite gauze of N,O-carboxymethyl chitosan/oxidized regenerated cellulose, RSC Adv. 6 (2016) 94429–94436. https://doi.org/10.1039/c6ra15983d.

[129] R.A. Nyquist, ed., Azines, Isocyanates, Isothiocyanates, and Carbodiimides, in: Interpret. Infrared, Raman, Nucl. Magn. Reson. Spectra, Academic Press, 2001: pp. 45–63. https://doi.org/https://doi.org/10.1016/B978-012523475-7/50183-2.

[130] C. Li, W. Sun, Z. Lu, X. Ao, S. Li, Ceramic nanocomposite membranes and membrane fouling: A review, Water Res. 175 (2020) 115674. https://doi.org/10.1016/j.watres.2020.115674.

[131] T. Fujioka, S.J. Khan, J.A. McDonald, L.D. Nghiem, Nanofiltration of trace organic chemicals: A comparison between ceramic and polymeric membranes, Sep. Purif. Technol. 136 (2014) 258–264. https://doi.org/10.1016/j.seppur.2014.08.039.

[132] M. Al Zarooni, W. Elshorbagy, Characterization and assessment of Al Ruwais refinery wastewater, J. Hazard. Mater. 136 (2006) 398–405. https://doi.org/10.1016/j.jhazmat.2005.09.060.

[133] H.J.H. Fenton, Oxidation of Tartaric Acid in Presence of Iron, J. Chem. Soc. 65 (1984) 899–910. https://doi.org/https://doi.org/10.1039/CT8946500899.

[134] C. Walling, Fenton's Reagent Revisited, Acc. Chem. Res. 8 (1975) 125–131. https://doi.org/10.1021/ar50088a003.

[135] V.N. Lima, C.S.D. Rodrigues, L.M. Madeira, Application of the Fenton's process in a bubble column reactor for hydroquinone degradation, Environ. Sci. Pollut. Res. 25 (2018) 34851–34862. https://doi.org/10.1007/s11356-017-0746-z.

[136] C.S.D. Rodrigues, R.A.R. Boaventura, L.M. Madeira, Application of Fenton's reagent for acrylic dyeing wastewater decolorization, organic matter reduction and biodegradability improvement, J. Adv. Oxid. Technol. 15 (2012) 78–88. https://doi.org/10.1515/jaots-2012-0109.

[137] A. Fernandes, M. Gągol, P. Makoś, J.A. Khan, G. Boczkaj, Integrated photocatalytic advanced oxidation system (TiO2/UV/O3/H2O2)for degradation of volatile organic compounds, Sep. Purif. Technol. 224 (2019) 1–14. https://doi.org/10.1016/j.seppur.2019.05.012.

[138] V. Pezzetta, C. Ulisse, M. Giorgetti, B. Conti, Method for Purification of Process Water from a Kerosene Desulfurization Plant, US 7,160,458 B2, 2007.

[139] R.M. Sellers, Spectrophotometric determination of hydrogen peroxide using potassium titanium(IV) oxalate, Analyst. 105 (1980) 950–954. https://doi.org/10.1039/an9800500950.

[140] M. hui Zhang, H. Dong, L. Zhao, D. xi Wang, D. Meng, A review on Fenton process for organic wastewater treatment based on optimization perspective, Sci. Total Environ. 670 (2019) 110–121. https://doi.org/10.1016/j.scitotenv.2019.03.180.

[141] J.H. Ramirez, F.J. Maldonado-Hódar, A.F. Pérez-Cadenas, C. Moreno-Castilla, C.A. Costa, L.M. Madeira, Azo-dye Orange II degradation by heterogeneous Fenton-like reaction using carbon-Fe catalysts, Appl. Catal. B Environ. 75 (2007) 312–323. https://doi.org/10.1016/j.apcatb.2007.05.003.

[142] J.H. Ramirez, C.A. Costa, L.M. Madeira, G. Mata, M.A. Vicente, M.L. Rojas-Cervantes, A.J. López-Peinado, R.M. Martín-Aranda, Fenton-like oxidation of Orange II solutions using heterogeneous catalysts based on saponite clay, Appl. Catal. B Environ. 71 (2007) 44–56. https://doi.org/10.1016/j.apcatb.2006.08.012.

[143] J.J. Rueda-Márquez, I. Levchuk, I. Salcedo, A. Acevedo-Merino, M.A. Manzano, Post-treatment of refinery wastewater effluent using a combination of AOPs (H2O2 photolysis and catalytic wet peroxide oxidation) for possible water reuse. Comparison of low and medium pressure lamp performance, Water Res. 91 (2016) 86–96. https://doi.org/10.1016/j.watres.2015.12.051.

Supplementary Information

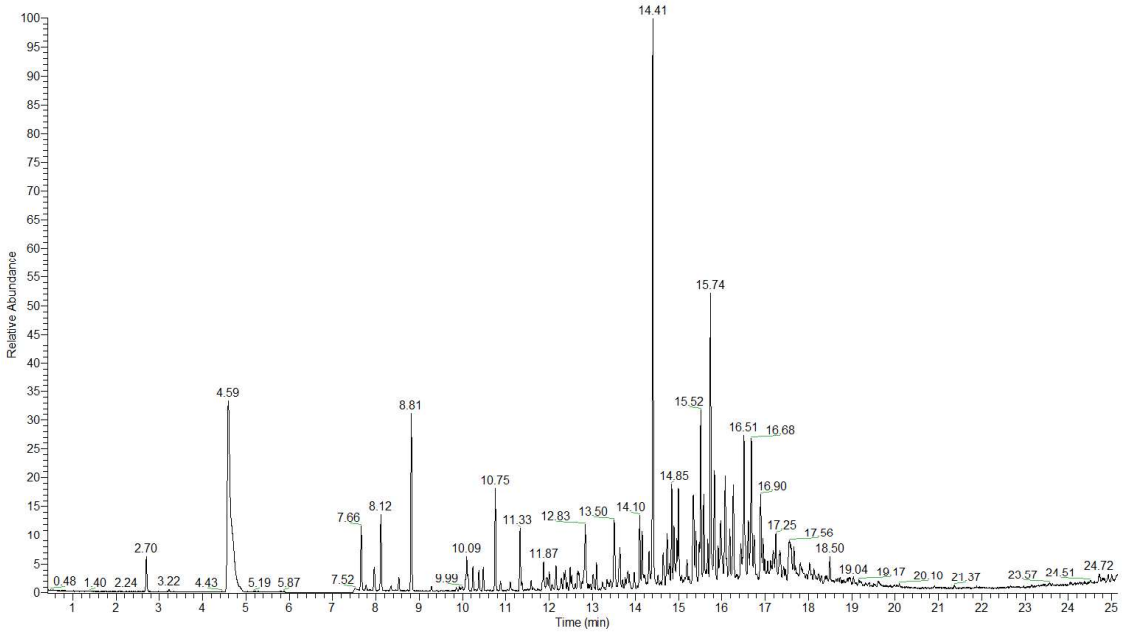

Figure A.1 - GC spectra of spent caustic sample collected in the 9th March 2018 in original form.

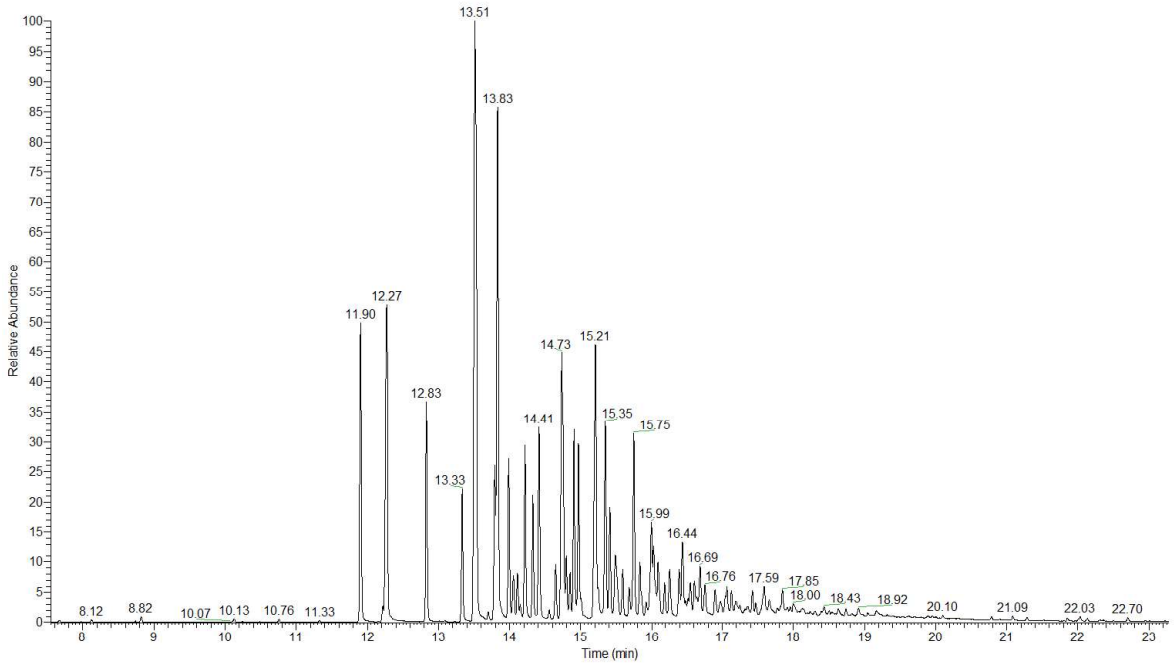

Figure A.2 - GC spectra of spent caustic sample collected in the 9th March 2018 in acidified form.

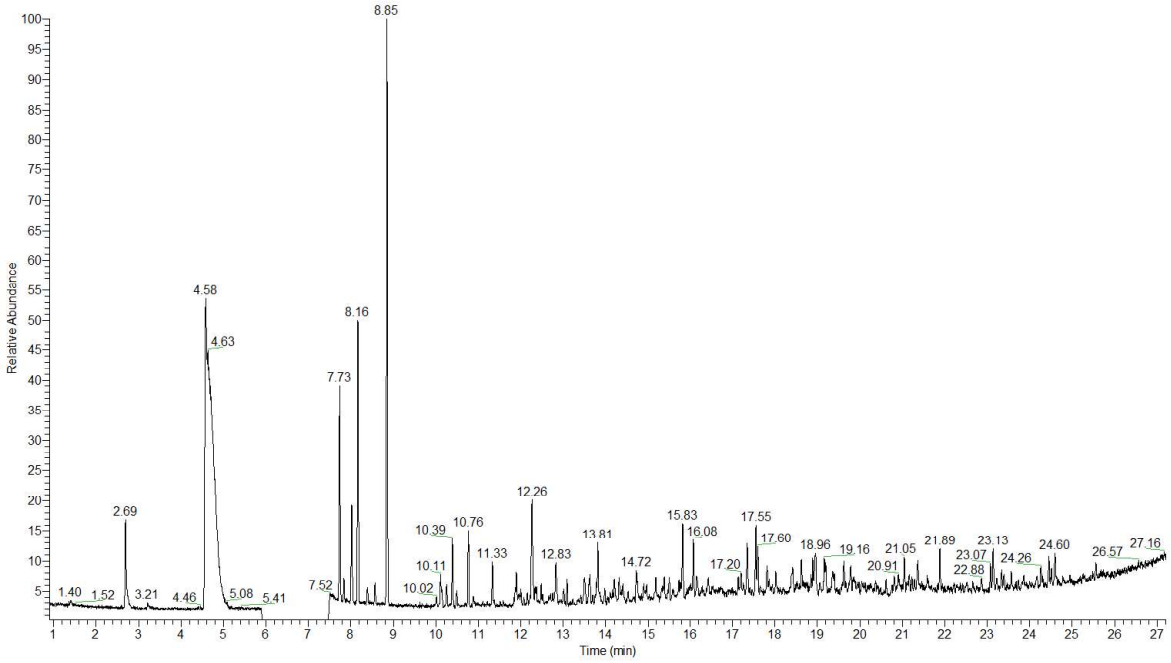

Figure A.3 - GC spectra of final wastewater collected in the 14th March 2018 in original form.

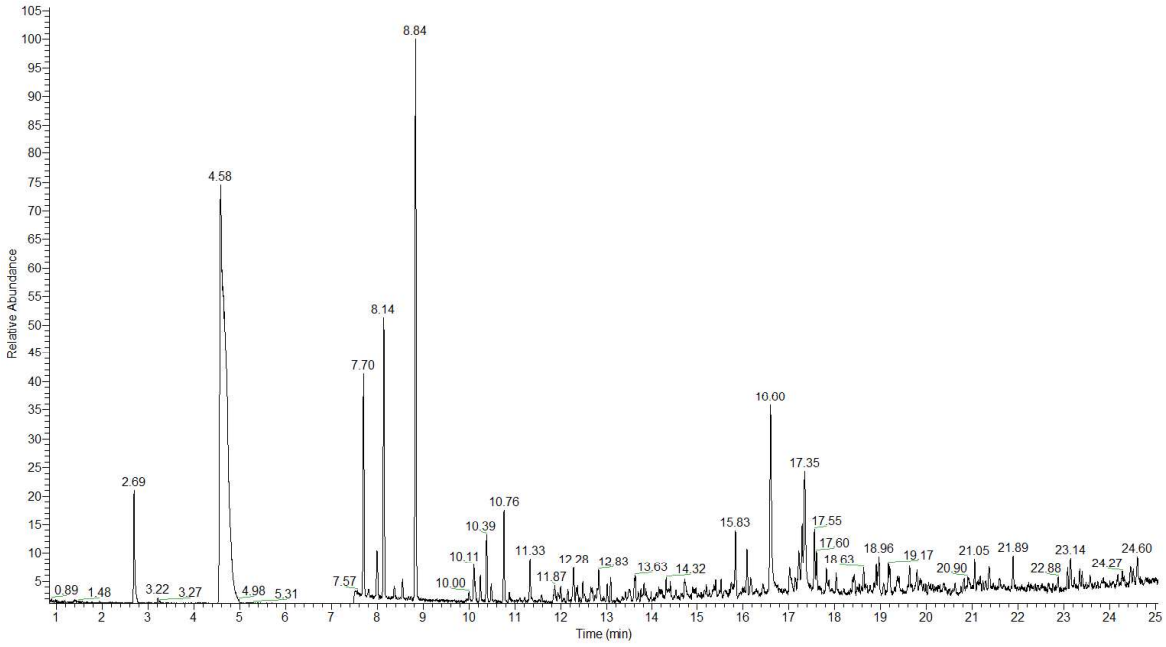

Figure A.4 - GC spectra of final wastewater collected in the 14th March 2018 in acidified form.

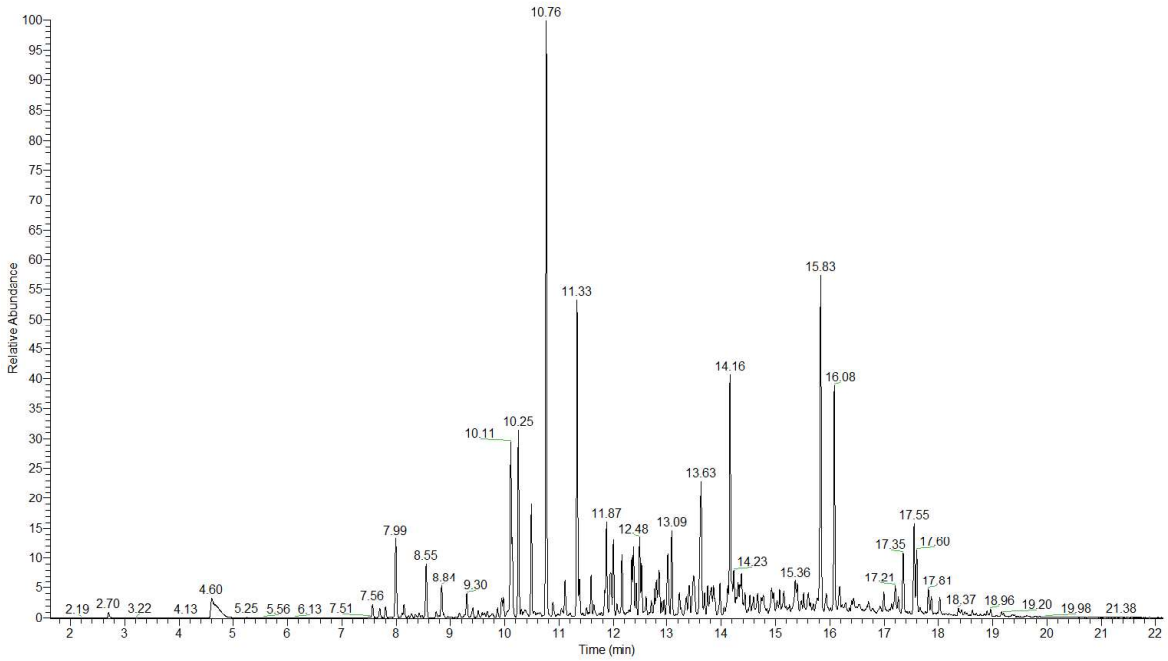

Figure A.5 - GC spectra of spent caustic sample collected in the 17th March 2018 in original form.

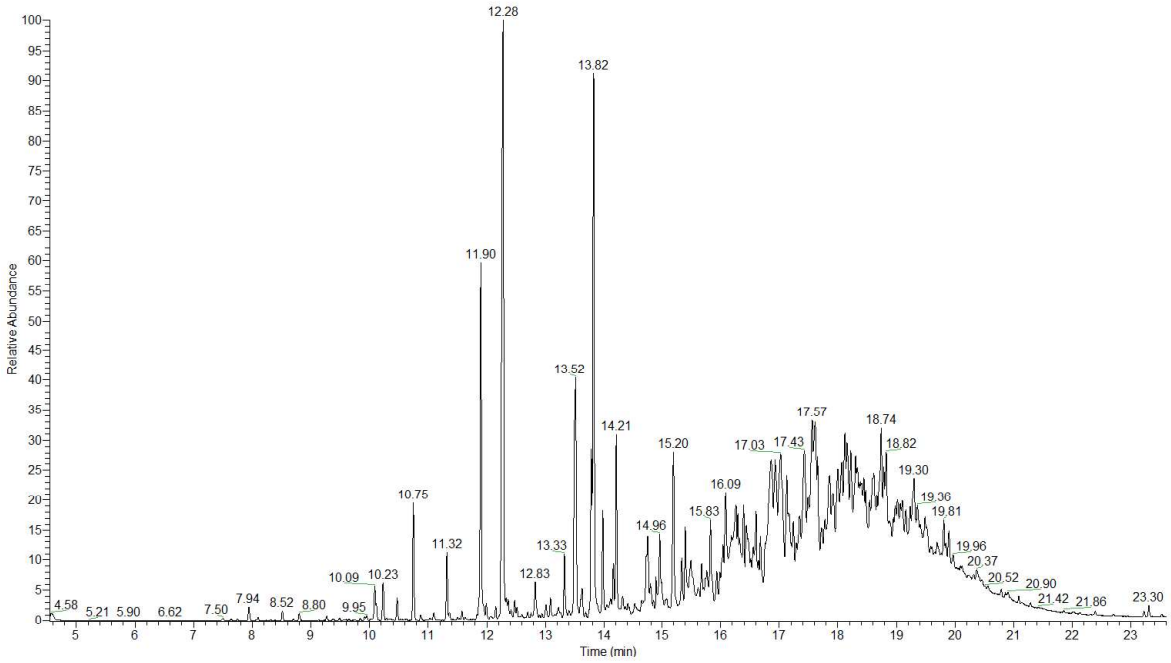

Figure A.6 - GC spectra of spent caustic sample collected in the 17th March 2018 in acidified form.

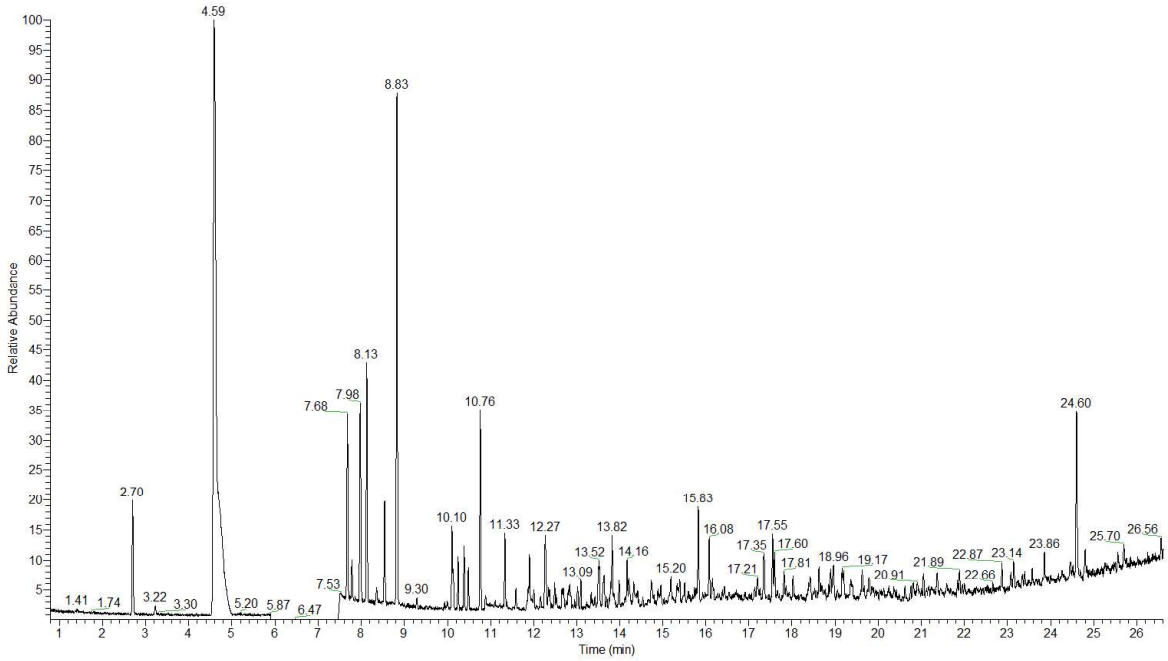

Figure A.7 - GC spectra of final wastewater collected in the 19th March 2018 in original form.

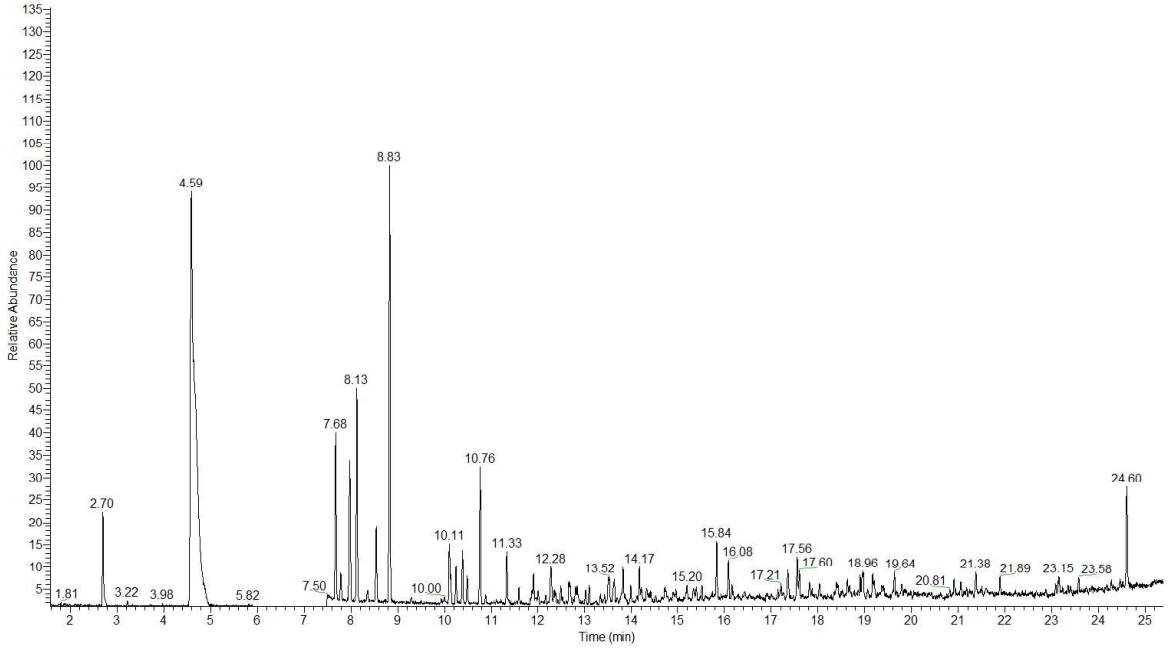

Figure A.8 - GC spectra of final wastewater collected in the 19th March 2018 in acidified form.